Ocjena zaštitnih svojstava organiskih prevlaka na različitim metalnim podlogama

Novak, Josip

Master's thesis / Diplomski rad

2019

Degree Grantor / Ustanova koja je dodijelila akademski / stručni stupanj: **University of Zagreb, Faculty of Mechanical Engineering and Naval Architecture / Sveučilište u Zagrebu, Fakultet strojarstva i brodogradnje**

Permanent link / Trajna poveznica: https://urn.nsk.hr/urn:nbn:hr:235:396214

UNIVERSITY OF ZAGREB
FACULTY OF MECHANICAL ENGINEERING AND
NAVAL ARCHITECTURE

MASTERS THESIS

Josip Novak

Zagreb, 2019.

UNIVERSITY OF ZAGREB
FACULTY OF MECHANICAL ENGINEERING AND
NAVAL ARCHITECTURE

MASTERS THESIS

Thesis advisor: Student:

Prof. Dr. Sc. Vesna Alar, dipl. Ing. Josip Novak

Zagreb, 2019.

I hereby declare that I have written this masters thesis independently, using only the knowledge acquired during the study and the listed literature.

Josip Novak

ACKNOWLEDGMENTS

I would like to thank my thesis advisor, Prof. Dr. Sc. Vesna Alar for guidance and support during the making of my thesis, as well as through years of study at the Faculty of Mechanical Engineering and Naval Architecture in Zagreb.

Special thanks go to Prof. Dr. Peter Weidinger for the dedicated supervision of the thesis at Brose Fahrzeugteile GmbH & Co. KG, for the constructive criticism, valuable advice and suggestions.

I would like to express my gratitude to Martin Kwiczala, for introducing me to contemporary coating processes and methods for corrosion evaluation on an industrial scale. I have greatly benefited from working by Martins side and without his persistent help this thesis would not have been possible.

I also received generous support from Marin Kurtela, whose assistance with comparative tests at the Laboratory for the protection of materials was invaluable.

Franziska Möhring and Andreas Erbisch made enormous contributions to electrochemical examinations in the thesis as well as set an example for diligence and attention to detail.

Finally, I would sincerely like to thank all the employees of the Brose materials laboratory, who welcomed me warmly and supported me and my work.

SVEUČILIŠTE U ZAGREBU
FAKULTET STROJARSTVA I BRODOGRADNJE
Središnje povjerenstvo za završne i diplomske ispite
Povjerenstvo za diplomske radove studija strojarstva za smjerove:
proizvodno inženjerstvo, računalno inženjerstvo, industrijsko inženjerstvo i menadžment, inženjerstvo materijala te mehatronika i robotika

Sveučilište u Zagrebu Fakultet strojarstva i brodogradnje	
Datum:	Prilog:
Klasa:	
Ur. broj:	

DIPLOMSKI ZADATAK

Student: **JOSIP NOVAK** Mat. br.: 0035192959

Naslov rada na hrvatskom jeziku: **Ocjena zaštitnih svojstava organskih prevlaka na različitim metalnim podlogama**

Naslov rada na engleskom jeziku: **Evaluation of corrosion protection properties of organic coatings on different metal substrates**

Opis zadatka:

Corrosion protection with coatings is the basic method of protecting metal structures. Increasingly strict ecological requirements, especially due to the emission of volatile organic solvents into the environment, have resulted in a wider application of environmentally friendly coatings.

The protection against corrosion via coatings needs to be carried out in greater detail in the paper. It is also necessary to further study and demonstrate the design of a protective coating system taking in to account the corrosive nature of the environment in which the structure will function, in accordance with the norm DIN EN ISO 12944. Additionally, it is necesary to study the literature, to analyze and display the properties and applications of powder coatings and coatings obtained by the electrophoretic process in an appropriate way.

In the experimental part of the paper, it is necesary to use the DC electrochemical method, by recording polarization curves, to determine the corrosion potential, the Ekor, the resistance, the Rp and the corrosion rate, the vkor, of the different metal substrates (aluminum, zinc and carbon steel) all of which are protected by powder coatings in a 3.5% NaCl solution. The EIS (Electrochemical Impedance Spectrometry) should then be used to follow the changes in the Ekor and in the coating resistance for a period of two months. It is necessary to determine the physical and chemical properties of the coating before and after its exposure to the salt and humidity chamber in accordance with norm DIN EN ISO 4628 (1-10).

Finally, it is necessary to critically consider the acquired results and the possibility of applying the analyzed coatings, depending on the substrate.
All references should be included in a reference list and an acknowledgement of all received help should be provided.

Zadatak zadan:
15. studenog 2018.

Rok predaje rada:
17. siječnja 2019.

Predviđeni datum obrane:
23. siječnja 2019.
24. siječnja 2019.
25. siječnja 2019.

Zadatak zadao:
prof. dr. sc. Vesna Alar

Predsjednica Povjerenstva:
prof. dr. sc. Biserka Runje

CONTENTS

LIST OF FIGURES

LIST OF TABLES

LIST OF ABBREVIATIONS

Al	chemical symbol for aluminium
BN	Brose standard (Brose Norm)
C	capacitance
CED	cathodic electrodeposition
CH	condensation atmosphere with constant humidity
CR4	grade 4 cold rolled steel according to ISO 3574
DBL	Daimler Benz delivery regulations (Daimler Benz Liefervorschrift)
DC	direct current
EIS	electrochemical impedance spectroscopy
E_{oc}	open circuit potential
EPS	electrostatic powder spraying
FSB	Faculty of Mechanical Engineering and Naval Architecture in Zagreb (Fakultet strojarstva i brodogradnje)
I_{corr}	corrosion current
KCl	potassium chloride
L	inductance
NaCl	sodium chloride
NSS	neutral salt spray test
R	electrical resistance
R_{corr}	corrosion rate
R_p	polarization resistance
SCE	saturated calomel electrode
SEM	scanning electron microscope
TL	technical delivery condition (technische Lieferbedingung)
UV	ultraviolet
VDA	German association of the automotive industry (Verband der Automobilindustrie)
Z	impedance
Zn	chemical symbol for zinc

SUMMARY

The aim of this masters thesis “Evaluation of corrosion protection properties of organic coatings on different metal substrates” is to examine the corrosion resistance properties of various CED and powder coatings, commonly utilized in the automotive industry. For this purpose, standardized steel, hot-dip galvanized steel and aluminium specimens are coated and subsequently tested in accelerated corrosion tests, the emphasis being on the climatic test according to VDA 233-102. The protective properties of the coatings are additionally studied using DC and AC electrochemical methods.

The main evaluation criteria are degree of rusting on surface and edges, degree of corrosion and delamination around a scribe, degree of blistering, cross cut test and Daimler scratch test. The utilized accelerated corrosion tests exhibit apparent differences in the onset and character of corrosion regarding those evaluation criteria. Key influencing factors for corrosion resistance, like coating thickness and pre-treatment methods are determined.

Key words: corrosion, organic coatings, accelerated corrosion tests, VDA 233-102 standard, electrochemical impedance spectroscopy

1. Introduction

To remain at the top position amongst car part manufacturers, Brose[1] has to offer high quality products with a competitive price tag. Guaranteeing the quality of all products, Brose employs a wide range of contemporary technologies, led by teams of capable engineers, complemented by an industrious work force.

A high diversity of products, ranging from seat adjusters, all the way to mechatronic components requires a vast level of expertise in various fields of engineering. Ensuring that all products work and look as intended, provide the driver with a comfortable driving experience and serve as a failsafe security measure in the case of a car crash is a very demanding task, which is backed up by constant series monitoring, a wide array of crash test and real time damage analysis.

Apart from the main function of any car part, an important quality is its longevity, especially in relation to tribological wear and the onset of corrosion. According to a survey from "IHS Markit", the average age of vehicles on the road is 11,4 years. It is also safe to assume that current car owners will own less cars in their lifetime, compared to the previous generation, as modern cars come out of the factory with better equipment and longer warranty periods [1].

Keeping the aspect of longevity in mind, a logical consideration would be to use materials that are shown to be optimal for such tasks. Materials, which provide both functional properties and protection against corrosion and wear, are not unknown, but the use of those materials usually comes at a great cost, namely their expense. When companies are mass-manufacturing parts in series of millions, possibilities to lover expenses, while keeping a reasonable degree of quality are considered on a regular basis. It is no secret that after optimizing and automatizing manufacturing processes, most profit can be saved by settling on a cheaper material, which, through certain processes, can behave the same as its more expensive counterpart. As an example, for some car parts, carbon steel is that material of choice. Steel has good mechanical properties, which come at the cost of high weight, moderate tribological properties and poor corrosion resistance. The latter downside is most commonly addressed by coating steel parts with metallic or organic coatings, which can provide exceptional corrosion resistance and aesthetic properties compared to its starting state. Like all competitors, Brose utilizes assorted coating methods that fulfil those longevity requirements and grant a distinct finish to their products.

[1]Brose is referring to Brose Fahrzeugteile GmbH & Co. KG

2. Motivation

Since the founding of the company in 1919, Brose has been on a steady rise in the automotive market. Key innovations, like the first electrically powered window regulator have secured a dominant position amongst competitive car part manufacturers and fortified a strong global presence for the company. By conquering new markets, the company had to adapt its production to meet the ever-growing demands of customers. Simply increasing the output and number of existing factories was not enough; therefore, Brose started cooperating with external companies in several stages of production.

The same is true when it comes to ensuring the corrosion resistance of their parts. Apart from having internal coating plants, Brose partnered up with external companies who specialize in coatings to meet the rising demand and provide a standardized quality of product. All coated parts are being examined by the Brose materials laboratory in Coburg prior to market release. Another important role of the laboratory is to evaluate new or experimental coating processes and approve those for future implementation. Upon conducting standard coating monitoring, the laboratory has detected certain issues in coating processes, a topic that must be addressed. One of the tasks of this thesis is to compare representative internal and external coaters[2] with each other, in various corrosion tests, and find out which coating system and pre-treatment method combination perform ideally.

The job of choosing the ideal coating system and process for the intended function is either simple, nor black or white, thus a multitude of variables must be considered for every single part separately. For the purpose of this thesis, parts from two Brose business divisions will be studied, the door and seat systems. A part representing the door system is a guide rail, most commonly made of galvanized steel or aluminium alloys, which are powder coated. A part of equivalent importance in the seat system is the seat adjuster, made from carbon steel with a cathodic electrodeposition coating. To eliminate some variables from the equation, instead of the previously mentioned car parts, standardized specimens with the corresponding coating will be used in the tests, so that the examined properties are resulting just from the coating process and the coating type.

The corrosion resistance properties of coatings are commonly tested in accelerated corrosion tests, which are carried out in standardized chambers. The tests promote the onset of

[2]Coaters are companies who specialize in coating application

corrosion in a relatively short period of time. Most car manufacturers, respectively customers[3], have standards with corrosion resistance requirements for their products regarding a specific test, test duration and evaluation criteria. Brose adheres to the customer requirements when testing parts specifically for any customer. The customer standards are also summarised in Brose internal standards, which will be revised as a part of this thesis.

Among the accelerated corrosion tests, the constant humidity and salt spray tests are well established, but they regularly do not paint the full picture nor have a good correlation to real time corrosion development. Therefore, new climate tests with intermittent phases were developed in hopes to reduce the testing time and expose the parts to conditions similar to day-to-day car use. A typical example is the climatic test according to VDA 621-415 standard, which has intermittent wet and dry phases and a salt spray phase. In 2013, VDA[4] released the latest iteration of a climatic test with the VDA 233-102 standard. The goal of the new test is to cause realistic corrosion propagation on aluminium alloys and galvanized steel while further reducing the required testing time. All of the coating variants will be compared in accelerated corrosion tests, in the Brose materials laboratory, with an emphasis on the new VDA test. In addition, comparative tests will be carried out in the Laboratory for the protection of materials at the Faculty of Mechanical Engineering and Naval Architecture in Zagreb.

Lastly, while accelerated corrosion tests provide valuable data and insight into the protective properties of coatings, corrosion, in the presence of a conductive medium is generally an electrochemical process, which can be observed from an electrochemical standpoint. To complement accelerated corrosion tests, electrochemical methods for inspecting corrosion properties of substrates, pre-treatment methods and coatings will be used. With the help of electrochemical impedance spectroscopy, coating properties in the starting condition will be compared to those of aged specimens.

[3]Customers are car manufacturers who purchase car parts from Brose
[4]VDA refers to The German Association of the Automotive Industry (Verband der Automobilindustrie)

3. Theoretical fundamentals

3.1. Corrosion

Corrosion is a process by which materials are unintentionally and detrimentally destroyed under the influence of physical, chemical or biological factors. Metals, the most commonly used material in engineering, are unstable in atmospheric conditions. This instability stems from their original state, namely ores, which must be artificially reduced through multiple metallurgical processes in order for them to be viable for utilization. When left unprotected, the same metals tend to return to their original states, hence forming corrosion products like oxides and sulphides [2].

Those changes follow the laws of thermodynamics, so when interpreting corrosion, it is imperative to talk about the corrosion system as a whole. Corrosion systems, or corrosion cells, include the material and its surroundings, the medium, which exchange energy and mass until said system reaches an energetically stable state. Fully understanding the interactions of materials and their environments also takes on the added dimension of chemistry and electricity [3]. Keeping that in mind, corrosion can be divided into two main mechanisms, chemical and electrochemical corrosion.

The former case describes corrosion in a medium, which is not electrically conductive, while electrochemical corrosion occurs in electrolytes and is the most common corrosion mechanism. Humidity, dew, water or seawater form conductive aqueous media, which exchange electrons between the material surface and the medium trough resulting galvanic currents. This process leads to the oxidation of metals, commonly observed when steel is exposed to a strong acid or a sodium chloride solution [3].

3.1.1. Types of corrosion

The main mechanisms of corrosion are responsible for many varying types of metallic corrosion. This chapter will focus on the most relevant ones for the thesis.

General (uniform) corrosion is characterized by an even rate of metal loss over the exposed surface. It is thought of as metal loss due to dissolution of the metallic component into metallic ions. In combination with oxygen, metallic ions form oxides, also known as scale, which ultimately flake off the surface, most commonly observed in rusting od iron. Metals can naturally

resist this type of corrosion by forming passive surface films, either by exposure to air or chemical treatment. In principle, those films are a form of general corrosion which prevents further degrading of the metal, provided it remains intact. Examples of such films are copper patina and the fogging of nickel. Aluminium also forms a thin and compact surface film that limits further degradation. The aluminium oxide film is stable in the pH range from 4 to 9, which makes aluminium applicable in many corrosive environments without the need for extra protection [2].

Pitting corrosion is both a corrosion mechanism and form of corrosion associated with other mechanisms. It is characterized by a highly localized loss of metal under an otherwise barely- or unaffected surface. The pit opening remains covered with corrosion products while the pit continuously penetrates deeper into the metal, making it difficult to detect. Furthermore, the absence of apparent reduction in wall thickness and the negligible loss in weight give little to no evidence as to the extent of the resulting damage. The main cause of pitting in electrolytes is the electrical contact between dissimilar metals, where the resulting difference of potential causes current to flow from the anode to the cathode. If the anodic area is relatively small, serious metal loss can occur. Pitting can also develop as a result of irregularities in the physical or chemical structure of the metal, even on clean surfaces [3].

Filiform corrosion can form on metals with semipermeable coatings or films. It manifests itself as numerous meandering threadlike filaments of corrosion just beneath the surface. Sufficient water permeability of the film, as well as defects and impurities in high humidity environments form ideal conditions for the onset of filiform corrosion. Each filament has an active head and an inactive tail, if the head crosses paths with another filament it is diverted and grows in another direction. Filiform corrosion has been observed on aluminium, zinc, steel and magnesium, usually under organic coatings such as paints and lacquers. Filiform corrosion is always very shallow in depth, thus not causing any serious damage to the metal beside cosmetic problems. In some cases, it can negatively affect paint adhesion and act as an initiation site for other forms of corrosion [3].

Other, most common types of corrosion include:

- Intergranular corrosion
- Galvanic corrosion
- Crevice corrosion
- Erosion corrosion
- Stress corrosion cracking

- Biological corrosion
- Selective leaching
- Hydrogen damage
- Liquid metal attack
- Exfoliation
- Corrosion fatigue [3].

3.1.2. Corrosion prevention

There are many ways to address corrosion prevention, most of which are based on the following two principles:

-nullifying the driving forces for the onset of corrosion

-increasing the systems resistance to those driving forces.

These principles can be exploited either by changing the characteristics of the construction material, the characteristics of the surrounding medium, or by simply separating the material from the medium [2].

In practice, corrosion can be prevented by thoroughly considering the design and technological properties of the product. Corrosion resistant materials for the specific environment should be used if possible. Materials in highly corrosive media, like seawater, require additional electrochemical protection in the form of sacrificial electrodes. Corrosion inhibitors can also be used to delay the onset of corrosion and, for example, enable longer storage times of half products. Ultimately, coatings represent a widely spread and cheap method of protection against corrosion with additional aesthetic and functional benefits. For constructions and parts that must be immutable to corrosion for years or decades an optimal combination of the mentioned measures should be taken into account [2].

3.2. Coatings

Coatings protect metals from corroding by forming a theoretically impermeable barrier between the surface and the surrounding medium. They can be made of one or more components that must be able to form a strong surface film. The effectiveness of any coating depends on not

only the properties of the used coating, but also on the metal substrate, application procedure, surface pre-treatment and compatibility with the substrate surface.

In addition to their protective properties, coatings usually have one or more of the following secondary functions:

-decorative purposes

-reduction or increase of electrical conductivity

-protection against mechanical wear

-regenerative properties, etc.

From a material standpoint, coatings are split into metallic and non-metallic groups. The former can be further divided, into sacrificial and noble coatings, depending on the mechanism of protection. Non-metallic coatings are further split into organic and inorganic classes [3].

The main form of corrosion protection on the examined parts are organic coatings applied by cathodic electrodeposition and powder coating processes, while hot dip galvanizing is used to additionally protect the steel substrate used for the guide rails.

3.3. Coated Brose parts

As mentioned in the motivation, this thesis will focus on parts of the two main Brose business divisions, the door and seat systems. The door system consists of products, which are built into car doors and provide them with various functionalities, the main one being the power windows. The power window assembly further breaks down into components like the electromotor, guide rail, cables and polymer parts. The guide rails, shown in figure 1, are made from aluminium

Figure 1. Powder coated guide rails

or hot dip galvanized steel and subsequently powder coated to receive their full range of protective and functional properties.

It is important to note, that the position of the door system is peculiar on itself, because it borders with the car's interior and exterior area. Naturally, the corrosion properties of exterior parts are tested more strictly as they are potentially exposed to a more corrosive environment and undergo larger temperature fluctuations. This is reflected both in the substrate and in coating choice. From the substrate standpoint, aluminium and hot dip galvanized steel are more corrosion resistant from the get-go than plain steel while the powder coating offers a greater coating thickness than cathodic electrodeposition.

As the name implies, the seat system consists of the metallic structures of the car seat and all its inner workings: the adjusters that secure the seat to the chassis, electro motors for all the adjustments and other security and supporting parts. Just like the power window guide rails, the seat adjusters, shown in figure 2, come in many shapes and material variants, the main material being steel with various carbon amounts and alloying elements.

Steel on its own, even being utilized in the relatively inert cars interior, does not showcase sufficient corrosion resistance nor aesthetic properties. Therefore, the seat adjusters are coated by the process of cathodic electrodeposition.

Figure 2. Cathodic electrodeposition coated seat adjusters

3.3.1. Metallic coatings

Metallic coatings are a popular stand-alone method of protection for structures made of metals, which are utilized in a relatively non-corrosive environment. They can also be used as a base coat within a multi layered coating system to substantially increase its protective properties. When designing any corrosion protection system with metallic coatings, the considered metals are classified by their standard electrochemical potentials, which describe the metals readiness to either receive or give electrons. The electrochemical potentials of metals in relation to a standard hydrogen electrode are well documented and are usually shown in form of electrochemical voltage series as in figure 3 [4].

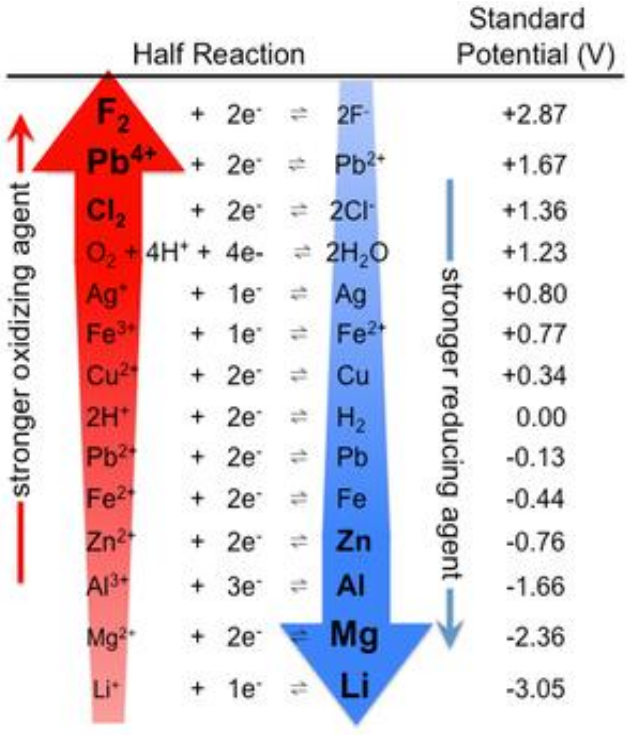

Figure 3. Metals in relation to their standard electrochemical potential [4]

Simplified, this figure shows how noble a metal is in relation to others. Metals with a lower value of the electrochemical potential, in contact with a corrosive medium “sacrifice” themselves to protect the more noble metal.

In the case of a zinc layer on steel in a corrosive, wet medium this manifests itself in the following way. If the zinc film is intact and no electrolyte comes into contact with the steel, there is no inherent danger for the substrate to corrode. When the protective zinc layer is damaged, and

the steel substrate exposed to the electrolyte, a galvanic element is formed. Based on the different potentials of zinc and steel, zinc electrons travel to the steel surface, turning it into a makeshift cathode and protect it from corroding. In that process, zinc corrosion products (white rust) are formed on the damaged area. This method of protection functions well, as long as there is a sufficient zinc layer left in that area (Figure 4) [5].

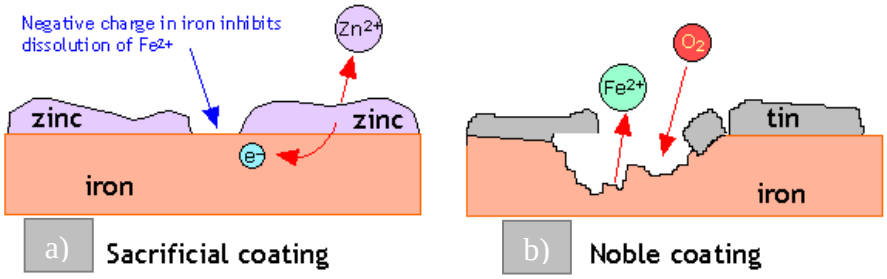

Figure 4. Differences in protection mechanisms between a) sacrificial metal coatings and b) noble metal coatings [5]

Hot-dip galvanization

Hot-dip galvanization is the most common metallic coating process for corrosion protection, either on its own or in combination with other coatings. In this process, a zinc coating is applied to sheet steel bands or components by immersing them into a molten zinc bath at around 450 °C. The whole process consists of several surface preparation steps, followed by the immersion in zinc and subsequent cooling and inspection. The resulting zinc coating is securely integrated into the steel, held together by a zinc-iron layer, as demonstrated in figure 5. Coating thickness can be varied from 10 all the way to 250 micrometres. The resulting layers are stable in atmospheric environments and can be use without any additional coatings, but in this case, the parts are additionally powder coated [6].

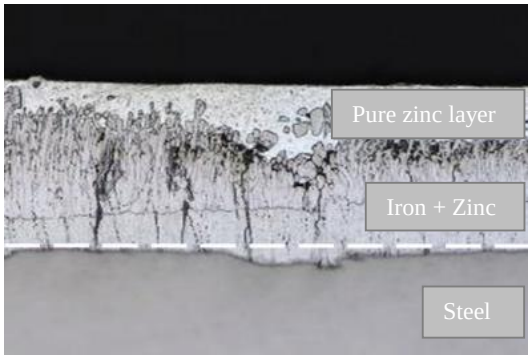

Figure 5. Crosscut sample of a hot-dip galvanized steel surface [6]

3.3.2. Organic coatings

Organic coatings are the oldest and most widely used method for corrosion protection of metals. They act as a barrier between the metal and the corrosive environment in order to protect the underlying substrate. As the name suggests, they stem from naturally occurring compounds like fish or rice oil, but today they largely consist of synthetic materials or the combination of both. The effectiveness of organic coatings depends on both the coating properties, the character of the metal substrate, surface pre-treatments and application methods. Therefore, it is necessary to take the properties of the whole system into account when opting for this method of corrosion protection.

Organic coatings get their protective and physical properties from a combination of the following ingredient classes: binders, pigments, fillers and additives [3].

Binder

The binder, also known as resin, is a continuous polymeric phase in which all other components can be incorporated, thus it is the matrix of the coating. The binder's density and composition are primarily responsible for determining the corrosion resistance, permeability and UV resistance of the coating. The binder can form a continuous film either by physical curing, chemical curing or the combination of those two [3].

Pigment

Pigments play a dual role in any coatings system. Firstly, they provide the coating with aesthetic properties, like colour and gloss, and secondly, they improve the corrosion resistance properties of the coating. For the latter purpose, flake shape pigments are added to form a layer parallel to the metal surface in order to prevent the permeation of corrosive media trough the coating by elongating their diffusion pathways. Alternatively, pigments that provide active protection against a corrosive attack can also be incorporated. In this case, they dissolve, or sacrifice themselves at endangered sites, thereby protecting the substrate metal actively or by passivating the attacked surface. Pigments must be compatible with the binder and should be somewhat resistant to the media of utilization [3].

Filler

Fillers generally increase the volume of the wet coating, as well as the dry coating thickness. They can also improve some coating properties, including, resistance to tribological wear, water

and oxygen permeability as well as enhanced edge deposition. Typical fillers like talc, mica and wood dust are low cost materials that make the coating more inexpensive [3].

Additive

Trace amounts of additives are added to a coating mixture in order to improve a very specific function of the coating. The amount of additives is usually around 0,01 to 1 % of the entire coating volume. They can fulfil the roles of surfactants, coalescing aids, emulsion stabilizers, drying agents, etc. Therefore, the use of a particular additive can be critical to the performance of coatings in certain conditions. Unfortunately, since they are only added in trace amounts, they are also the hardest component to detect while analysing the paint [3].

Solvent

Another very important component of organic coatings is the solvent. Without the proper solvent, coatings have a very high viscosity and are often heterogeneous, as the relatively heavy pigments and additives sink to the bottom of the container. Solvents reduce the viscosity coatings, making them easier to mix and achieve a homogenous composition.

The role of the solvent prior and after paint application is inherently contradictory. Before application, coatings should form a stable solution or dispersion of all before mentioned components. All of the components should be spread out equally, where solvents act as a repulsive force between them to avoid clustering and inhomogeneity. Oppositely, after the coating is applied, the components have to form a continuous film by coming closer together. Therefore, the solvent should be able to evaporate uniformly across the whole surface to let the film cure uniformly. This enables the application of very smooth and thin films of coatings on specific surfaces [3]. Naturally, coatings without any solvents are not uncommon either, like the powder coatings used on the Brose parts.

3.3.2.1. Mechanisms of protection

Simply knowing the building blocks of a coating does not provide enough insight into the complex matter of corrosion protection. However, when the roles of each individual component are combined, the following mechanisms of protection become evident; formation of a barrier and active corrosion inhibition by pigments.

In actual practice, the passive barrier properties of organic coatings are fairly limited. They always remain permeable to oxygen and water to some extent. In outdoor environments, organic coatings are saturated with water about half of its service time, while for the remainder they contain a quantity of water comparable to a high humidity environment. Moreover, the diffusion of oxygen trough some coatings is high enough to allow unlimited corrosion. Taking these factors into account, it is obvious that at least a part of the protective properties results from other mechanisms. Additional protection is achieved by resistance inhibition, which is a part of the barrier mechanism on the electrochemical level. Corrosion reactions are greatly slowed down by inhibiting the charge transfer between cathodic and anodic sites, since organic coatings increase the ionic resistance of the metal surface in the corrosion cycle [3].

3.3.2.2. Failure of organic coatings

For corrosion to take place under an intact coating, it is necessary to establish an electrochemical double layer, or break the adhesion between the substrate and the film. Corrosion processes through a coating take place in the following steps:

-migration of water, oxygen and ions trough the coating

-development of an aqueous phase at the coating/substrate interface

-activation of the substrate surface for the anodic and cathodic reactions

-deterioration of the coating/substrate interface bond [3].

3.4. Cathodic electrodeposition (CED, German; KTL)

Cathodic electrodeposition, also known as cathodic dip coating, is a specific process under the umbrella of electrophoretic deposition. Other processes from the same family include electro coating, anodic electrodeposition, electrophoretic painting, which are all very similar for the most part. The differences between cathodic and anodic film deposition are depicted in figure 6 [3].

CED became mainstream in the seventies with the advancements made with water-based solvents and process technologies related to coating application. Today it is a widespread method of applying a uniform primer film for corrosion protection, especially in the automotive industry.

In most cases, CED is a fully automated process in which an organic coating is applied to a metal part by immersing it into a water dispersion or paint solution baths with the help of electric current. Coating particles, which contain macroions, travel to the oppositely charged part, the cathode, while water travels in the opposite direction, resulting in an almost dry coating out the bath. Once a certain coating thickness has been achieved, the coating itself acts as a resistor and prevents further film build-up. CED processes have the ability to coat parts with a very complex geometry and achieve a uniform coating thickness [7].

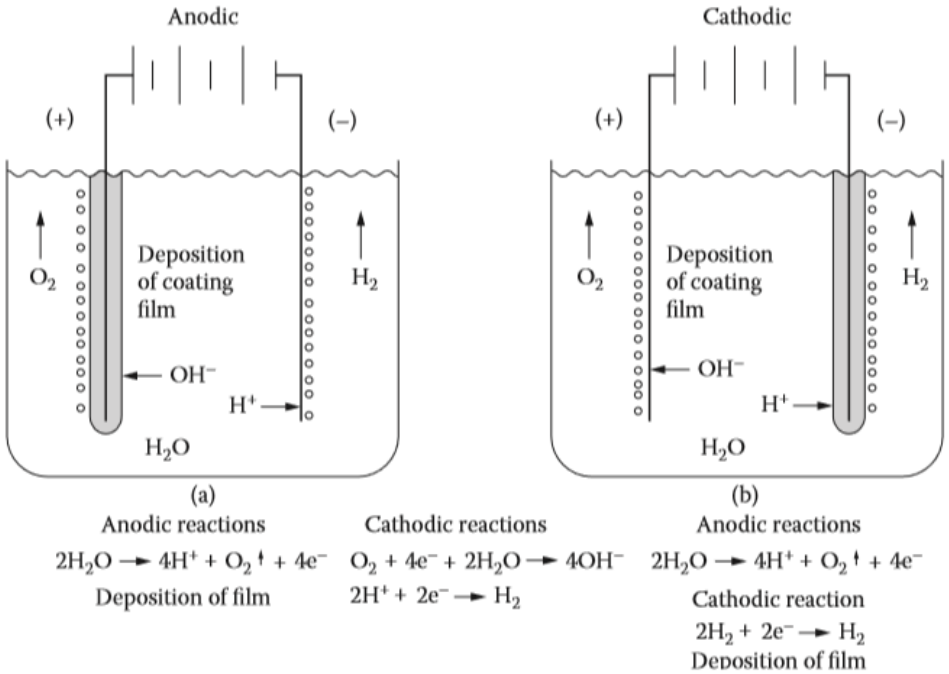

Figure 6. Schematic depiction of a) anodic and b) cathodic electrodeposition processes additionally described with chemical equations [3]

CED coating application

Before applying any coating to a metal substrate certain pre-treatment processes have to take place to condition the surface and ensure an ideal film formation. It has been proven that most cases of coating failures can be traced down to failures in the pre-treatment methods, rather than the coating process or coating type. Therefore, pre-treatment is a very important step which cannot be overstated [8].

Various pre-treatment methods are used to clean the metal surface, remove already formed corrosion products, contaminants or existing coatings. At the same time, the surface can be chemically activated, and the desired surface roughness can be achieved. Lastly, thin conversion layers which further promote coating adhesion and have anticorrosive properties can be applied. Pre-treatment methods vary from process to process, but they usually consist of a combination of the following steps: degreasing, mechanical pre-treatment, chemical pre-treatment, removal of existing coatings. Since these steps are highly customizable, Brose employs multiple pre-treatment variations. Nevertheless, typical pre-treatment steps will be further explained in continuation [7].

Degreasing

Metal parts are usually delivered to the paint shop with a layer of oil from the earlier reshaping processes or for corrosion resistance purposes during storage and transport. These oils would make it impossible for the coating to adhere to the surface, therefore they must be removed, as well as all other organic surface impurities.

Integrated at the start of an automated coating process, degreasing consists of several washing and solvent soaking steps. Depending on the type of metal and degree of impurities the following solvents can be applied; organic solvents, alkaline water suspensions, acidic water suspensions, inorganic water suspensions, in specific cases even incineration. Integrated in the sample degreasing process are either alkaline, acidic or neutral water suspensions, where the surface is cleaned by those chemicals activated by heat. After the whole degreasing process, the surface would be sufficiently clean for paint application, but this is not good enough for today's standards [8].

Surface activation

Surface activation is a chemical pre-treatment method, which ensures optimal conditions for the phosphating step. During activation, crystallization nuclei are formed on the metal surface,

which help in the development of the phosphate layer. The phosphate film also forms faster which reduces overall phosphate thickness. This is important if parts encounter mechanical stress, because a thinner phosphate layer does not break as easily.

Phosphating

Subsequently to degreasing, a layer forming pre-treatment method is employed. The achieved surface has better roughness for film formation and provides with additional corrosion protection. Typical processes include phosphating and chroming [9]. Since the latter method is frowned upon from an environmental standpoint, Brose has opted for the phosphating route.

Phosphating is a method in which steel or galvanized steel substrates are treated with a solution of phosphoric acid and phosphate salts, in order to form a crystalline phosphate layer. The produced conversion layer prevents the onset of corrosion during the coating process itself, conditions the surface for better coating adhesion and prevents the spreading of corrosion in final products to a degree. The most common phosphating methods include iron, zinc, manganese and tricationic phosphating, the former two will be covered in more detail.

Iron phosphating is in wide use as a base for parts that have a relatively low corrosion resistance requirement. The process itself is also relatively inexpensive, compared to zinc or manganese phosphating, and the replacement and sanitation of the baths is simpler. Unlike both zinc and manganese phosphates, in which the metal cation is found in the phosphating solution, the iron in the iron phosphate is contributed by the coated metal. The resulting phosphate film has a very low thickness and is susceptible to corrosion between coating steps [10].

Differing from iron phosphating, zinc phosphating is used for highest corrosion resistance requirements. This process is carried out with an alkaline degreasing step and a subsequent phosphate bath. The bath consists of zinc phosphate and phosphoric acid which form, which react with the substrate. As a result of this reaction, a crystalline phosphate layer is formed, which adheres extremely well to the substrate. This layer is thicker than the iron phosphate layer, therefore it offers more corrosion protection and potentially even better coating adhesion [9].

Tricationic phosphate also contains zinc, with the addition of manganese and nickel. It can be considered as a more advanced zinc phosphate with slightly better protective properties. Tricationic phosphate forms an extremely fine and compact layer, resulting in extremely low porosity. This contributes to even better coating adhesion and corrosion resistance properties.

Surface passivation

Right after the phosphating, a passivation bath can chemically treat the newly formed layer to increase its quality. In this process, the surface is made inert to prevent further oxidation and mid process corrosion [11].

Coating application

Following a variant of the pre-treatment methods, the coating can now be applied to the prepared surface. CED involves submerging the part into a container with the coating solution which is integrated after the pre-treatment line. The bath is usually acidic, with a pH value between 3 and 6, which is achieved by adding oxalic or acetic acid. This process is appropriate for most binders, including epoxides, acrylates, polyesters and alkyds.

Direct current is then applied to the bath using electrodes to stimulate the positively charged coating solution to move towards the negatively charged substrate, the cathode. The dissolution of the metal substrate is therefore minimized, but unwanted gas formation can be a problem. Cathodic processes are usually operated at higher current voltages than the anodic ones. The voltage varies from 50 to 500 volts and it mostly remains constant during the process. The applied voltage also determines the coating thickness. The formed coating on the substrate has a higher resistance than the substrate itself, the increase of coating thickness is proportional to the resistance. Thus, at the pre-set process voltage, the electric current slowly decreases as the film gets thicker, until the deposition stops occurring. This guarantees a uniform coating thickness of about 15 to 50 micrometres, depending on the used voltages and coatings [7].

After a successful coating application, the parts emerge out of the bath and the excess wet coating solution must be washed off, which is typically a twostep process carried out by jets of deionized water.

Curing

Since the coating is organic, composed of a resin, the binder must be additionally cured to materialize in its final form. Curing is the final step in the coating process, where the applied coatings are dried, and the binder polymerizes with all the other ingredients to from a uniform film. Coatings are classified by various film forming mechanisms, such as solvent evaporation, coalescing, phase change and conversion. In addition to that, they are also classified as room-

temperature curing or baking, both of which are applicable for thermosetting and thermoplastic coatings [3].

3.5. Powder coating

Powder coating is a method for applying dry, solid, finely dispersed resinous coatings to conductive materials, developed in the 1950ies. Most common procedures include:

- electrostatic powder spraying
- electrostatic fluidized bed
- rotational coating of pipes
- centrifugal casting etc [3].

The following section will describe electrostatic powder spraying, as it is the powder coating method utilized by Brose.

Electrostatic powder spraying (EPS)

In this process, electrostatically charged particles are applied to a grounded metal using a specialized spray gun (Figure 7). The spray gun has a charged electrode in the nozzle powered by

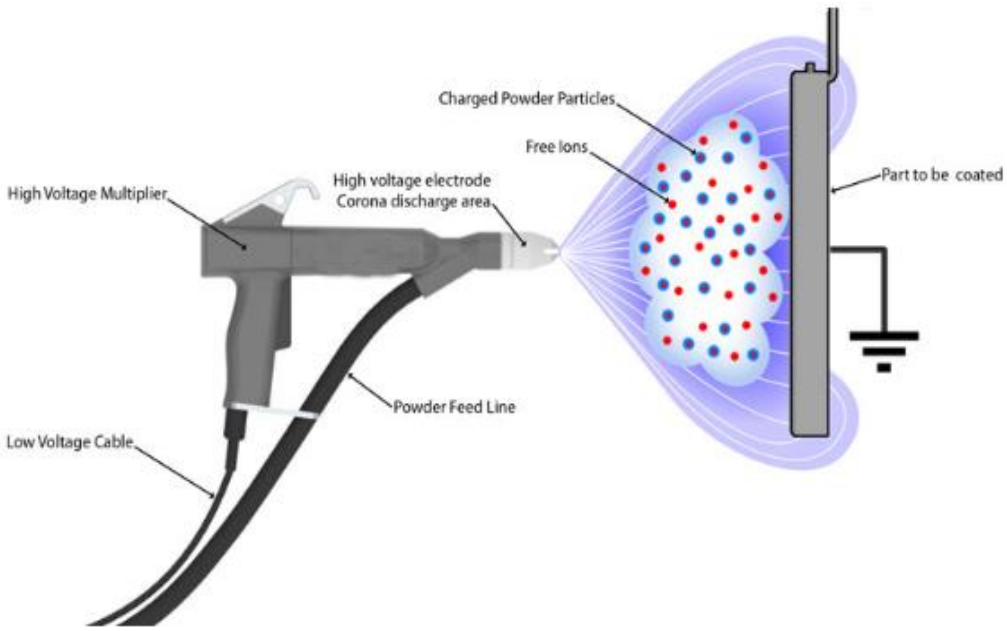

Figure 7. EPS process with spray gun and powder trajectories [35]

a high-voltage DC power pack. A powder and air mixture is supplied from a small fluidized bed in a powder reservoir through a hose.

The powder and the substrate have opposite electrical charges, therefore, the powder is attracted to the substrate surface where it forms a predetermined layer. Moreover, the electrical forces can determine the layer thickness and serve as a type of electrical adhesion. This adhesion prevents the powder to fall of the substrates in the presence of other forces, like gravity.

The trajectories of the sprayed particles are also shown in figure 7. It is clear that they reach around the surface facing the spray gun, which enables uniform powder deposition on the rear site of the substrate.

EPS is environmentally friendly because the powder does not contain any components, which can evaporate into the air and cause pollution. The excessive powder can be re-used after it is collected, so there is practically no material loss in this process. EPS is also fully automatized which further reduces operating costs.

Similar to CED, parts meant for electrostatic powder coating have to undergo a rigorous pre-treatment process. This process is analogous to the one previously described but has to be adjusted for hot-dip galvanized steel and aluminium substrates [12].

Curing of powder coatings

Just like CED coatings, powder coatings must be cured after the application. The film is subsequently formed by heating and baking of the applied powder. The mechanism of curing depends on the individual reaction system of a specific powder and is carried out in dryers for continuous operation attached directly after powder application. The powder and the substrate should be heated uniformly to the curing temperature, so that the phase change reactions are not hindered by premature crosslinking. The standard curing temperatures are around 110 °C to 250 °C and times between 5 and 30 minutes. Suitable curing parameters are necessary to avoid over burning and secure a consistent degree of gloss [12].

3.6. Chosen coatings for the thesis

As mentioned in the Motivation, Brose is a global supplier of car parts, with production and coating plants spread throughout the globe. Apart from the huge benefits of having a global market at one’s disposal, this fact brings further complexity into all aspects of production,

including corrosion protection of their parts. Laws, guidelines and standards are not uniform across the globe, and for every new market, they must be taken into consideration separately. In short, this means, that applicable and acceptable technologies in Asia might be prohibited in North America. Moreover, Brose cannot depend on just one coating manufacturer in any region. At least one back-up option has to be available in case the demand surpasses the supply capabilities. Theoretically, all utilized coatings should be equivalent and exhibit the same properties. Finally, even though any singular coating has to fulfil any regional demands, logistic and economical cost have to be taken in to account too.

In an effort to minimize this scattering and fulfil all those requirements, Brose could not settle just on one coating process and coating brand, so they chose a couple leading companies. Purchasing their paints from market leaders, they can adapt to new markets without making any sacrifices in terms of coating quality. Additionally, Brose materials laboratory rigorously tests any new coating process, with new pre-treatment variations and upcoming coating types to ensure that those processes are valid and fulfil all corrosion resistance requirements. Once a process is greenlit, constant series monitoring of the final product and the coating line is carried out, to have an insight in any process changes or eventual quality decline.

One of the goals of the thesis is to compare representative coaters and their respective processes and discover any and all differences between them. Moreover, differences between pre-treatment methods and coatings should be explored in order to find out which coating and pre-treatment combination performs best in standardized corrosion test to be able to make a recommendation for the future. State of the art processes should be strived for.

This experiment would be to comprehensive to perform on the total of more than 60 active internal and external coaters, therefore a representative sample was chosen. The coaters were chosen so that every coating type and pre-treatment combination is included in the test. Additionally, an experimental coater with a modified coating technology is included, so that a deeper look can be had in the decision-making process while choosing a new process and/or coating. Both internal and external coaters are selected for the CED process, while only external EPS coaters will be examined. Table 1 and 2 present the full range of the selected coaters, the respective coatings and key pre-treatment steps that distinguish each coating process. The tables are purposely encoded, in order to prevent the leak of Brose internal manufacturing secrets.

Table 1. CED coated specimen codes, specific to selected coaters, with key coating

Specimen code	Coating brand name	Coating type	Degreasing	Phosphate	Follow-up treatment	Components	Binder	Pigments
COB	AQUA-EC 3000 AS	CED Epoxy System	Alkaline + Acidic	Iron phosphate	None	Epoxy resin: 90 % Dibismuth trioxide: 1% Soot: 9%	RESL - 90384	8A36-97457
COV	Powercron 6000	CED Epoxy System	Alkaline + Acidic	Iron phosphate	None	Polyurethane resin: 88 % Dioctyltin oxide: 1 % Kaolin: 10 % Soot: 1 %	CR 691 K	CP 458A
LON	AQUA-EC 3000 AM	CED Epoxy System	Alkaline + Acidic	Iron phosphate	None	Epoxy resin: 90% Dibismuth trioxide: 1% Soot: 9%	EK-2150	6292347
QUA	Cathoguard 960s	CED Epoxy System	Alkaline + Acidic	Iron phosphate	None	Polyurethane resin: 83 % Kaolin: 11,5 % Soot: 1,5 % Bismuth: 1,5 % Barium sulfate: 2 %	QT38-9962	QT37-9960
C	Framecoat II	CED Epoxy System	Alkaline	Tricationic phosphate (Zn, Ni, Mg)	Passivation	Polyurethane resin: 88 % Dioctyltin oxide: 2 % Kaolin: 9 % Soot: 1 %	MR2200	MP3200
F	Powercron 6200 HE	CED Epoxy System	Alkaline	Tectalis Nanoceramic	None	Polyurethane resin: 90 % Dioctyltin oxide: 1 % Kaolin: 8 % Soot: 1 %	CR 693	CP 523 F
J	590-534	CED Epoxy System	Alkaline	Tricationic phosphate (Zn, Ni, Mg)	Passivation	Polyurethane resin: 84 % Dioctyltin oxide: 1 % Kaolin: 13 % Soot: 2 %	One component product CF590-534	
P	Powercron 6100 HE	CED Epoxy System	Alkaline	Tricationic phosphate (Zn, Ni, Mg)	None	N.A.	CR 681	CP 524

Table 2. Powder coated specimen codes, specific to selected coaters, with key coating process

Specimen	Coating	Coating type	Degreasing	Phosphate	Follow-up treatment	Components
Zn_EXP	PE55	Epoxy-Polyester Powder coating	Alkaline	Tricationic phosphate (Zn, Ni, Mg)	Passivation	Polyester resin: 34 - 40 % Epoxy resin: 22 - 28 % Calcium carbonate: 32 - 38 % Other additives: 1 - 4 %
Zn_G Al_G			Alkaline	Tricationic phosphate (Zn, Ni, Mg)	Passivation	
Zn_L Al_L			Alkaline	Tricationic phosphate (Zn, Ni, Mg)	None	
Zn_EP Al_EP	EP5000	Epoxy-Polyester Powder coating	Acidic	Iron phosphate	Oxsilan passivation	Epoxy resin: 41 - 46 % Polyester resin: 32 - 37 % Calcium carbonate: 10 - 12 % Other additives: 1 - 4 %
Zn_EN Al_EN	EN155G	Epoxy-Polyester Powder coating	Acidic	Iron phosphate	Oxsilan passivation	Polyester resin: 36 - 40 % Epoxy resin: 23 - 27 % Calcium carbonate: 36 - 39 % Other additives: 1 - 4 %

3.6.1. Customer requirements

Setting the laws and regulations aside, the final entity, which determines a specific quality of a product, is the customer. When developing a new product or rehashing old ones, customers compile a bundle of specification documents with all the corresponding drawings and product description. Somewhere, in this sea of documents, corrosion resistance requirements are clearly mentioned, most commonly in form of an internal customer standard. Those standards include all of the required test methods for any particular corrosion protection systems. Although addressed in the internal standards, accelerated corrosion tests often refer to familiar ISO or VDA standards for the matching test method.

At this point, the matter or corrosion protection seems to be completely outlined, but the test durations and the evaluation criteria are not considered yet. Most customers have their own demands in that respect, together with prescribed evaluation data ranges, which have to be met. Therefore, these evaluation factors vary across the board. The evaluation criteria are also mostly based on the part position in the car. Parts that are on the inside, generally have reduced testing times and less strict criteria compared to the parts on the outside.

In hopes to summarize all customer standards and have a collective overview of the testing methods, durations and evaluation criteria, Brose composed two principal internal standards. One for powder coated parts (BN 587000-112) and one for CED parts (BN 562161-107). This effort was a step in the right direction, but it could not quite unite every single customer requirement.

An additional effort of unifying the customer standards has been made as a part of this thesis. While the data for all tests and subsequent evaluation has been compiled, no single duration or evaluation standard for accelerated corrosion tests could replace all customer demands simultaneously. Resulting was the conclusion that Brose would either have to know the capabilities of all utilized coating processes, unite them in the Brose standards, and offer the products with predetermined properties to customers. The second option would be to cater to each customer separately, as is the common practice at this time.

3.6.2. Acquisition of the new chamber

With the constant development of technology, new testing methods are slowly being integrated in the previously mentioned customer standards. The new tests apply different stresses to the coatings in hopes to make the resulting corrosion damage more analogous to real-life corrosion and reduce testing times. The effects of those stresses differ vastly from the ones in already established accelerated corrosion tests and should be examined thoroughly.

It is obvious that Brose must test their parts according to those new tests and document the outcome in order to sell products that are satisfactory to the customers. Consequently, the company invested in a new climatic-test chamber, "HKS 700", which can carry out virtually any standardized accelerated corrosion test (Figure 8).

Figure 8. "HKS 700"climatic test chamber

The practicality to have one machine, which can run a plethora of different tests on demand, is undeniable. Moreover, Brose can now test their parts according to the contemporary VDA 233-102 test, as well as the Volvo and Ford tests with shower phases.

As an integral part of the thesis, the new VDA 233-102 climatic- test has to be examined and characterized. Since the chamber is new, its functionality also has to be verified in a series of tests. Subsequently, the coatings have to be tested in the new chamber and the results compared with the already standard climatic-tests.

4. Experimental details

From figures 1 and 2, as well as the description of the chosen car parts it is clear that their size and geometry are complex and differ from each other. Through years of experience, Brose materials laboratory has detected differences in corrosion formation and the degree of corrosion resulting just from the shape variables of observed parts and their placement within the climatic test chambers. Furthermore, this claim was confirmed in 2009 by Helena Mick in her master's thesis, where she described those effects in detail. In order to characterize and evaluate just the selected coatings and coating processes, this known effects have to be eliminated. Therefore, instead of the mentioned parts, standardized specimens[5] will be used in the tests. The specimen materials as well as the coating process and the coating itself corresponds to those of the described parts. By using specimens, some influential, but unwanted variables can be eliminated to ensure a more objective examination. Furthermore, the testing can be made more extensive due to the compact size of the specimens.

This chapter will focus on the groundwork for the experimental execution as well as substrate[6] and specimen characterization. The possible effects of the chosen substrates on the coatings will be examined and explained. Furthermore, the evaluation methods for the specimens after the accelerated corrosion tests will be specified. Lastly, initial values of the key specimen characteristics will be defined, in order to have a reference point for the upcoming evaluation.

[5]Specimen – an individual coated piece used as a representative example of its type for scientific study

[6]Substrate – a material with defined geometry and composition on which the coatings are deposited

4.1. Substrate characterisation

As already mentioned in the previous part, coated specimens will be used for the testing instead of actual car parts. In order to stay true to the original parts, the chosen substrates are virtually identical to those of the parts. The selected coatings will be applied to three different substrates; steel, hot dip galvanized steel and aluminium, all from the company "Chemetall". Displayed in figure 9, "Gardobond OC" stands for the steel substrates, "Gardobond HDG 6 "for the hot-dip galvanized steel substrates and "Gardobod AA6014/2" for the aluminium substrates shown in figure 9. The chosen substrates have a rectangular shape, 190 mm long, 105 mm wide and 0,8 mm thick, the only exception being the aluminium substrate with 1.2 mm of thickness. All substrates also have two holes, one in the bottom and one in the top, in order to be adequate for various coating methods.

Figure 9. The chosen substrates from the company "Chemetall"

Just like the car parts, the substrates are manufactured by shearing the shape out of a continuous metal coil with the help of a punch and a die. The process of shearing is already established in the automotive industry and its many variations are well described. Generally, it is carried out in a press where a sheet of metal is placed on a die. While the blank holder immobilizes the sheet, the punch cuts the metal with a high shearing force around the die. Shearing is characterized by low costs, high productivity and the ability to be automatized. Figure 10 shows the shearing process with its distinctive edge formation [13].

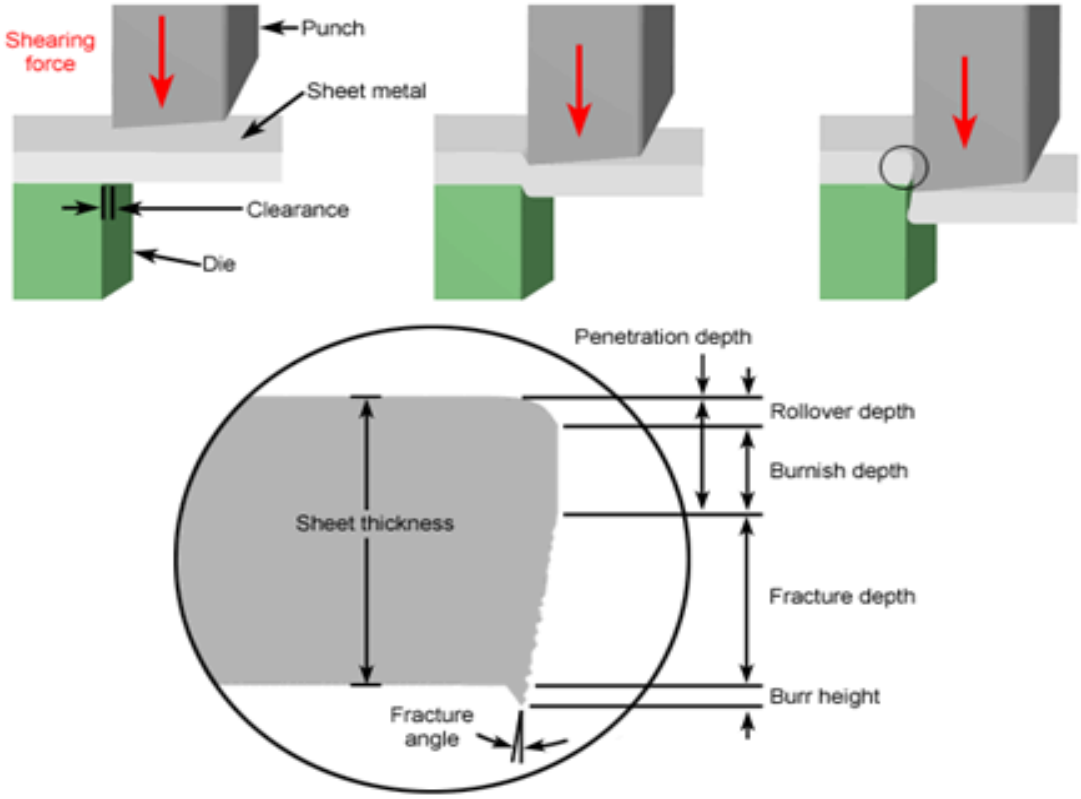

Figure 10. Sheet metal shearing process with shearing surface details [36]

The edge of the substrate has a couple of distinct areas after the shearing, the burnished and the fractured surface, the same is true for the two punched holes. The properties of the punched edge depend on the material type, the punching tool and used parameters. The proportion of the smooth and rough part varies, as well as the roughness itself. This critical area will be further examined in order to make conclusions about the specimen placement in the accelerated corrosion tests. Moreover, these findings might affect the evaluation of the specimens after the tests.

4.1.1. Materialographic sample preparation

While metallography uses microscopic methods to study the structure and components of metals exclusively, materialography is a broader term, in which all material groups are included. In order to perform any materialographic examination a specific sample preparation procedure must take place [14]. The sample preparation starts by addressing the size of parts or specimens, to be examined, which are usually too big to fit under any microscope. After the samples have been cut to form and embedded, the observed surface can be prepared by grinding and polishing. The most important thing to keep in mind during sample preparation is that the sample is representative of the whole part or that it displays the individual properties in a representative way. This ensures that valid conclusions can be drawn from the sample.

Separating defines any process by which a representative sample is separated from the starting part. Saws that operate in dry or wet conditions are usually the tool of choice for this step. Dry cutting is used when the sample should not be affected by the coolant, although wet cutting typically produces higher quality cuts with better properties of the separating surfaces. When separating a sample, additional care should be had with clamping the parts in place, as not to damage the future sample in any way. Depending on the choice of the tool, the cutting edges may display a certain degree of burr or heat effected area. These effects are always unwanted and have to be eliminated from the sample. The edges usually undergo a rough grind right after cutting to minimize those effects and enable better positioning during the follow-up embedding process.

Embedding or mounting is a process in which the samples are braced in a polymer mass. As a result, the rounding of the samples edges is minimized, and they become much easier to handle in the following steps. The former is extremely important when examining thin coatings on metal substrates because there is no potential warping of the coated edges. Mounting is also necessary when an automated grinding and polishing machine is used to enable safe gripping of the samples. The choice of the embedding material, usually polymer granulate, also has a big impact on the final sample. The polymers come in many colours, which effect the visibility of the edge and can have additional properties like electrical conductivity for Scanning Electron Microscopy.

Grinding and polishing is the last step in the materialographic sample preparation. It is carried out after the embedded samples have cooled and hardened. The process can be done either manually or by using an automated machine. The manual grinding and polishing can yield better

result, depending heavily on the operator, while the automated process has a greater throughput and a more uniform quality. Grinding starts at smaller grits, which indicate the roughness of the grinding paper. In gradual steps, it moves upwards from those small grits until a satisfactory grind has been achieved. The whole process can end at that point if there is no need for polishing.

Polishing uses even smaller abrasive particles, mixed together with a lubricant to give a mirror like finish to a metal surface. Since those particles are mixed within a suspension, polishing is considered a water free step. Having a water free polishing and cleaning step is especially important to preserve the look and shape of thin zinc layers, which tend to react unfavourably when exposed to water.

4.1.2. Sample preparation steps

The substrate and specimen samples will first be separated by a band saw, after which an automated wet abrasive chop saw will be used for a more precise cut. The burrs will be removed by wet grinding the edges with an 80-grit grinding paper.

The samples will then be mounted using a “Struers CitoPress” mounting press. White “IsoFast” granulate from “Struers” will be used as the mounting polymer. The white colour of the polymer will provide a great contrast to the black coatings, which have to be clearly visible.

The embedded samples (Figure 11) will be ground in a “Struers Tegramin” automated grinding and polishing machine. The last grinding step will be at 4000 grit, after which a manual water free polishing step at 1 micrometre will follow.

Figure 11. Embedded specimen samples for optical microscopy

Optical microscopy is a widespread method of producing a magnified image of an examined sample area. The magnification is a result of series of lenses being aligned in the objective and ocular [15]. By having an enlarged picture of the substrate surface and the coatings, statements about coating thickness, adhesion and any imperfections can be made.

"Zeiss SmartZoom" and "Zeiss" optical microscope will be used to examine the embedded samples and give clear statements about the state of the edges and the coating surface. The same devices will be used to characterize the scribing tools and edge optimization properties of select coatings.

Scanning electron microscope (SEM) produces images of a sample by scanning the surface with a focused beam of electrons. The electrons interact with the atoms on the surface and produce signals that contain valuable information about the surface topography and even the composition of the sample. SEM can achieve greater magnifications than optical microscopes and provide additional data about the sample, which otherwise might have been overseen [16]. "Zeiss EVO MA 25" SEM will be used to examine additional properties of substrate and specimen samples.

4.1.3. Substrate assessment

The edges of all substrates are first examined with "Zeiss SmartZoom" with a 150x magnification. The distinct shearing zones can be seen with a problem as shown in figure 12.

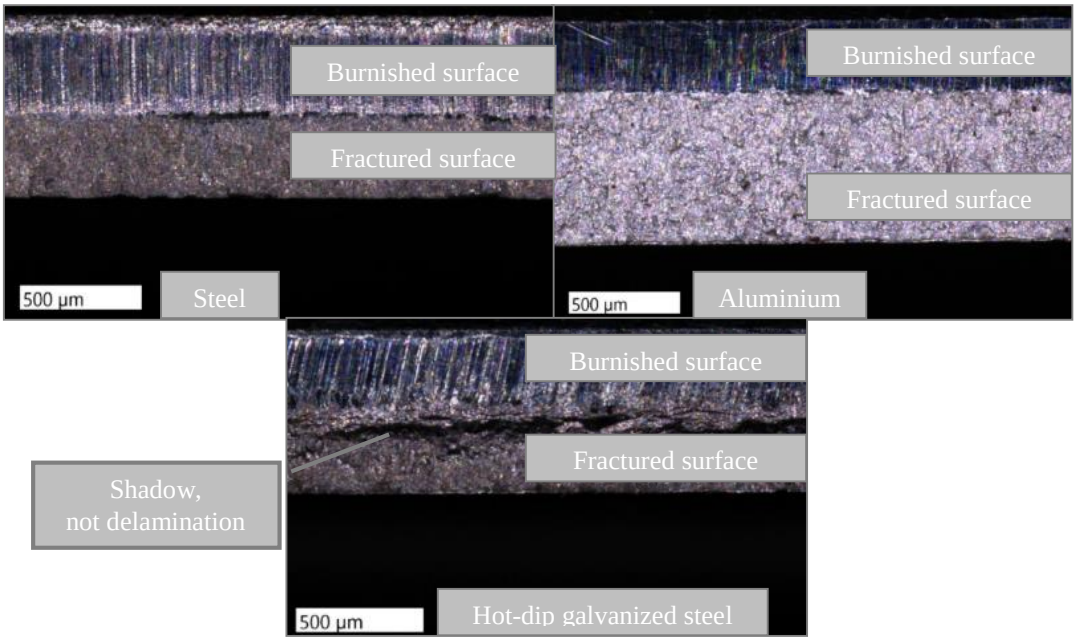

Figure 12. Substrate edges with two distinct shearing surfaces

The proportion of the burnished and fractured surface varies for each substrate, but no detrimental defects, such as flaking, or delamination are detected.

Upon further optical examination, it is clear that the shearing process was carried out in two separate motions. First the long side of the substrate was separated and then the shorter side. Therefore, the corners of the specimens are also examined, as the only area of the specimen where this shearing phenomenon is visible. For the vast majority of the assessed substrates, the cut is made in the same direction (Figure 13 b), but there were some seemingly random outliers too (Figure 13 a).

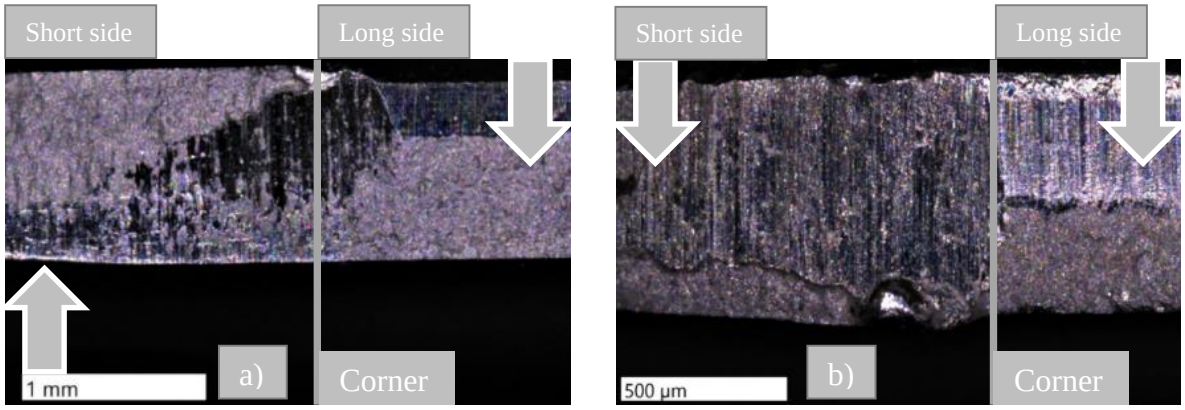

Figure 13. a) shearing process in opposite directions b) shearing process in the same direction

To further investigate the edges of the substrates, cross-section samples were prepared as described in the previous section. When examined with an optical microscope, the samples reveal another problematic area of the edge. A sharp bur is formed alongside the substrates as a result of the shearing process (Figure 14).

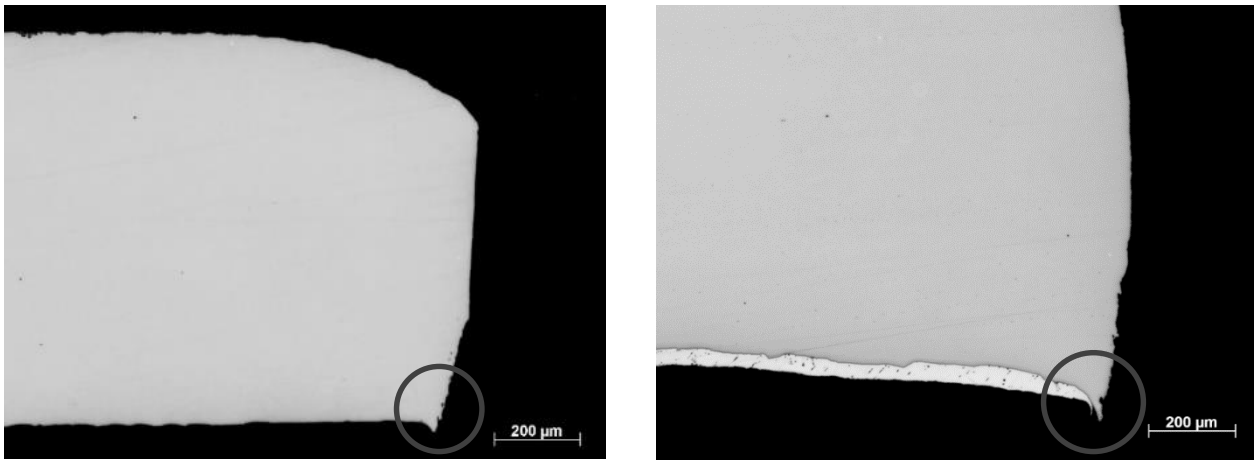

Figure 14. Cross-section substrate samples, a) steel substrate with burr b) hot-dip galvanized steel substrate with burr

Specimen characterisation

In order to differentiate from coating specific properties and substrate influences, the coated specimens also have to be examined. It is critical to discover the potential failure areas of coatings in order to have a consistent evaluation process. As a result, some areas of the specimens may be excluded from the evaluation.

4.2.1. Edges and holes

The edges and holes of the substrates present the most challenging area for any coating to cover fully. Responsible for that are the fractured surfaces and the burrs from the shearing process. While organic coatings and the selected coating processes can coat almost any surface, crevice and complex geometries, the coating might be much thinner at those critical points. The roughness of the fractured surface effects the coating thickness negatively, while the thin, razor sharp line of the burr prevents coating deposition altogether [17].

For optimal corrosion protection, it is imperative that minimal coting thickness, specified by the coating manufacturer or coater, is met. While this issue could be addressed by increasing the coating thickness altogether, economic aspects force the coaters to apply coatings in the lower acceptable range of the coating thickness. Many coating manufacturers have addressed this issue by adding additives that promote extra coating build-up around edges. The success of those additives is still limited because of the overall dependence on the coating thickness for absolute coverage.

The holes of the specimens can additionally suffer from adhesion and coating thickness problems resulting from the coating process itself. In both CED and powder coating, the specimens are suspended from the holes in specialized carriers. Throughout the CED pre-treatment process the carriers shield the holes from jets of washing and degreasing fluid, which makes them relatively dirty in comparison to the substrate surface. As a result, the coating cannot adhere fully to the surface around the hole, which makes that area more susceptible to any kind of corrosion attack. During the powder coating process, the carrier might interfere with the deposition of the powder, which usually leads to a decreased coating thickness around that hole.

4.2.2. Specimen assessment

The edges of the CED and powder coated specimens were examined using optical microscopy and SEM. Cross section samples were prepared following the method described in part 4.1.2.

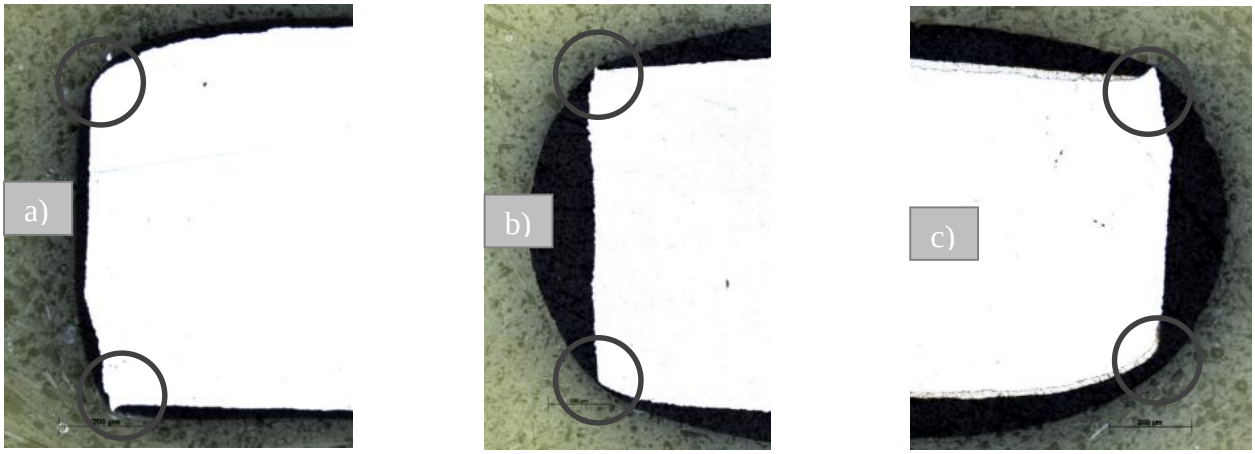

Figure 15. Cross-section specimen samples, a) CED coated specimen b) Powder coated specimen (aluminium substrate) c) Powder coated specimen (hot-dip galvanized steel substrate)

The marked areas in figure 15 show reduced coating thickness on the edges of the specimens. The sharp burrs in some specimens even protrude out of the coating. SEM comparison images of the edges with burrs can be seen in figure 16.

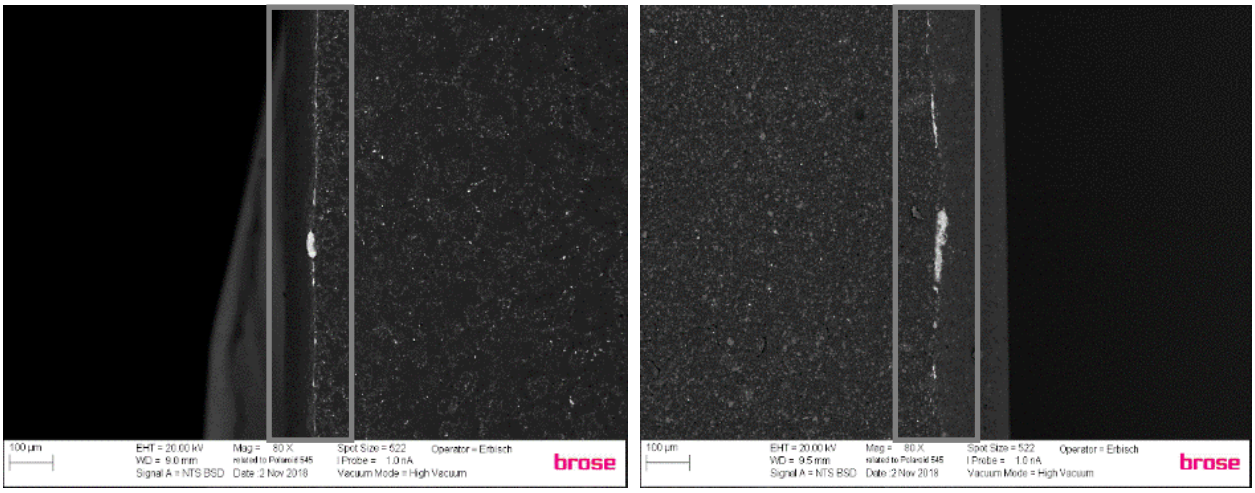

Figure 16. SEM pictures of specimen edges with the burr

It is evident that one side of the specimens would be more prone to corrosion, simply because the edges are not fully protected by the coating.

These findings could lead to complications and mischaracterization of the coatings at the examination level. At this point, a decision was made regarding the placement and examination of

the specimens. In the accelerated corrosion tests, the specimens will be placed in such way that the attacked surface is the one without the burr. Consequently, the examined surface and edge will be the ones without the burr.

As described in the previous part, the holes of the substrates are very unreliable regarding the protection properties of coatings. Therefore, the holes of the specimens, as well as the area around the holes will also be excluded from the examination. This decision was made in an attempt to make the testing more consistent, in order for the results to be coating dependant and not caused by substrate characteristics.

4.2.3. Scribe lines on specimens

Scribe lines are geometrically defined scratches purposely introduced to a coated specimen prior to testing in accelerated corrosion tests. Scribe lines have to pierce the coating and expose the underlying metallic substrate to the surrounding medium. They are used to examine properties like the degree of corrosion and delamination around scribe marks [18].

Having to comply to customer standards, Brose materials laboratory generally utilizes one of three standardized scribing tools. The scribing pen with the tip according to van Laar, the handcutter 428 with the tip according to Clemen and scribing stylus with the tip according to Sikkens. These scribing tools are shown in figure 17.

Figure 17. Scribing tools with respective scribing tips a) Sikkens b) Clemen c) Van Laar

All three comply with the standard for the introduction of scribe marks trough coatings (EN ISO 17872), where a scribe width of 0,2 to 1 millimetre as well as the ability to pierce the coating layer are prescribed.

4.2.4. Scribing experiment

Prior to the accelerated corrosion testing, a decision has to be made, which scribe tool is going to be used for the purposes of scribing the specimens for this thesis. In order to have exemplary scribing results, new tips are inserted in every tool. Every specimen will have three parallel scribe lines, each from a different tool (Figure 18). All lines have sufficient spacing between them to prevent any interference. The line marked with 1 is made with the Sikkens tool, line 2 is made with the Clemen tool and line 3 with the van Laar pen. This order of the scribe lines will remain the same for the entire scribe experiment.

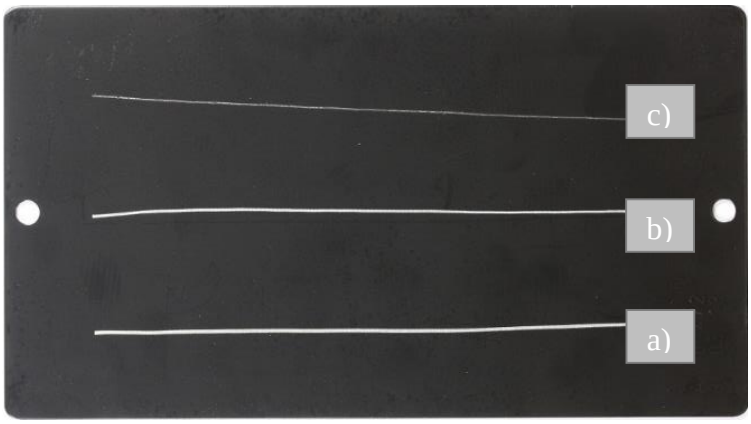

Figure 18. Scribe lines on a CED coated specimen, made with standardized tools a) Sikkens b) Clemen c) van Laar

In the next step, representative crosscut samples are made from scribed specimens in order to define the scribe marks from a different perspective (Figure 19).

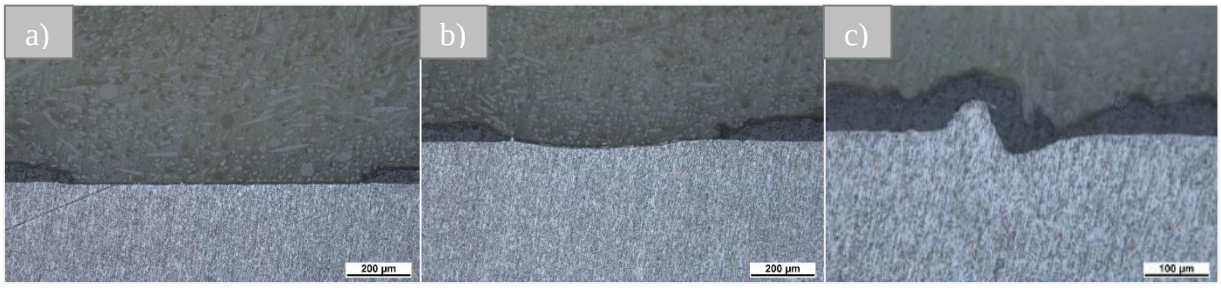

Figure 19. Cross section samples of the scribe lines a)Sikkens b) Clemen c) van Laar

The tip according to Sikkens leaves a one millimetre wide scribe line with the substrate fully exposed across the whole surface. The tip according to Clemen, leaves a slightly narrower U shaped groove, while the van Laar pen makes a slightly angled V shaped groove. The angle of the groove is most likely connected to the nature of handling the tool like a pen, when scribing. Peculiarly, the groove made by the van Laar pen is seemingly filled with the coating of the specimens. This appearance, together with the other scribe lines will be additionally examined in the SEM (Figure 20).

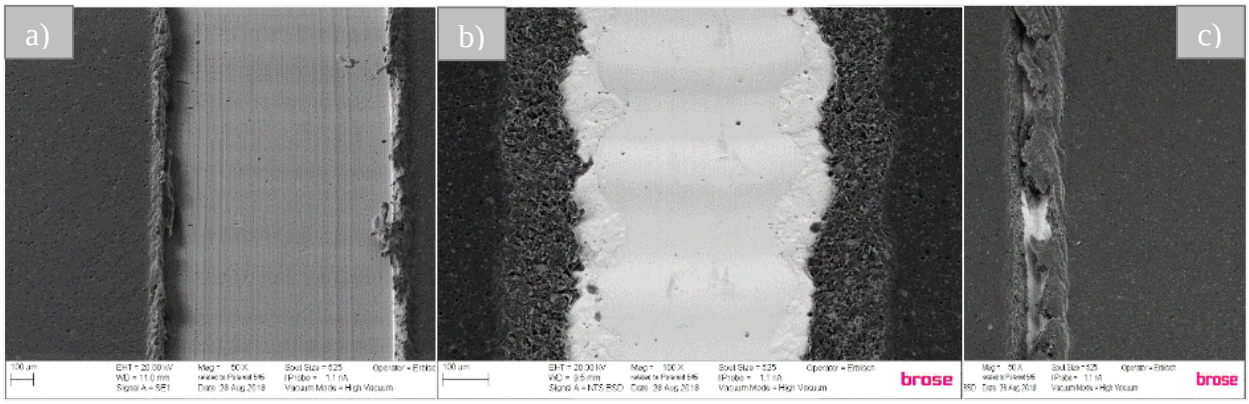

Figure 20. SEM images of scribe lines on a hot-dip galvanized steel powder coated specimen a) Sikkens b) Clemen c) van Laar

The SEM images uncover an interesting phenomenon when it comes to the scribing pen. On the powder coated specimens, the coating is pierced from one side resulting in leftover, loose coating remains from the other side. The remains are left above the scribe line, like an umbrella protecting the exposed surface. This finding would explain why the scribe lines were full of coating in the optical microscopy samples. The leftover coating was simply pressed into the groove under the influence of high pressure and temperature during the embedding process.

As the final part of this experiment, three CED and three powder coated specimens, each with scribe lines from all three tools, are stress tested for 480 hours in the neutral salt spray test. The powder coated aluminium substrates did not show any degree of delamination, thus they are excluded from the examination. In contrast, steel and hot-dip galvanized steel specimens exhibit a substantial amount of corrosion and delamination around the scribe lines (Figure 21). The choice of the scribing tool seemingly has a big effect on the powder coated specimens. The Sikkens and Clemen tools show identical degrees of corrosion and delamination (Figure 21 a and b), while the scribe made with the van Laar pen looks almost pristine (Figure 21 c). This can be explained by

the smaller surface which the pen exposes as well as the umbrella effect of the coating as seen in the SEM pictures.

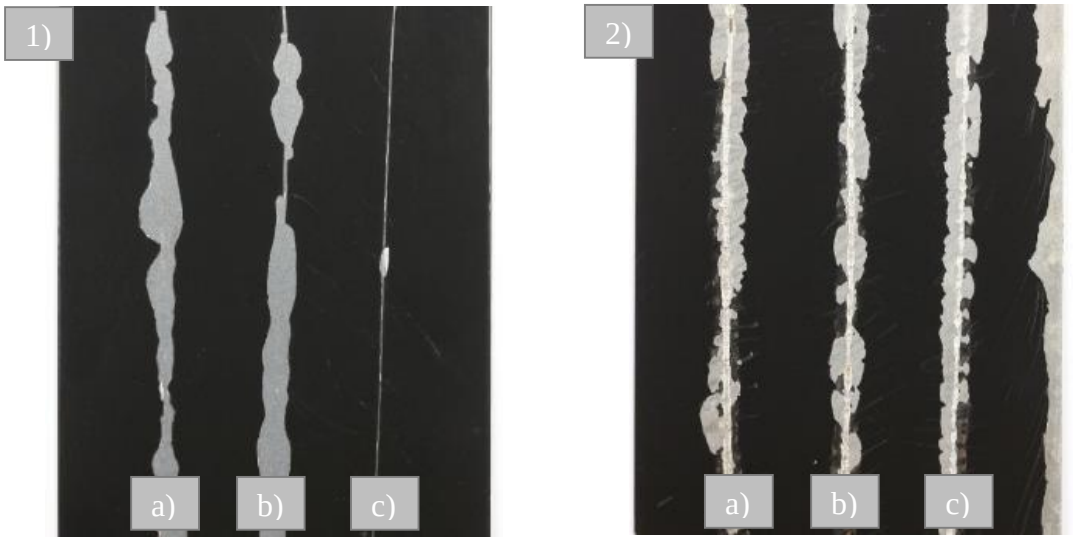

Figure 21. Degree of delamination around different scribe lines after 480 hours of NSS test 1) Powder coated hot-dip galvanized steel substrate 2) CED coated steel substrate, with matching scribe lines a)Sikkens b)Clemen c) van Laar

Resulting from this experiment is the choice of the scribing tool. Although Clemen and Sikkens make similar scribes with identical corrosion and delamination effects, for the purpose of this thesis the Sikkens tool was chosen. The stylus according to Sikkens is far more practical to use on even surfaces because of the implemented guiding wheel. The scribe lines can be reproduced more easily and should be more consistent across all specimens. The Clemen tool is generally more versatile and practical to use on actual car parts as it does not require a flat surface to operate on. As for the van Laar pen, the validity and the cases for implementation should be thoroughly examined, as it does not show the same extent of corrosion damage around a scribe on powder coated specimens, compared to other tools.

4.3. Evaluation criteria

A repeating theme trough the previous parts are the customer standards and requirements Brose has to adhere to in order to deliver satisfactory product quality. This is no different for the evaluation criteria of the parts and specimens. The customers, besides demanding certain climatic tests, also prescribe evaluation methods and criteria for those tests.

Having no reason to neglect the customer demands, the evaluation criteria are selected from a pool of customers. Even though all of the evaluation methods are standardized, custom ratings will be applied for some of them. Every evaluation procedure will be carried out as uniformly as possible, in order to have consistent results. In specific cases, a colleague with superior experience in the field will serve as council for the evaluation and subsequent conclusion.

The evaluation will take place after a 24-hour conditioning period at standard atmospheric conditions, but all unusual findings will be noted directly after the test. Overview pictures of whole specimens will be taken before and after the evaluation.

4.3.1. Degree of rusting on surface and edges according to DIN EN ISO 4628-3

The degree of rusting will be determined separately on the surface and on the edges of the specimens. Both surface and edge corrosion will be judged in percentages instead of the predetermined grading system described in the standard. The standardized grades, which range only from 0 to 5, are based on predetermined degree of rusting values which are not flexible [19]. This might conceal some subtle differences between the specimens.

It is important to say that same specimens may have faulty areas, most likely due to transportation. Those will be marked beforehand and not taken into consideration when judging the degree of rust after the tests. The area around the edges and holes will also be excluded, as those are problematic areas. The same is true for the edges. All edges facing up in the tests will be evaluated, and the ones on the backside excluded (Figure 22).

The degree of rusting on hot-dip galvanized steel specimens will exclusively refer to white rust (zinc corrosion). Should those specimens exhibit any degree of red rust (steel corrosion), this will be mentioned separately.

Figure 22. Example specimens with marked areas, which are excluded from the degree of rusting evaluation

4.3.2. Degree of delamination and corrosion around a scribe according to DIN EN ISO 4628-8

Scribe lines leave the surface of the specimen unprotected by the coating, exposing an ideal place for a corrosion attack in accelerated corrosion tests. While in those tests, corrosion can attack the substrate in different ways, depending on the type of the substrate and the corrosive medium or intermittent cycles. Scribe lines are used to compare this phenomenon among the specimens while various conclusions can be made as why that happened. This degree of delamination and corrosion around a scribe line is standardized in the DIN EN ISO 4628-8.

After a predetermined testing time, corrosion products are formed around the scribe line, causing the loss of adhesion between the coating and substrate. To measure the degree of this damage, loose corrosion products, together with the coating, are removed from the scribe with a

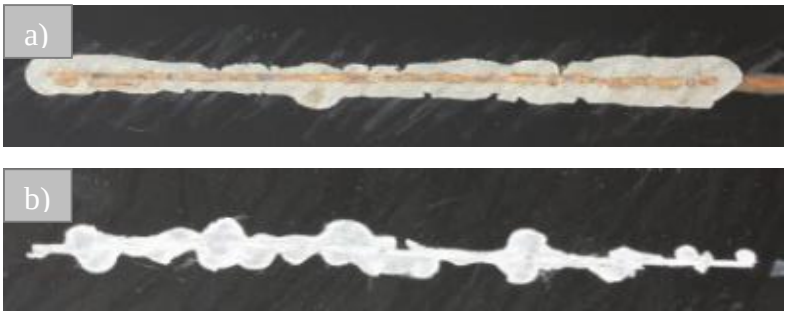

Figure 23. Typical delamination patterns on a) CED and b) powder coated specimens

scalpel, to expose the delaminated area (Figure 23). The delaminated area is then measured with a ruler in six different points, which are about 10 mm apart from each other. Upper- and lowermost areas of the scribe line are excluded from the evaluation.

The measured values are rounded to 0,5 mm and with the help of equation 1, the average width of the delaminated area is calculated.

$$d_1 = \frac{a + b + c + d + e + f}{6} \quad (1)$$

Where d_1 is the arithmetic mean of the measured points in millimetre and *a*, *b*, *c*, *d*, *e*, *f* are the individual measurements in millimetre. The delamination value is then calculated according to equation 2.

$$d = \frac{d_1 - w}{2} \quad (2)$$

Where *d* is the delamination in millimetre and *w* is the width of the scribe line, in this case one millimetre.

Following the standard, one scribe mark parallel to the long edge will be made on the steel and hot dip galvanized steel substrates (Figure 24 a). The scribe must be drawn at least 20 millimetres from the top, bottom and side edges of the specimen. Aluminium specimens will receive two scribes, one parallel and one vertical to the longer edge, as prescribed in the standard

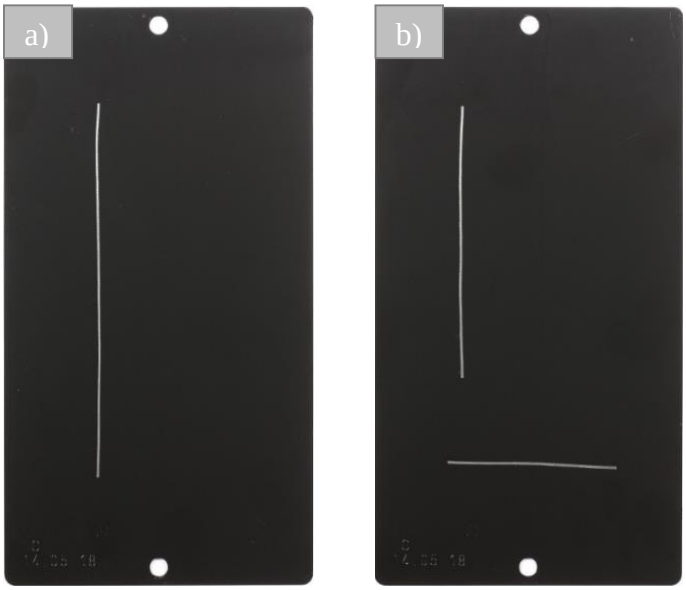

Figure 24. Sample scribe lines on a) steel and hot-dip galvanized steel specimens and b) aluminium specimens

(Figure 24 b). The same rule for the distance applies here too; the scribes must be at least 20 millimetres from the edges and each other [20].

For simplicity purposes, the degree of corrosion and delamination around a scribe will be described just as delamination in some cases.

4.3.3. Cross cut test according to DIN EN ISO 2409

The cross cut test is a method for determining the level of adhesion between a coating and a substrate. This examination can be carried out before any other testing, in order to measure the coating adhesion in its initial state. The same can be executed after accelerated corrosion tests, to determine if the adhesion was influenced by those tests.

Figure 25. Cross cut tool with brush and magnifying glass from „Erichsen“

The test is carried out by a specialized tool from the company “Erichsen” (Figure 25), which makes six parallel lines in one pull. The magnifying glass is used for the evaluation, while the brush can be used to remove excess coating remains after cutting. Six parallel lines are cut into the specimen, piercing the coating all the way to the substrate. Another six lines, at a 90° angle, cross those lines, resulting in 25 square shaped tiles (Figure 26) [21].

Depending on the coating thickness, varying spacing between those lines are used. The standard for CED coatings, or up to 60 micrometres coating thickness is a 1 mm gap. For powder coatings, typically 60 to 120 micrometres coating thickness, a 2 mm gap is used.

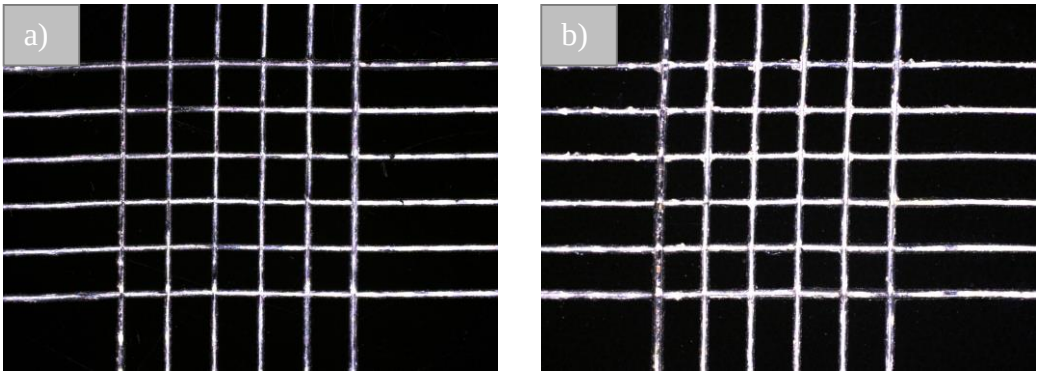

Figure 26. Sample cross cut hatches on CED coated specimens a) grade 0 b) grade 1 (1 mm spacing between the grooves)

In the continuation, an adjustment is made for powder coatings which coating thickness is less than 60 µm. Those coatings were randomly tested with both 1 and 2 mm gap cross cut. The results of both cross cuts on those specimens were continuously the same.

For the evaluation, any loose flakes of the coating are removed by gently adhering and pulling off a standardized adhesive tape. The area is then examined with a magnifying glass and compared to sample cross cut pictures in the standard with matching grades from 0 to 5. Grade 0 is the best possible grade, indicating exceptional adhesion, while grade 5 indicates a high degree of delamination from the cross cut.

4.3.4. Degree of blistering according to DIN EN ISO 4628-2

As described in the theoretical part, corrosion can take place under an intact coating too. For this to occur, a small amount of electrolyte must penetrate the coating trough diffusion pathways and reach the surface of the substrate. Corrosion under an organic coating most commonly manifests as blistering on the surface of specimens or parts. Meaning that the degree of blistering is a measurement of a coatings permeability to the exposed medium.

The degree of blistering will be examined on the same surface as the degree of rusting, neglecting the edges and holes of the specimen. The same is true for all of the marked faulty areas. Degree of blistering is determined by comparing the surface with the reference pictures in the standard (Figure 27) [22].

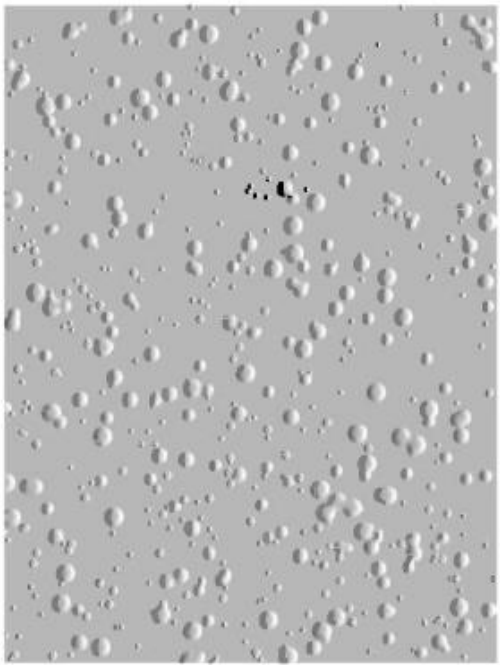

Figure 27. Example picture for degree of blistering evaluation, grade 4(S4) [22]

4.3.5. Daimler scratch test according to DBL 7382

This is a specific test enforced by the customer Daimler. The test is another method for determining the adhesion between a coating and a substrate. The test can be carried out both prior and after accelerated corrosion tests. The initial test grade can then be compared to the grade after testing to determine if any decrease in adhesion occurred. The test is carried out by a special knife prescribed by Daimler (Figure 28).

Figure 28. “Wolfcraft” knife used to scratch the specimen surface

The coating is scratched by holding the blade vertical to the substrate surface and pulling it while simultaneously pressing down. The resulting scratch is then graded from K0 to K5 according to the descriptions in the DBL standard [23]. Figure 29 depicts the first four grades of the scratch test.

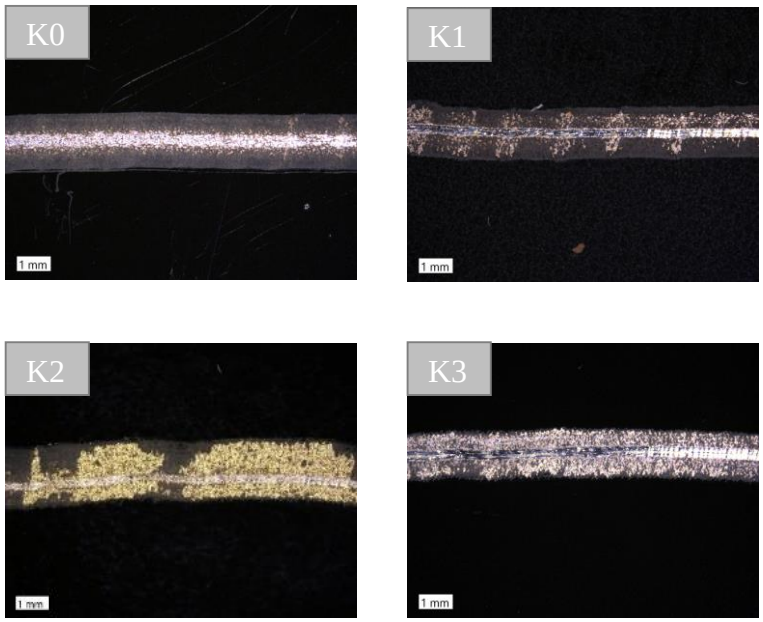

Figure 29. Scratch marks on CED specimens with matching scratch test grades K0, K1, K2, K3

Grade K0 describes the best possible adhesion between the substrate surface and the coating, while grade K5 stands for the worst possible adhesion. This test is appropriate for coatings with relatively low coating thicknesses, as it requires the tester to scratch the coating uniformly across the length of the scratch. From the initial trials, this has proven to be very difficult for powder coatings, with a coating thickness greater than 60 µm. In those cases, the coating is not scratched, but pulled by the knife, resulting in bunching and breaking of the coating. The interpretation of these results is difficult and inconsistent, as they can only be compared to written descriptions from the standard. Therefore, the Daimler scratch test will only be carried out on CED coated specimens.

4.4. Initial specimen properties

Taking an overview picture before starting any testing is common practice in engineering, the same applies to climatic tests. The initial values of evaluation criteria have to be established, in order to be able to compare the differences after those tests. Other initial values are there to characterize the properties of coatings and serve as confirmation that the coating process was successful, i.e. coating thickness.

4.4.1. Coating thickness

As one of key characteristics of any coating or coating system, coating thickness directly influences the protection properties for the underlying substrate. Coating manufacturers usually specify a range for coating thickness, in which the coating is working as intended without any shortcomings. For a satisfactory quality of products, coaters have to abide by those specifications, which proves to be difficult in some cases. Economic reasons force the coaters to apply as little coating as possible, while still being in the acceptable range [17]. This can lead to insufficient coating thickness on specific areas of products or specimens, resulting in reduced corrosion protection properties.

Figure 30. „Dualscope MP 40“coating thickness measuring device with a) ferrous substrate probe b) aluminium substrate probe

In this specific case, the acceptable range for CED coatings, defined in the BN 562161-107, is 15 µm to 30 µm. For powder coatings, the range is set much higher, from 40 µm to 120 µm, as defined in BN 587000-112. Coating thickness of the specimens will be measured with "Dualscope MP 40" measuring device (Figure 30), based on the magnetic induction principle.

Coating thickness is measured at five points on two random specimens for every coating variant, within the grey area indicated in figure 30. Measurements on two separate specimens are made in order to better approximate the average coating thickness across all specimens. Conflictingly, this slightly increased the scattering of the coating thickness, indicated with error bars in the following charts. Figure 31 shows the average coating thickness of CED coated specimens, where the green area indicates the acceptable coating thickness range prescribed in the Brose standard.

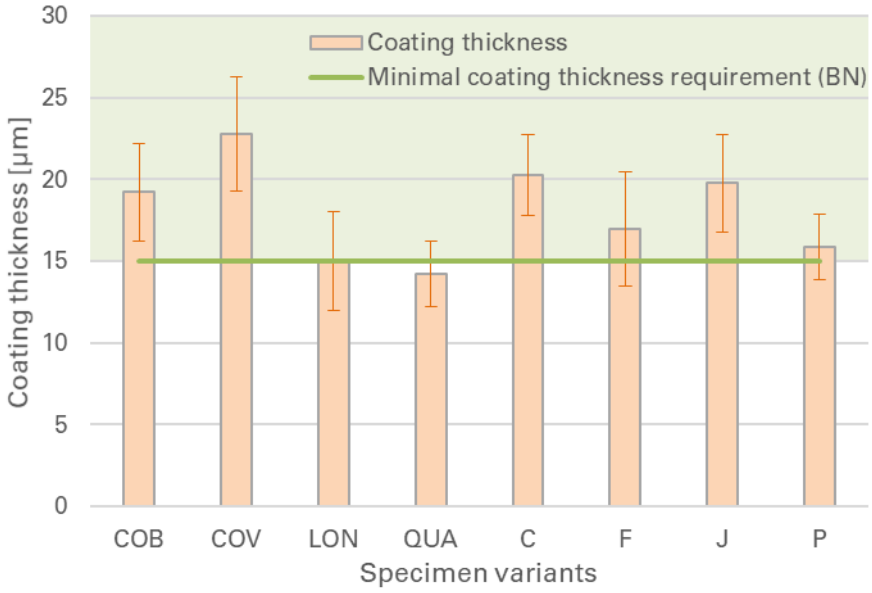

Figure 31. Average coating thickness of CED coated specimens (error bars indicate scattering)

Evident from figure 31, average coating thickness of specimen QUA is below the minimal coating thickness requirement prescribed in the Brose standard. Measured coating thickness on specimens LON, F and P is also below the requirement at some points.

Figure 32 displays the average coating thickness of powder coated specimens, where the green area indicates the acceptable coating thickness range prescribed in the Brose standard.

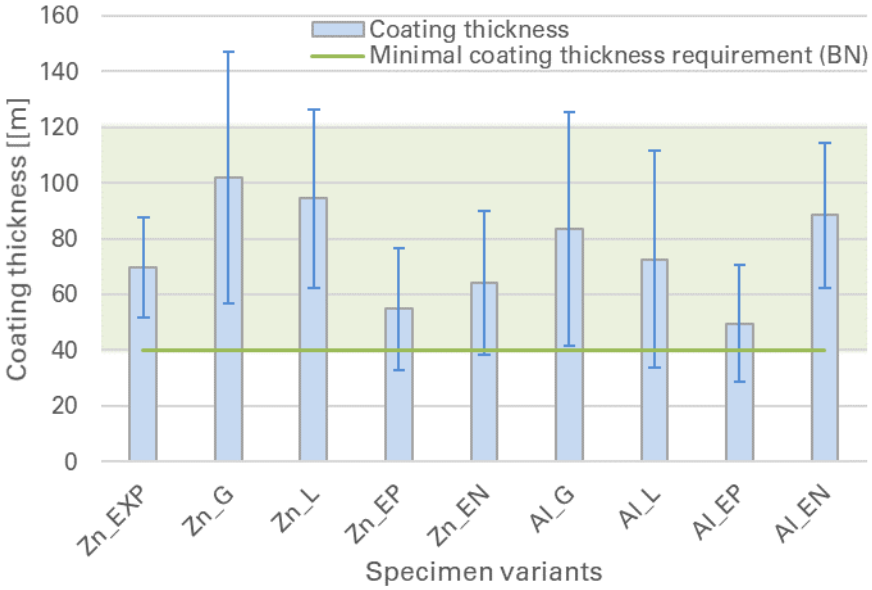

Figure 32. Average coating thickness of powder coated specimens (error bars indicate scattering)

The average coating thickness value of all measured powder coatings is within the acceptable range defined in the Brose standard. However, specimens Zn_EP and Al_EP exhibit borderline coating thickness values, with multiple measured points below 40 µm.

4.4.2. Daimler scratch test

Apparent from the description of the scratch test, the evaluation of the scratches is somewhat subjective, as there are not comparison images in the standard. Therefore, the resulting values are depicted in a range of grades, where a single grade could not be determined. Additionally, some specimens exhibit varying scratch test results when tested across the whole surface. The same range of grades is used to describe those specimens, i.e. COB and COV from figure 33.

Figure 33 displays the initial scratch test grades on CED coated specimens. Defined in the Brose standard BN 562161-107, the maximal acceptable scratch test grade is K2, both in the initial state of parts and specimens and after accelerated corrosion tests. For the initial evaluation, five

scratch lines are made on two separate specimens for each specimen variant. In its initial state, all specimens received a grade within the acceptable range.

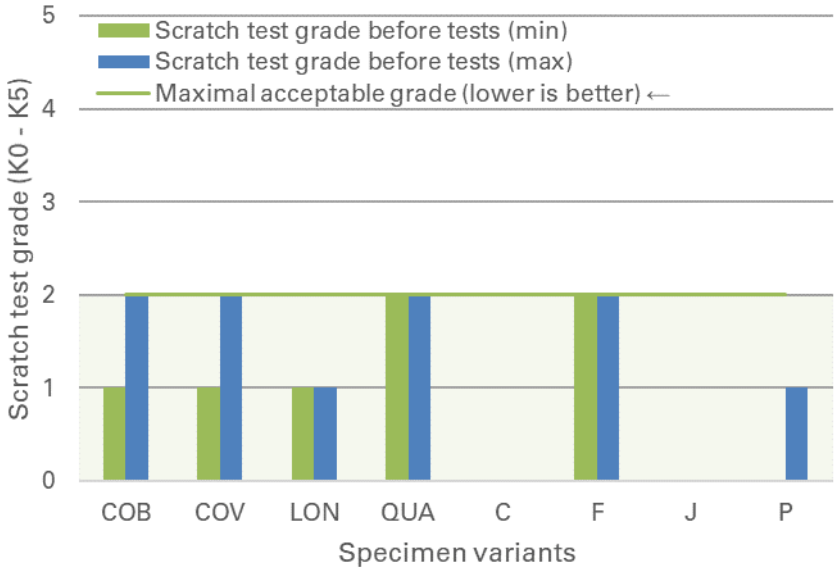

Figure 33. Initial scratch test grades on CED coated specimens

4.4.3. Cross cut test

Initial cross cut test grades are shown in table 3 and 4 for CED and powder coated specimens. The grades were established by carrying out two cross cut tests on one specimen for each specimen variant. The only outlier is specimen QUA, where one of the cross cut tests exhibited a grade of 1. This value is still within the acceptable range, 0 to 1, defined in the Brose standard.

Table 3. Initial cross cut test grades for CED coated specimens

CED coated specimens	Cross cut test grade
COB	0
COV	0
LON	0
QUA	0-1
C	0
F	0
J	0
P	0

Table 4. Initial cross cut test grades for powder coated specimens

Powder coated specimens	Cross cut test grade
Zn_EXP	0
Zn_G	0
Zn_L	0
Zn_EP	0
Zn_EN	0
Al_G	0
Al_L	0
Al_EP	0
Al_EN	0

5. Experimental methods

Organic coatings provide a long-lasting corrosion protection for metal substrates, which can span up to decades. Therefore, it is impossible to test the behaviour of a coating and its corrosion resistance properties to the full extent of its life-cycle. Moreover, a coating which is applied to a transportable object, like a car, will rarely be in contact with the same climatic conditions and medium for an extended period of time.

In hopes to have a consistent and objective testing method for the evaluation of coating properties, accelerated corrosion tests were developed. These tests are well defined in their respective standards and should be used as a valid and time saving method to examine the corrosion resistance of materials and coatings. The results of the accelerated corrosion tests can also be reproduced in certified laboratories all over in the world. Accelerated corrosion tests are now the go to method for part inspection in the automotive industry and will be utilized extensively in this thesis.

With the development of computers and specialized software technologies, new methods for electrochemical corrosion testing have emerged. Corrosion of metals is inherently an electrochemical process which can be observed and characterized from an electrochemical standpoint. With the introduction of potentiostats and galvanostats new ground-breaking advancements in the understanding of the mechanism of corrosion were made. Apart from being able to define all corrosion mechanisms, electrochemical methods offer a wide range of tests which can aid in material selection and corrosion resistance testing of coatings.

5.1. Accelerated corrosion tests

By definition, accelerated corrosion tests simulate conditions which cause an accelerated corrosion attack on specimens or parts. The tests are carried out in climatic chambers which operate under controlled parameters. All of the parameters are established in the respective standards for those tests. When executed correctly, accelerated corrosion tests should yield reproducible results, independent of any external influences.

Many standardised accelerated corrosion tests are currently in use, especially in the automotive industry. Car manufacturers rigorously test every part to in order to ensure their flawless functionality and prevent the onset of corrosion by choosing a suitable coating. Since the

same is true for car part manufacturers, Brose tests all their parts using contemporary accelerated corrosion tests. In this case, the tests are often prescribed by the customers, which demand a certain quality of product. Test durations, as well as evaluation criteria are also individualized according to specific customer requests.

After summarizing and categorizing all customer requirements, Brose materials laboratory found the following accelerated corrosion tests to be most relevant for their products:

-Condensation atmosphere with constant humidity according to DIN EN ISO 6270-2 (CH)

-Neutral salt spray test according to DIN EN ISO 9277 (NSS)

-Cyclic corrosion test according to DIN EN ISO 11997-1, Cycle-B

-Cyclic corrosion test according to PV 1210

Even though the tests are standardized, the durations and subsequent evaluation criteria are determined between the companies. The customers have their own idea of which duration particular parts should be subjected to, as well as the criteria, rather the extent of the corrosion damage caused by the tests.

The new climatic test, according to VDA 233-102 will also be described and compared to the standard tests in the following part.

5.1.1. Condensation atmosphere with constant humidity (CH) test according to DIN EN ISO 6270-2

The CH ("**CH test**" will be used when talking about the "Condensation atmosphere with constant humidity test") accelerated corrosion test simulates an extremely humid environment in combination with increased temperature (Figure 34). The warm and humid medium causes condensation on the specimens, which makes them absorb water. The corrosion stress on the specimens is mild but shows great results when testing the adhesion or blistering of organic coatings. The simulated stresses in this test do not represent realistic stresses that car parts are subjected to, but the corrosion resistance of coatings can be compared, since every specimen is exposed to the same stresses.

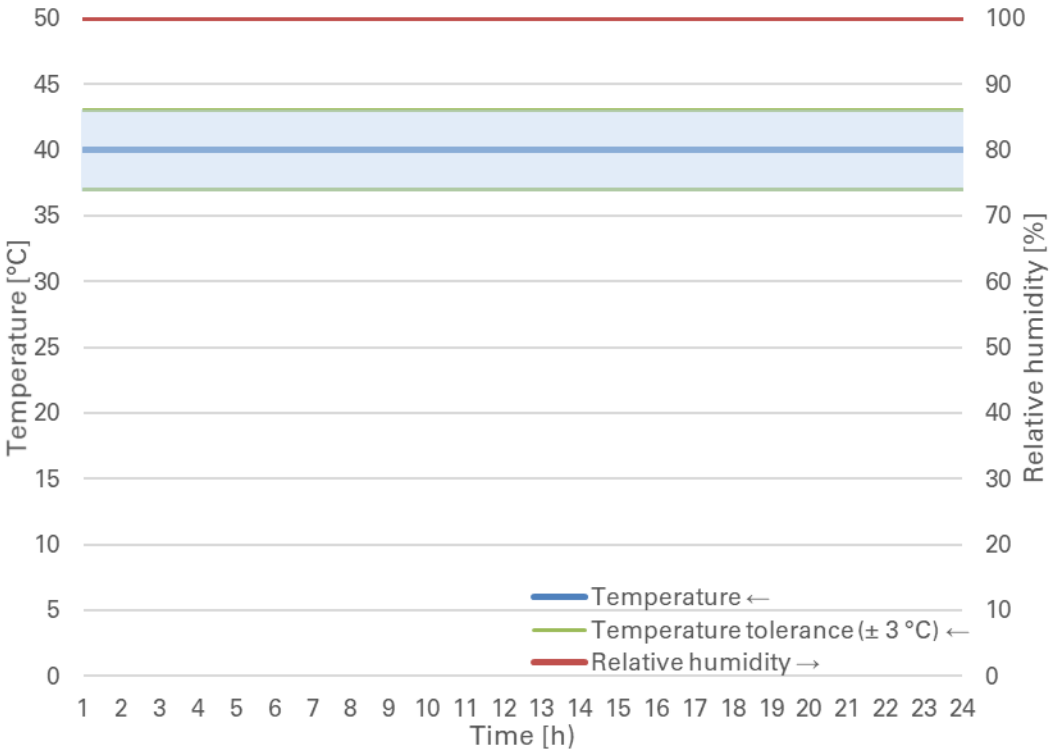

Figure 34. CH test operating parameters

The test is carried out in the "HK 400 M" climatic chamber. During the test, the bottom of the chamber is filled with at least 10 mm of deionized water. Specialized heaters raise and maintain the temperature at 40 °C. Water evaporates from the resulting heat but cannot exit the chamber, which makes the inside environment extremely humid. Condensation drops form on the surface of the specimens, as their temperature is lower than the surrounding temperature.

According to the standard the specimens are placed at least 100 mm from the chamber walls, 200 mm from the water surface and 20 mm from each other. It is also important to ensure that no condensate is dripping on the specimens during the test. The standard also prescribes, that the examined surface should be angled at 60° or greater to the horizontal plane [24]. Therefore, as the most practical solution, the specimens are hung from polymer rods by waxed strings, shown in figure 35.

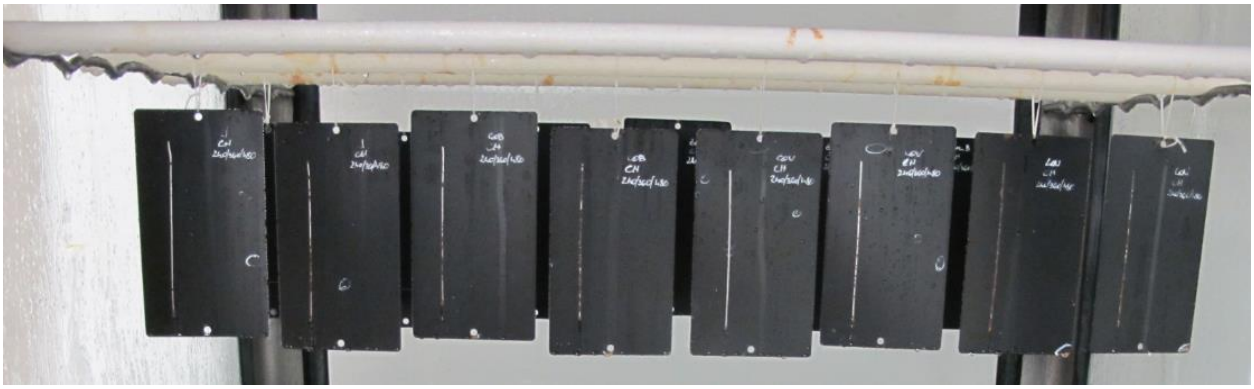

Figure 35. Placement of the specimens in the CH test chamber

The DIN EN ISO 6270-2 standard does not ask for nor define the scribing of the specimens, but for the sake of comparability with other tests, all of the specimens had scribe lines.

CH test at the Faculty of Mechanical Engineering and Naval Architecture in Zagreb

CH test for comparative purposes will also be carried out at the Laboratory for the protection of materials at Faculty of Mechanical engineering and Naval Architecture in Zagreb. The operating parameters of the CH climatic chamber are identical to the ones at the Brose laboratory. The only difference being the placement of the specimens. At the faculty, the specimens will be placed in polymer carriers, with the scribed surface facing upwards at a 70° angle from the horizontal plane, which also complies with the standard.

5.1.2. Neutral salt spray test (NSS) - DIN EN ISO 9277

The NSS ("**NSS test**" will be used when talking about the "Neutral salt spray test") test is yet another classic accelerated corrosion test in the automotive industry. The use of this test started in the 1940ies and is still prevalent today. In the NSS test, the parts are exposed to a 5 % sodium chloride solution mist at 35 °C (Figure 36).

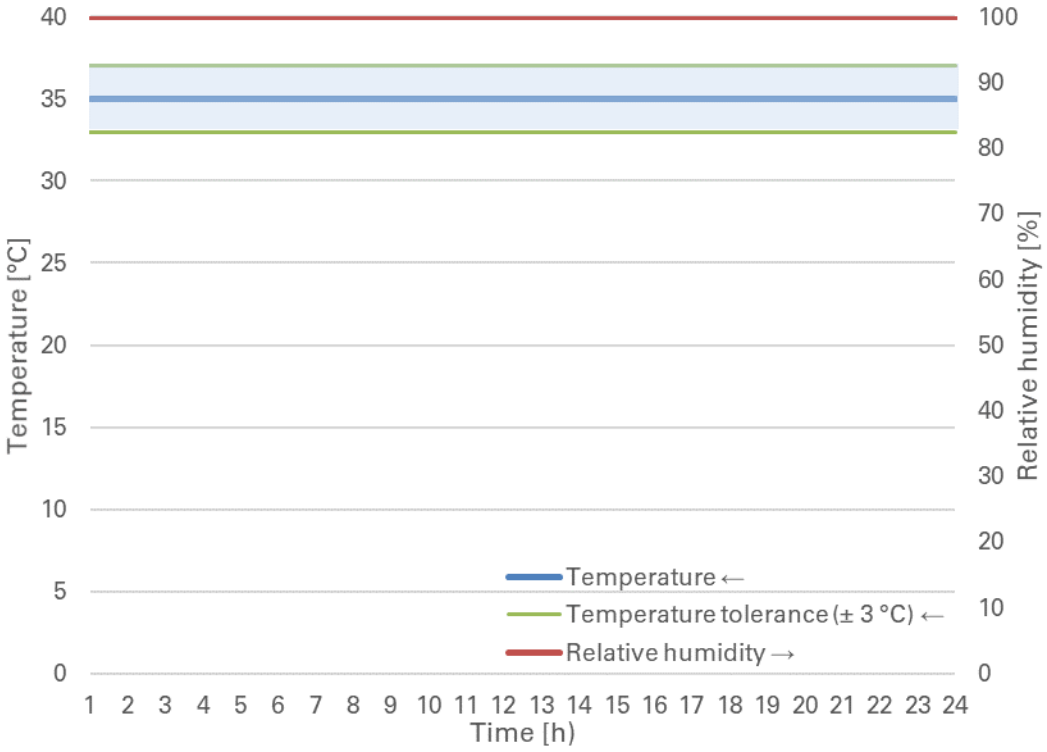

Figure 36. NSS test operating parameters

The NSS test is useful to find weaknesses, like pores and faulty areas, in metallic and organic coatings. The simulated stresses in this test do not represent realistic stresses that car parts are subjected to, but the corrosion resistance of coatings can be compared, since every specimen is exposed to the same stresses.

The test is carried out in the "HK 1000 M" climatic chamber. In addition to the chamber, the NSS test requires a container with a special salt water solution, as described in the standard. The relative density of the sodium chloride solution must be between 1,029 g/l and 1,036 g/l at 25 °C. The pH value must stay in the neutral range, form 6,5 pH to 7,2 pH at 25 °C. The properties of the sodium chloride mist in the chamber must mirror those of the solution in the tank. The amount of the sprayed mist is measured in two collecting containers, which have a collecting area

of 80 cm^2. The atomizer nozzles have to distribute one to two millilitres of the mist within an hour, uniformly across the whole chamber [25].

According to the standard, the specimens, with scribe lines, are place on specialized polymer carriers. When the carriers are placed in the chamber, none of the specimens can be in direct contact with the walls of the chamber, nor get hit directly by the spray beam from the nozzle. One side of the specimens is facing upwards at a 20° angle to the vertical plane, as shown in figure 37. The previously defined side with the burr is facing downwards in this case. The carriers also ensure that the specimens do not shield each other from the sprayed mist.

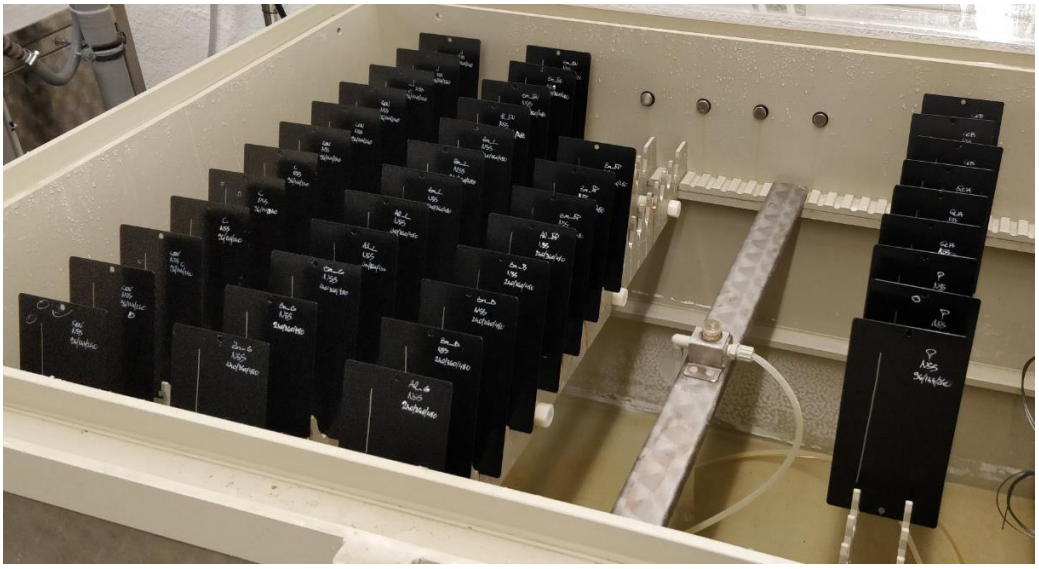

Figure 37. Placement of the specimens in the NSS test chamber

NSS test at the Faculty of Mechanical Engineering and Naval Architecture in Zagreb

NSS test for comparative purposes is also carried out at the Laboratory for the protection of materials in Zagreb. The test is operated according to DIN 50021 SS in a climatic chamber from the company "Ascott", but the parameters are identical to the ones in the DIN EN ISO 9277. The specimens are be placed in polymer carriers, with the scribed surface facing upwards at a 20° angle from the vertical plane.

5.1.3. Cyclic corrosion test according to DIN EN ISO 11997-1, Cycle-B

The Cycle-B ("**Cycle-B test**" will be used when talking about the "Cyclic corrosion test according to DIN EN ISO 11997-1, Cycle-B") test was developed to simulate the conditions a car part might encounter in its life cycle. It can also promote faster forming of corrosion in order to reduce testing times. The test is composed of three distinct phases, a wet salt spray phase, a constant humidity phase and a dry phase. Combined, these three phases form one cycle of testing which lasts for one week, as shown in figure 38. The cycle starts with a 24-hour salt spray phase, which is followed by four days of intermittent constant humidity and dry phase. It is concluded with a two-day dry phase, during which the specimens can be taken out for assessment. The solution and temperature for the salt spray phase are identical to the NSS test, with a 5% sodium chloride solution being sprayed at 35 °C. The constant humidity phase is also identical to the CH test. During the dry phase, the chamber operates at 25 °C and 50% relative humidity [26].

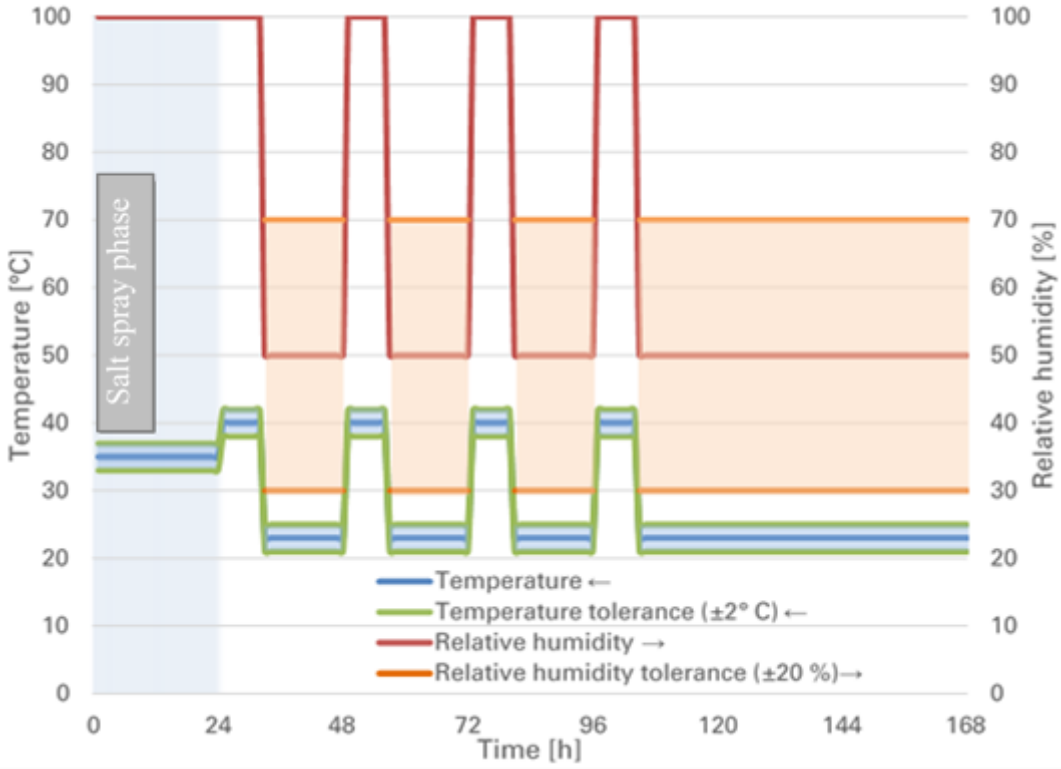

Figure 38. Cycle-B test operating parameters

The test is carried out in the "HKS 1000" climatic chamber. The specimens with scribe lines are placed in identical simple carriers as in the NSS test, with one side facing up at a 20° angle to the vertical plane (Figure 39). Just like it the NSS test, it is imperative that none of the specimens is hit by the direct spray beam of the nozzle during the salt spray phase and that no excess fluids drip directly onto the specimens.

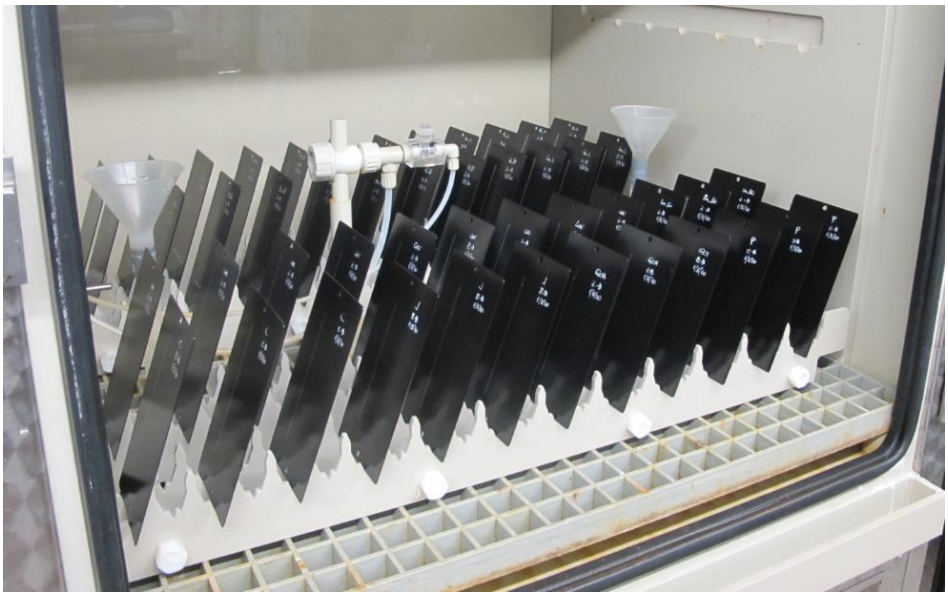

Figure 39. Placement of the specimens in the Cycle-B test chamber

5.1.4. Cyclic corrosion test according to PV 1210

The PV 1210 ("**PV 1210 test**" will be used when talking about the "Cyclic corrosion test according to PV 1210") test is an internal cyclic corrosion test designed and prescribed by the company Volkswagen. Similar to the Cycle-B test, it consists of three phases which are compounded to form one cycle. All of the phases are running within a 24-hour period for a total five days, after which a two-day resting period follows (Figure 40). This means that five cycles are completed after one week of testing [27].

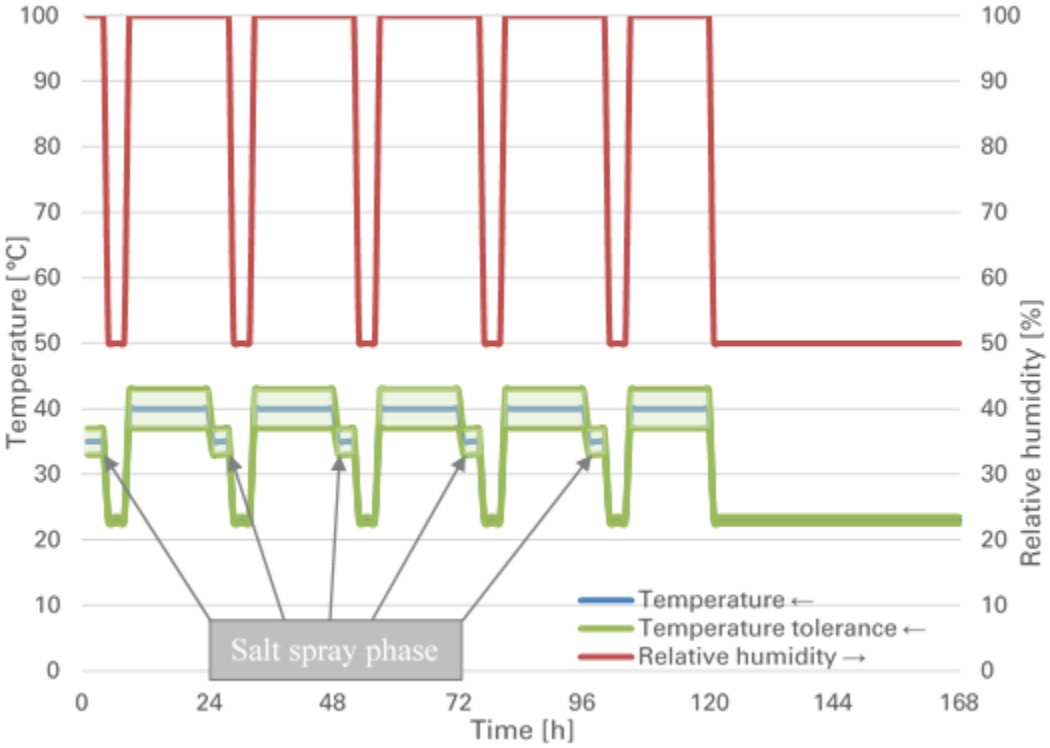

Figure 40. PV 1210 test operating parameters (humidity tolerance too narrow to bet indicated -1,5 %)

The salt spray phase is the same as the NSS test. The constant humidity phase is also identical to the CH test. The dry phase is carried out at 23 °C and 50% relative humidity, according to VW 50554-23/50, but with extremely narrow tolerances of just 0,5 °C for the temperature and 1,5% for the relative humidity.

The test is carried out in the “HKS 1000” climatic chamber. The sample carriers are identical to the ones used in the NSS and Cycle-B test (Figure 41).

Figure 41. Placement of the specimens in the PV 12010 test chamber

5.1.5. Cyclic corrosion test according to VDA 233-102

The VDA-new ("**VDA-new test**" will be used when talking about the "Cyclic corrosion test according to VDA 233-102") cyclic corrosion test has been created by the German Association of the automotive Industry, short VDA (Verband der Automobilindustrie), in cooperation with the steel and aluminium industry. The test is used for assessing the corrosion behaviour of blank metals, coated components or specimens and of adhesive coatings. In the focus of the test are delamination around a scribe mark, surface and edge corrosion as well as perforation corrosion in flanged areas.

The VDA-new test was design to mimic the harsh atmospheric conditions a car might encounter during its utilization and generate results, which correlate well with natural weathering. The corrosion patterns formed on steel, galvanized steel and aluminium after the test, should reflect real-life corrosion phenomena very closely (Figure 42) [28].

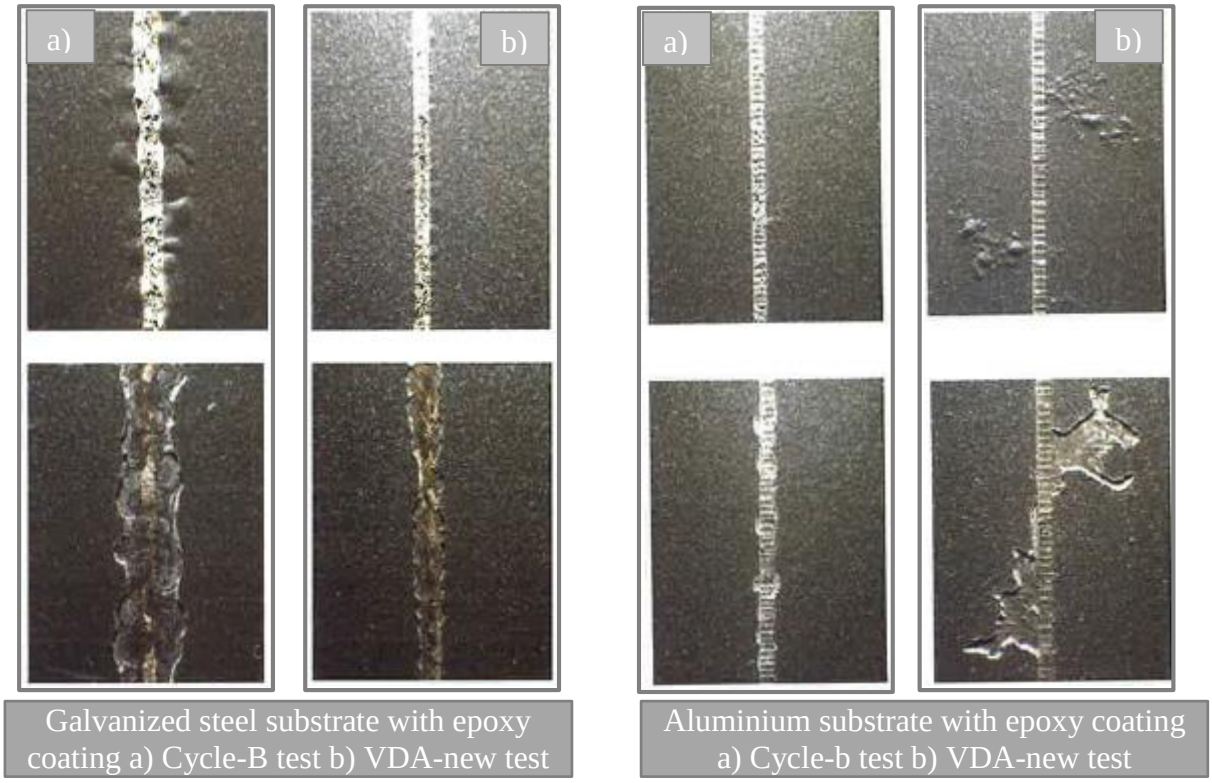

Figure 42. Comparison of the delamination around a scribe on galvanized steel and aluminium substrates in the Cycle-B and VDA-new test (upper images are before removing of the delaminated coating, bottom images are after removing of the delaminated coating [28]

The test should be carried out in an automatized combination chamber, which allows temperature, humidity and salt spray programming, so that all phases can be run with minimal disturbance.

Execution of the VDA-new test

The VDA-new test is carried out in the "HKS 700" cyclic corrosion chamber. In addition to the chamber, the test requires a container with a special 1% sodium chloride solution, as described in the standard. The relative density of the sodium chloride solution must be between 1,0045 g/l and 1,0055 g/l at 25 °C. The pH value must stay in the neutral range, form 6,5 pH to 7,2 pH at 25 °C. The properties of the sodium chloride mist in the chamber must mirror those of the solution in the tank. The amount of the sprayed mist is measured in two collecting containers, which have a collecting area of 80 cm^2. During the salt spray phase, the atomizer nozzles have to distribute two to four millilitres of the mist within an hour, uniformly across the whole chamber [29].

One cycle of the test takes one week to complete and consists of three different phases, which are repeated in the sequence shown in figure 43. All of the phases A, B, C, differ from the phases in previously described accelerated corrosion tests.

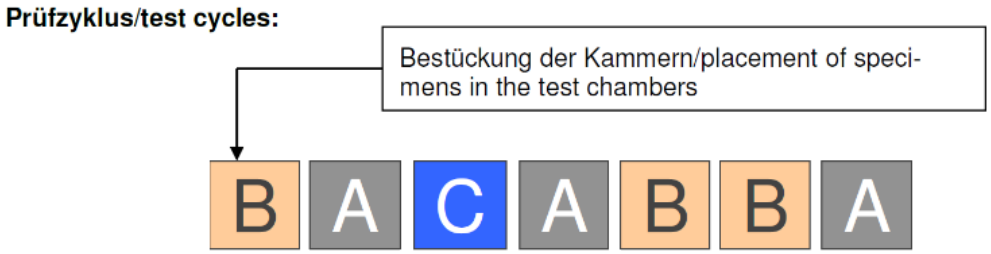

Figure 43. Arrangement of individual phases in one cycle of VDA-new test [29]

Phase A starts with a salt spray period of three hours, with the 1% sodium chloride solution. Shortly after the spraying the temperature ramps up from 35 °C to 50 °C (Figure 44).

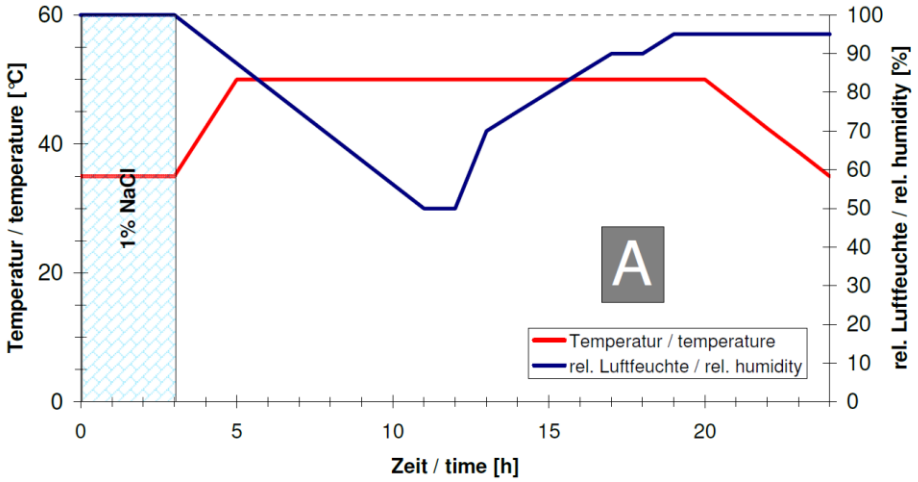

Figure 44. Graphical representation of phase A in the VDA-new test [29]

Phase B is similar to a dry phase but with custom-made temperature and humidity ramps, allowing for the opening of the chamber and specimen evaluation (Figure 45).

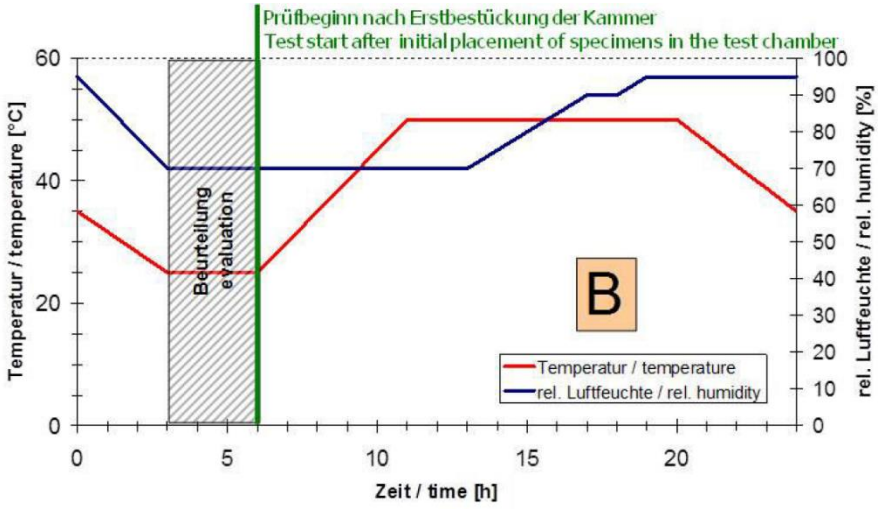

Figure 45. Graphical representation of phase B in the VDA-new test [29]

Phase C is entirely different from the others, because it includes a freezing period at -15 °C (Figure 46). This freezing period is the underlying characteristic of this test and should contribute to the most differences in corrosion formation in comparison to other climatic tests.

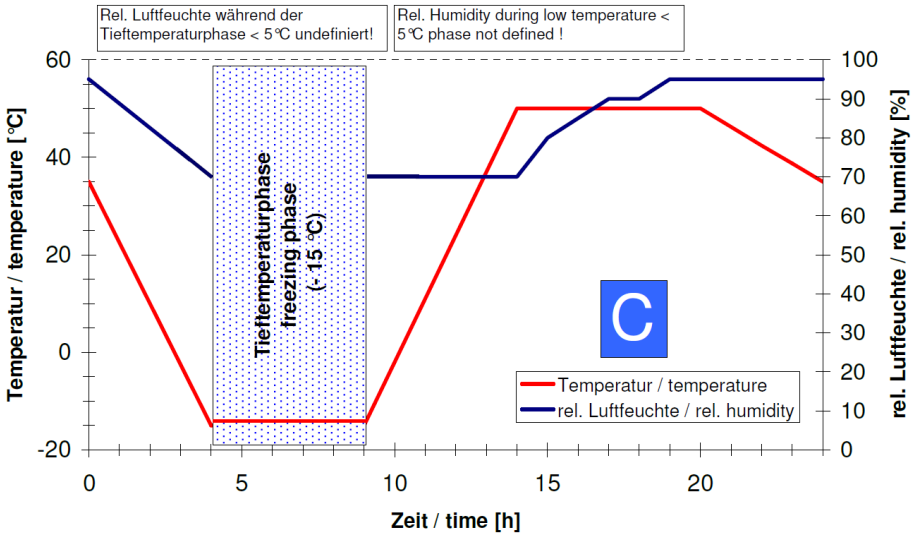

Figure 46. Graphical representation of phase C in the VDA-new test [29]

Specimens with scribe lines are placed in identical simple carriers as in the NSS test, with one side facing up at a 20° angle to the vertical plane (Figure 47).

Figure 47. Placement of the specimens in the VDA-new test chamber

Monitoring of the system

Since this is a completely new chamber installed in the Brose materials laboratory, the reproducibility of the VDA-new test has to be demonstrated. The applied method for corrosiveness evaluation via mass loss specimens is described in the DIN EN ISO 9227.

The mass loss specimens are CR4 steel plates, with the dimensions 150 mm x 70 mm x 1 mm, as defined in the ISO 3574. After thorough cleaning, measuring and weighing, the backside of the specimens is taped, in order to prevent corrosion. Then they are placed in the same polymer sample carriers as the coated specimens and have to undergo three cycles or three weeks of testing. After three weeks, the mass loss specimens are taken out of the chamber and all of the corrosion products are removed according to ISO 8407. This is achieved by pickling the specimens in a hydrochloric acid and hexamethylenetetramine solution for one hour and scraping the corrosion products off gently with wooden sticks (Figure 48).

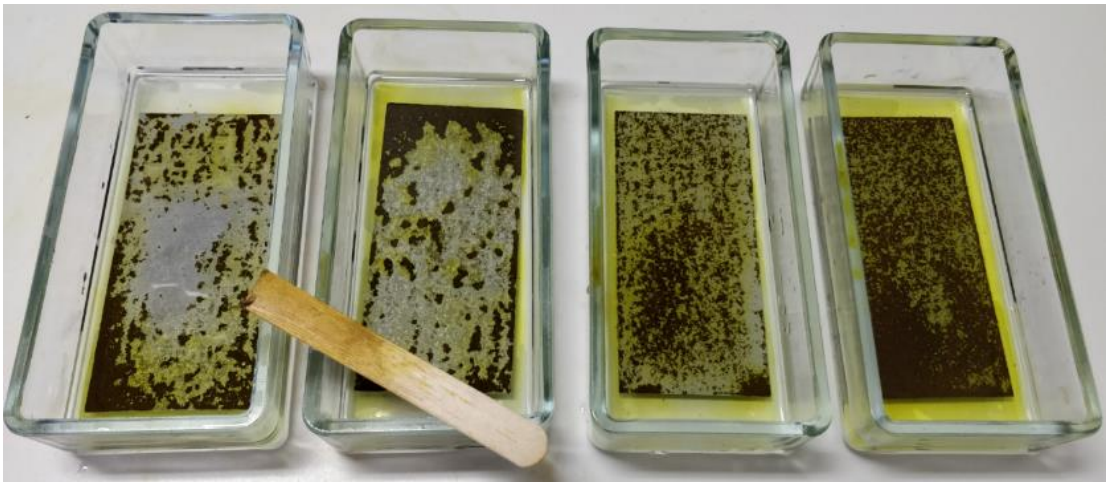

Figure 48. Mass loss specimens after the first layer of rust was removed

Since the specimens were weighed prior to the test, the mass loss is evaluated gravimetrically, by weighing them afterwards too. The difference in mass is divided by the exposed surface area in order to calculate mass loss in gram per square meter. If the average mass loss of the three of four specimens is within the tolerances, 680 g/m^2 to 1120 g/m^2, the test chamber is working satisfactory. The results of this test are in table 5.

Table 5. Measurements from steps in the corrosiveness experiment

Mass loss samples	Starting weight [g]	Weight after 3 cycles of VDA-new test [g]	Weight change [g]	Sample lenght [m]	Sample width [m]	Corroded surface [m^2]	Mass loss [g/m^2]	Average mass loss [g/m^2]
Sample 1	81,746	73,549	8,197	0,1499	0,0701	0,0105	**780,073**	**770,255**
Sample 2	81,876	73,443	8,433	0,1498	0,0701	0,0105	**803,297**	
Sample 3	82,106	74,456	7,650	0,1499	0,0702	0,0105	**727,395**	
Sample 4	81,987	74,939	7,048	0,1499	0,0701	0,0105	**670,919**	-

Sample 4 has been excluded from the final corrosiveness measurement because the exhibited mass loss was slightly below the tolerance defined in the standard. It is important to note that the corrosiveness of the chamber would have been within the tolerances even if the fourth sample were included in the calculation.

5.2. Electrochemical testing

The bulk of metal corrosion occurs by electrochemical reactions at the metal-electrolyte interface. In anodic reactions, metals are oxidized, releasing their electrons. The opposite takes place in the cathodic reaction, where the solution is reduced, removing electrons from the metal. Corrosion normally occurs at a rate determined by an equilibrium between the anodic and cathodic reactions. The net flow of electrons in each direction is balanced exactly at the equilibrium point, which results in a no net electron flow [30].

These reactions can be measured with a potentionstat, resulting in a Tafel plot (Figure 49). The curved line is the total current, the sum of the anodic and cathodic currents. The straight lines represent the extrapolated values for the anodic and cathodic reactions. The reaction changes from anodic to cathodic at the sharp point of the curved line, due to the logarithmic scale.

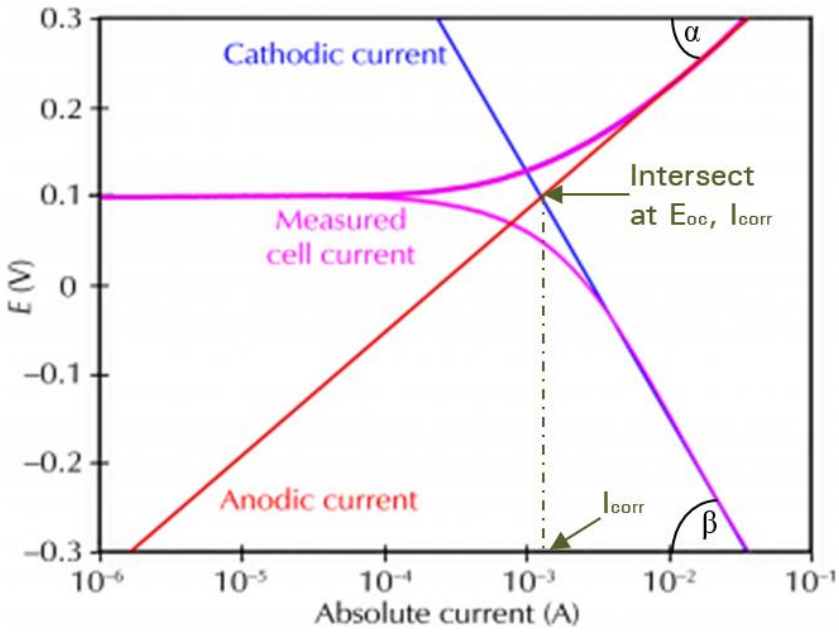

Figure 49. Sample Tafel plot with indicated E_{oc} and I_{corr} intersect [30]

The current from the anodic and cathodic reactions depends on the electrochemical potential of the metal. If too many electrons are released in the anodic reaction, the excess of electrons shifts the potential of the metal more negative, thus slowing the anodic reaction and speeding up the cathodic reaction. This equilibrium potential, where there is no electrical connection to the metal is called open circuit potential (E_{oc} or E_{corr}) and is usually measured before any electrochemical corrosion experiments. From the same figure 49, the value of the anodic or

cathodic current at E_{oc}, called corrosion current (I_{corr}) can be seen. By determining the I_{corr} one can calculate the corrosion rate of the metal [30].

The corrosion current is calculated with the help of the Stern-Geary equation 3:

$$I_{\mathrm{corr}} = \frac{\beta\mathrm{a} * \beta\mathrm{c}}{2.303 * (\beta\mathrm{a} * \beta\mathrm{c})} * (\frac{1}{R\mathrm{p}}) \quad (3)$$

Where I_{corr} is the corrosion current in [A], β_a is the anodic beta Tafel constant in [V/decade], β_c is the cathodic beta Tafel constant in [V/decade], R_p is the polarization resistance in [Ω].

The act of forcing the potential of the sample, in a solution, away from E_{oc} is called polarizing the sample. The response of the sample is measured in a polarized state and used to develop a model of the sample's corrosion behaviour. Polarization resistance is defined as an increased resistance to the flow of current in an electrochemical corrosion system. Meaning that high R_p of a metal implies high corrosion resistance and low R_p implies low corrosion resistance. It is usually measured in a separate experiment, where the cell voltage is swept over a small range of potential very near to E_{oc}. The numerical fit of the resulting curve yields a value for R_p, an important parameter in the calculation of the corrosion rate (Figure 50) [31].

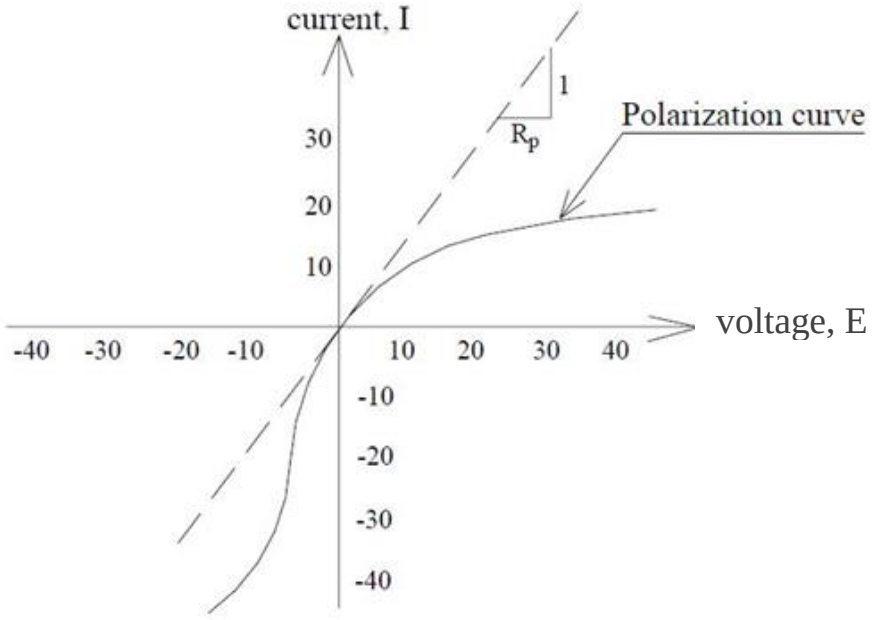

Figure 50. Sample polarization resistance curve, with a linear approximation line [37]

Once the current is known, it is easy to calculate the corrosion rate of materials with the following equation 4:

$$R_{\text{corr}} = \frac{I_{\text{corr}} * K * EW}{d * A} \quad (4)$$

Where R_{corr} is the corrosion rate in millimetres per year [mmpy], I_{corr} is the corrosion current in [A], K is a constant that defines the units for the corrosion rate, EW is the equivalent weight in [g], d is the density in [g/cm^3] and A is the sample area in cm^2.

In electrochemical tests, a sample with a small surface area of just a couple of square centimetres is sufficient to model its behaviour in a corrosive medium. The samples are immersed in a solution typical of the sample's exploitation environment together with additional electrodes. All of the submersed parts are then connected to a potentiostat. This device can change the potential of the sample in a controlled manner and draw a model for the sample's corrosion behaviour based on the generated electrical current response [30].

Electrochemical methods can capture a wide range of corrosion phenomena and have the ability to measure extremely low corrosion rates. These measurements are also relatively fast and reliable, corrosion measurement systems have become a standard in modern laboratories. Electrochemical impedance spectroscopy is one of the top methods to measure the protection properties of coatings.

5.2.1. Electrochemical impedance spectroscopy of organic coatings (EIS)

Electrochemical impedance spectroscopy measures the response of an electrode to a sinusoidal potential modulation at different frequencies. Those AC modulations can be superimposed either onto applied anodic or cathodic potential or onto open circuit potential. EIS is based on the Ohm`s law, where the resistance is defined as a ration between voltage *E* and current *I*, equation 5.

$$R = \frac{E}{I} \tag{5}$$

This well-known relationship is applicable to only one circuit element, the ideal resistor. In reality, there are many elements of a circuit that exhibit more complex behaviours. Therefore, the concept of resistance is exchanged with impedance. Impedance is also a measure of the ability to resist the flow of electrical current but is not limited by the properties of an ideal resistor [32].

Electrochemical impedance is measured by applying and AC potential to an electrochemical cell and measuring the current trough the cell. If a sinusoidal potential excitation is applied, the response is also a sinusoidal current signal with a phase shift shown in figure 51.

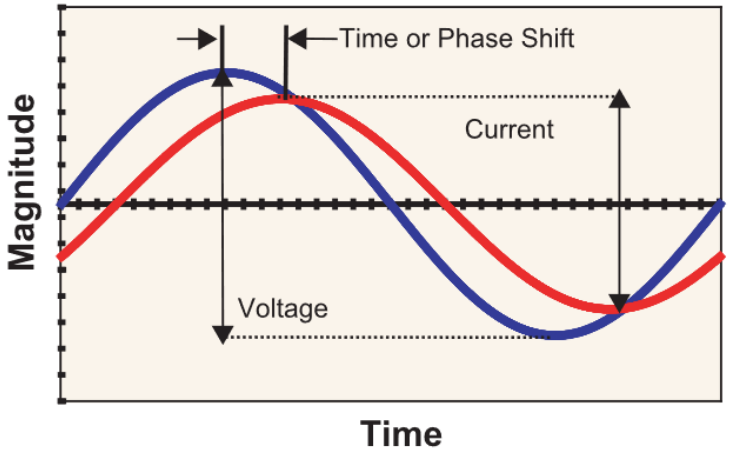

Figure 51. Sinusoidal excitation and response signals with a phase shift [33]

The excitation signal has the following form, equation 6:

$$E_t = E_0 sin(\omega t) \tag{6}$$

Where E_t is the potential at time t, E_0 is the amplitude of the signal, and ω is the radial frequency. Radial frequency ω (in radians/second) can be expressed in relation to frequency f (in Hz) with equation 7:

$$\omega = 2\pi f \tag{7}$$

The response signal I_t, in a liner system, has a different amplitude I_0 and is shifted in phase ϕ, using equation 8:

$$I_t = I_0 \sin(\omega t + \phi) \tag{8}$$

The impedance (Z) of the system can now be expressed analogous to Ohm`s law, using equation 9:

$$Z = \frac{E_t}{I_t} = \frac{E_0 sin(\omega t)}{I_0 sin(\omega t + \phi)} = Z_0 \frac{sin(\omega t)}{sin(\omega t + \phi)} \tag{9}$$

The impedance is expressed in terms of magnitude, Z_0 and a phase shift ϕ [32].

EIS data presentation

Prior to the availability of modern EIS instrumentation, impedance measurements were show as a "Lissajous figure" on oscilloscope screens (Figure 52). This oval was a result of plotting the sinusoidal signal E_t on the X-axis and the sinusoidal response signal I_t on the Y-axis of a chart.

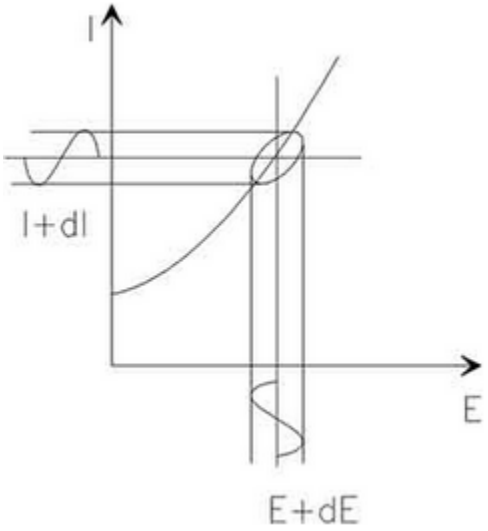

Figure 52. Sample Lissajous figure [38]

Using the Euler relationship,

$$\exp(j\omega\phi) = cos\phi + jsin\phi \tag{10}$$

impedance can be expressed as a complex function where the potential is expressed as

$$E_t = E_0 exp(j\omega t) \tag{11}$$

and the response current as

$$I_t = I_0 \exp(j\omega t - \phi) \tag{12}$$

resulting in the impedance as a complex number:

$$Z(\omega) = \frac{E}{I} = Z_0\, exp(j\phi) = Z_0(cos\phi + jsin\phi) \tag{13}$$

The expression for $Z(\omega)$ consists of a real and an imaginary part. When the imaginary part is plotted on the X-axis and the real on the Y-axis of a chart, the "Nyquist plot" emerges. Each point on the Nyquist plot represents the impedance at one frequency. It is also important to note that the Y-axis is negative. The impedance can be shown as a vector of the length Z on the Nyquist plot. The phase shift, ϕ (arg Z) is the angle between the vector and the X-axis (Figure 53).

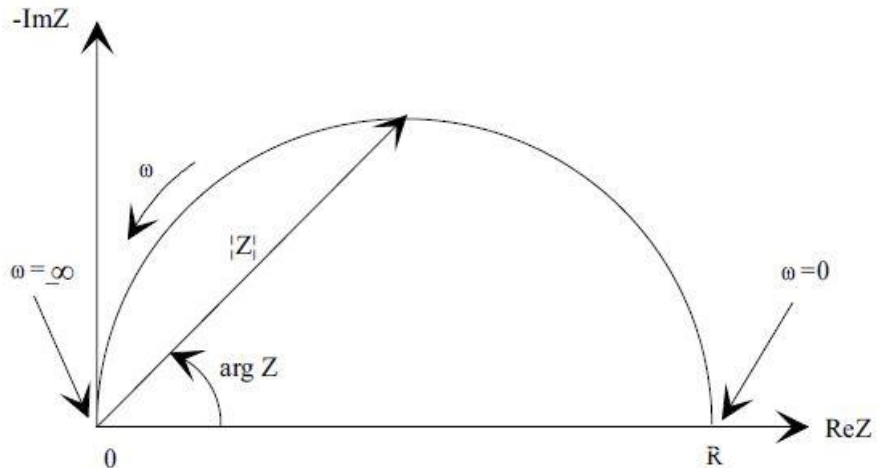

Figure 53. Sample Nyquist plot with impedance vector [38]

The Bode plot is a different presentation method of the measured impedance, which tries to address one of the shortcomings of the Nyquist plot, namely the absence of the data for the frequency, which is used to record the impedance. On the Bode plot, the impedance is plotted with log frequencies on the X-axis and both the absolute values of the impedance and the phase shift on the Y-axis (figure 54.).

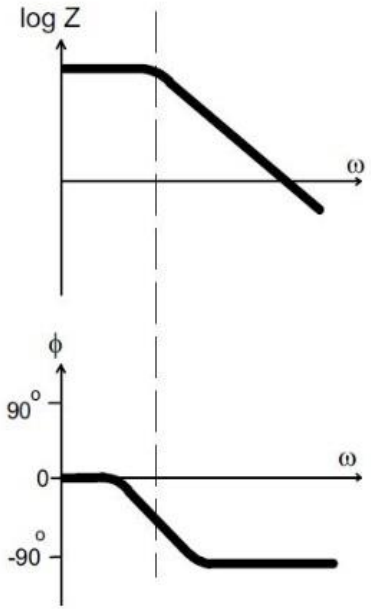

Figure 54.Sample Bode plot with the corresponding phase shift [38]

5.2.2. Equivalent electrical circuits

Electrochemical systems such as coated surfaces or corroding metals behave like simple electric circuits. Thus, EIS date is commonly analysed by fitting it to an equivalent electrical circuit. The most common circuit elements include resistors, capacitors and inductors, as shown in table 6.

Table 6. Circuit elements with impedance correlation to resistance

Component	Impedance
Resistor	$Z = R$
Inductor	$Z = j\omega L$
Capacitor	$Z = j\omega C$

The resistors impedance is independent of frequency and has no imaginary component. The current through a resistor stays in phase with the voltage across the resistor. The impedance of the inductor increases with the frequency. As inductors have just the imaginary impedance component, the current trough an inductor is phase shifted by -90° with respect to the voltage. Capacitors behave the opposite of inductors, their impedance decreases as the frequency rises. As they also have just an imaginary component, the current through a capacitor is phase shifted by 90° with respect to the voltage. To be valid and useful, the assembly of the elements in the model should have a basis in the physical electrochemistry of the system. Figure 55 shows an equivalent circle, which represents an organic coating on a metal substrate.

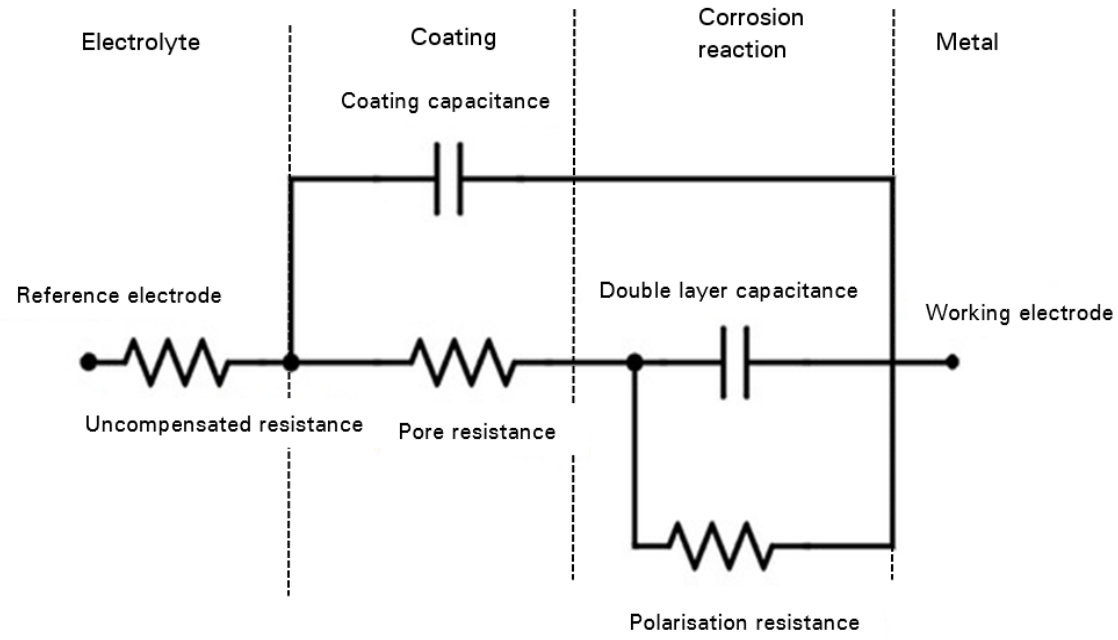

Figure 55. Sample electrical circle representing an organic coating in EIS results evaluation [39]

EIS can provide valuable quantitative data which relates to the quality of an organic coating on a metal substrate. It can indicate changes in the coating long before there is any visible damage. EIS is not an absolute measurement, and its data is only valuable when compared to another EIS spectrum. This can be both coating variants or a multiple measurement of the same coating before and after an outside stress is applied. By making periodic EIS measurements during a stress process, a rate of coating failure can be estimated. EIS remains a non-destructive method, so it is easy to carry out multiple measurements on the same spot and track the condition of a coating as it changes. In most cases it is also possible to identify the cause of coating failure.

5.2.3. EIS test setup

EIS is most commonly run in three electrode mode. The working electrode is represented by the coated specimen, the counter electrode is usually graphite or platinum. There are many choices for an independent reference electrode, saturated calomel electrodes (SCE) and silver/silver chloride being most common ones. The electrodes are then mounted into a cell which contains an electrolyte of choice. Electrolytes are generally chosen to reflect the service condition, the most common ones being sodium chloride solutions. The electrode area of the sample exposed in the cell should be relatively large. Statistically, a larger area has a higher probability of highlighting a defect in the coating while also working with higher currents, which speeds up the measuring process. A larger area also guarantees that no singular coating imperfection has a major influence on the results [33]. A Faraday cage is often used to negate outside electrical disturbances and ensure a smooth measurement.

Figure 56. „Gamry Reference 600“ potentiostat [40]

The EIS tests for this thesis will be carried out in the “Gamry Paracell” (Figure 57) cell connected to the “Gamry Reference 600” potentiostat (Figure 56).

It is important to note that this cell is not optimal for EIS measurements due to its relatively small exposure surface area of 2,85 cm^2. This could lead to capturing a surface imperfection or mechanically damaged spot and interpreting the result as valid. To prevent that, three areas will be predetermined for EIS measurements on every specimen. Obvious false measurements will be neglected, while the average result from the three areas will be used for further analysis. Valid comparative measurements can be made by measuring the exact same spot before and after aging of the specimens.

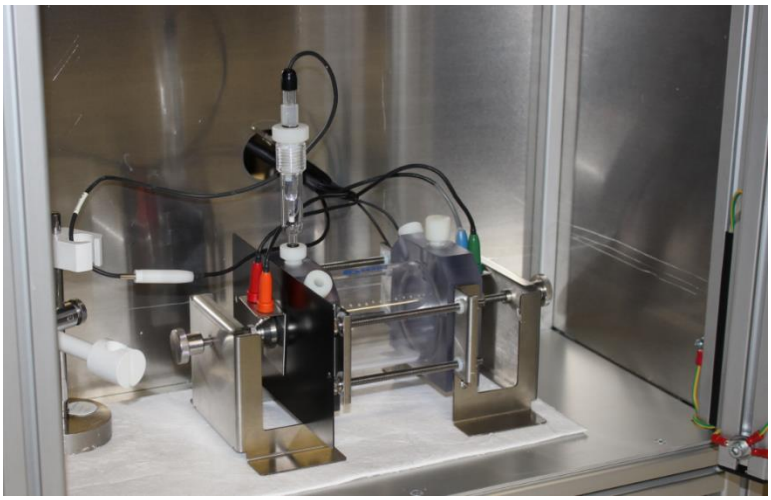

Figure 57. EIS test setup with „Gamry Paracell“ in a Faraday cage

A graphite block will serve as the counter electrode, while the reference electrode will be an SCE (in saturated KCl solution) electrode. Due to the cell setup and the long distance between the electrodes, saturated sodium chloride solution will be used as the electrolyte, instead of 3,5% or 5% sodium chloride solution. A saturated solution is generally more conductive than its unsaturated counterpart, thus ensuring a more stable current flow from the electrodes and less noise during the measurement.

Finally, the cell will be put into a Faraday cage and the electrodes connected to the potentiostats leads. The working and working sense cables will be connected to the exposed substrate, the reference to the reference SCE electrode and the counter and counter sense cables to the graphite electrode. The ground lead will be connected directly to the Faraday cage.

The experiment will be carried out using “Gamry Framework” software and the subsequent analysis by using “Gamry Echem Analyst”. Under Electrochemical impedance, Potentiostatic EIS is selected. In the pop-up window the parameters will be chosen, like in figure 58.

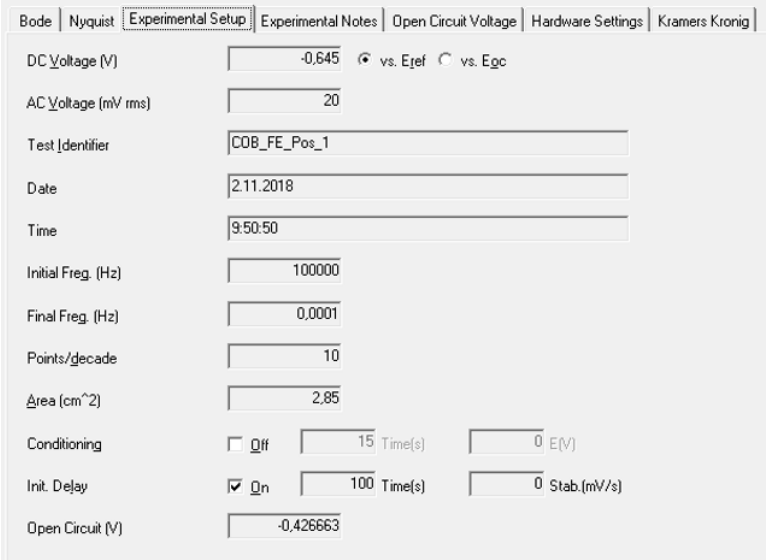

Figure 58. "Gamry Framework" test parameters utilized in EIS evaluation

Bode plots will be used for the result evaluation, as it is interpretation is more intuitive. The equivalent circuit used for the evaluation is the same as in figure 55.

The impedance of the examined coatings will be measured twice. First the impendance of the intact and unaged coatings will be measured. These values will serve as a reference point for the second set of measurements. The coatings will then be left in 5% sodium chloride solution for one month, after which the EIS measurements will be carried out on the same marked areas than before. These values will then be compared to see if the coatings have degraded in the sodium chloride solution. Taking the relatively small surface area of 2,85 cm^2, which is used for the measurements into account, the impedance of coatings might appear surprisingly high.

5.2.4. Corrosion rate test setup

The test setup for the corrosion rate measurement will be virtually identical to the one used for EIS measurements. The only major difference will be the medium, 5% sodium chloride solution, which proved to work best for corrosion rate measurements in the chosen cell. Corrosion rate will be measured on all three substrates using "Gamry Paracell" in the Farraday cage. "Gamry Framework" software will be used to portray Tafel plots and polarisation resistance curves for the substrates, which will then be analysed in "Gamry Echem Analyst".

5.3. Test plans

The experimental part of the thesis is extensive and spread out across multiple testing methods and laboratories. Therefore, test plans for each individual method will be used to clarify the intended testing procedures and make part 6 easier to follow. The specimens will be distributed into accelerated corrosion tests as well as electrochemical tests at the Brose materials laboratory. Additionally, comparative CH and NSS tests will be carried out at the Faculty of Mechanical Engineering and Naval Architecture in Zagreb.

5.3.1. Test plan for accelerated corrosion tests

All specimens will be divided into groups for the five accelerated corrosion tests described in part 5. Three identical specimens will be placed in every accelerated corrosion test, one per each specific duration. The test plan for every climatic test is shown in table 7.

Table 7. Accelerated corrosion test plan for CED and powder coated specimens

One specimen per coating and test duration	CED coated specimens			Powder coated specimens		
	Duration			Duration		
CH test	240 h	360 h	480 h	240 h*	360 h*	480 h
NSS test	96 h	144 h	240 h	240 h*	360 h*	480 h
Cycle-B test	1 Cycle	3 Cycles	6 Cycles	3 Cycles	6 Cycles	10 Cycles
PV 1210 test	5 Cycles	10 Cycles	15 Cycles	15 Cycles	30 Cycles	60 Cycles
VDA-new test	1 Cycle	3 Cycles	6 Cycles	3 Cycles	6 Cycles	9 Cycles

The shorter durations of the accelerated corrosion tests are either prescribed by customers or by the internal Brose standards. Since the protection systems are designed to perform well in all corrosion tests while exposed for the prescribed amount of time, limited corrosion build-up is expected for those durations. Therefore, testing the specimens exclusively within those periods of time would yield limited results, since only miniscule differences could be seen between various coatings and substrates.

Accordingly, the other set of durations has a benchmark character, and should strain the capabilities of the coatings to the full extent. It is expected that the specimens would exhibit a greater degree of corrosion damage after being exposed to the tests for a prolonged period of time, or even completely fail to protect the substrate. Critical failure points could be detected more evidently, while at the same time further conclusions could be derived from those results.

Important notice: The "240 h*" and "360 h*" marked durations for the powder coated specimens exclude the following specimens: Al_G, Al_L, Al_EP, Al_EN for the "240 h*" duration in both the CH and NSS test. Al_G, Al_EP, Al_EN are excluded for the "360 h*" duration in both the CH and NSS test. This exception had to be made due to the lack of aluminium specimens.

However, all of the specimens were included in the 480 h duration of the CH and NSS test. A preliminary assessment of those specimens was made after 240 and 360 hours in both tests as a compromise. Since no corrosion damage or irregularities were detected during those inspections, the specimens were left in the chambers to complete the final duration.

5.3.2. EIS test plan

EIS measurements will be carried out on every coating variant, but not every substrate and coating combination. This compromise had to be made due to the lack of powder coated specimens. Since coating properties are in the forefront of this examination, substrate variations should not impact the final results. In addition, EIS measurements carried out for this thesis are purely comparative in nature and should capture the coatings behaviour before and after aging, independent from the substrate.

All specimens for the EIS examination are shown in table 8., together with all aging times in 5% sodium chloride solution.

Table 8. EIS test plan with aging times

One specimen per coating variant	Initial measurement	Aging in 5% NaCl solution	One specimen per coating variant	Initial measurement	Aging in 5% NaCl solution
CED coated specimens	Time (days)	Time (days)	**Powder coated specimens**	Time (days)	Time (days)
COB	0	24	**Zn_EXP**	0	25
COV	0	24	**Zn_G**	0	25
LON	0	24	**Zn_L**	0	25
QUA	0	25	**Al_L**	0	25
C	0	27	**Al_EP**	0	25
F	0	27	**Al_EN**	0	25
J	0	25	-	-	-
P	0	25	-	-	-

5.3.3. FSB Zagreb test plan

Comparison CH and NSS tests will be carried out in the Laboratory for the protection of materials at the Faculty of Mechanical engineering and naval architecture in Zagreb, as described in parts 5.1.1. and 5.1.2. The specimen count for those tests was fairly reduced, due to transportation limitations and chamber capacities. The selected specimens and test durations are shown in tables 9 and 10.

Table 10. FSB Zagreb CH test plan

CH test			
CED coated specimens	Duration		
COB	240 h	360 h	-
LON	240 h	360 h	-
QUA	240 h	360 h	-
Powder coated specimens	Duration		
Zn_EXP	-	-	480 h
Zn_G	-	-	480 h
Zn_L	-	-	480 h
Zn_EP	-	-	480 h
Zn_EN	-	-	480 h
Al_G	-	-	480 h
Al_L	-	-	480 h
Al_EP	-	-	480 h
Al_EN	-	-	480 h

Table 9. FSB Zagreb NSS test plan

NSS test			
CED coated specimens	Duration		
COB	-	144h	240 h
LON	96 h	144h	240 h
QUA	-	144h	240 h
Powder coated specimens	Duration		
Zn_EXP	240 h	360 h	480 h
Zn_G	240 h	360 h	480 h
Zn_L	240 h	360 h	480 h
Zn_EP	240 h	360 h	480 h
Zn_EN	240 h	360 h	480 h
Al_G	-	-	480 h
Al_L	-	-	480 h
Al_EP	-	-	480 h
Al_EN	-	-	480 h

6. Results and discussion

This section will summarize the results from individual accelerated corrosion tests, compare the results of those tests with each other, as well as display the results from the electrochemical tests. The specimens will be evaluated based on the evaluation criteria from part 4.3. The results of those evaluations will be displayed in individual charts for any noteworthy finding. Since corrosion testing can have a multitude of influencing factors and is not always strictly objective, i.e. degree of rusting, a brief discussion will follow the portrayed results.

Important notice

Before the results of the accelerated corrosion tests are revealed, some critical findings must be discussed. The findings are concerning only the Zn_EXP specimen across all accelerated corrosion tests. The Zn_EXP specimen displays a very low level of adhesion in all durations of the CH, Cycle-B and PV 1210 test, as shown in figure 59. The same phenomenon is demonstrated in the CH test at the Laboratory for the protection of materials in Zagreb.

Figure 59. Zn_EXP specimens with poor coating adhesion after 480 hours of CH, 60 cycles of PV 1210, and 10 cycles of Cycle –B test

The coating can be peeled off from the scribe line with a scalpel without any difficulty. This can also be replicated at any part of the specimen where the coating is not mechanically damaged. As seen from the specimen characterization in part 4.2.2., this anomaly was not detected during initial value assessment for Zn_EXP specimens.

The exception for this phenomenon are NSS and VDA-new test, where Zn_EXP does not show any adhesion issues after all durations (Figure 60).

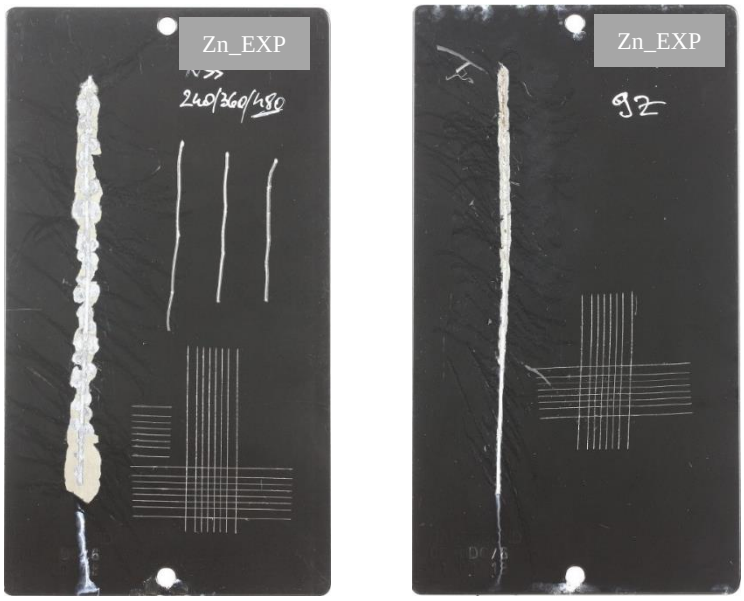

Figure 60. Zn_EXP specimens with adequate coating adhesion after 480 hours of NSS and 9 cycles of VDA-new test

The results for the Zn_EXP specimen will be displayed in the charts as if this problem did not occur. Therefore, it might seem that the properties of this coating and the coating process are considerably better than they are in actuality.

The causes for this behaviour are only speculative, but most likely connected with the nature of the coating process. Zn_EXP was coated by an experimental coater, who is still in a development phase with the whole coating process. Since the reasoning behind this anomaly is well beyond the scope of this thesis, attention to those findings was brought to Brose employees. They will carry out additional examinations on specimens and parts coated by the experimental coater, in order to resolve this issue.

6.1. Results from individual accelerated corrosion tests

To have comparable results from accelerated corrosion tests, the specimens are divided into the CED and powder coated group. As mentioned previously, the test duration for those groups will vary in most cases, as powder coated specimens are expected to be more corrosion resistant in the same conditions as CED specimens. The results are displayed in charts for each relevant evaluation criteria. As the first point of evaluation, they are assessed in relation to the Brose standards for CED (BN 562161-107) and powder coated (BN 587000-112) parts. All results that fall in line with those standards are enclosed in the green area of the charts.

The symbols in the charts represent individual results, which are connected with dotted lines. The sole purpose of the lines is to provide a better visual representation of the trends which occur with increased testing durations. The lines do not represent any measured values and serve exclusively for visualization purposes. A legend, specific to every test, is displayed just above the results. The arrows in the legend indicate the axis that is connected to a particular set of data.

The results from the accelerated corrosion tests are just a snapshot of a coatings behaviour after a predetermined stress time. Hence, any predictions about a coating's behaviour after a different stress time are purely speculative. It is also important to remember that just one specimen was used for any given duration of any test, therefore, some findings could be falsely interpreted as dominant or valuable even though they can be specific just to that particular specimen. Consequently, trends and analogies should be the main focus of this evaluation, as they can better illustrate the effects of the tests on the coated specimens.

The error bars on particular symbols indicate the degree of uncertainty of the evaluation. Edge corrosion is a value, which is not easily quantified, especially in a sample size large as this one. Therefore, the results are an approximation of the objective edge corrosion values. In order for the evaluation to be consistent, specialist colleagues were asked to approximate the edge corrosion on select specimens. Since the values of all approximations were corresponding with each other, within a small deviation, the results are regarded as valid. In some cases, the approximation was made difficult by the build-up of corrosion products which were flowing onto other edges, these specimens are also marked with an error bar.

Please note that the scaling of the data on the y axis often changes, depending on the test. Without taking the scaling into consideration, the results could be interpreted falsely.

Since there is a plethora of results for each evaluation criteria and accelerated corrosion test for both CED and powder coated specimens, the result presentation might seem somewhat unclear. Therefore, for all evaluation criteria with results that can be displayed in charts, this will be the case (green cells in table11). For all other results this method would be impractical, since i.e. for degree of rusting on surface every value would be 0. Striking results from evaluation criteria, not shown in charts (orange cells in table 11) will be summarized at the end of this part. The entirety of the results will be available in appendix A.

Table 11. Depiction of every evaluation criteria and accelerated corrosion test, where green cells indicate graphical portrayal

Coating type	Accelerated corrosion test	Degree of rusting on surface	Degree of rusting on edges	Degree of corrosion and delamination around a scribe	Cross cut test	Degree of blistering	Daimler scratch test
CED coating	CH						
	NSS						
	Cycle-B						
	PV 1210						
	VDA-new						
Powder coating	CH						
	NSS						
	Cycle-B						
	PV 1210						
	VDA-new						

6.1.1. CH test – CED specimens

6.1.1.1 Degree of rusting on edges (Edge corrosion)

Figure 61 displays the edge corrosion results on CED specimens after 240, 360 and 480 hours of CH test. Marked with green triangles, edge corrosion even after prolonged 240 hours of testing is well below the Brose requirement of 5% after 144 hours. The value of 0,5%, or less than 1%, is used to indicate a minimal degree of rusting.

None of the specimens exhibit a significant degree of rusting, which is most likely connected to the nature of the CH test and its relatively mild stresses.

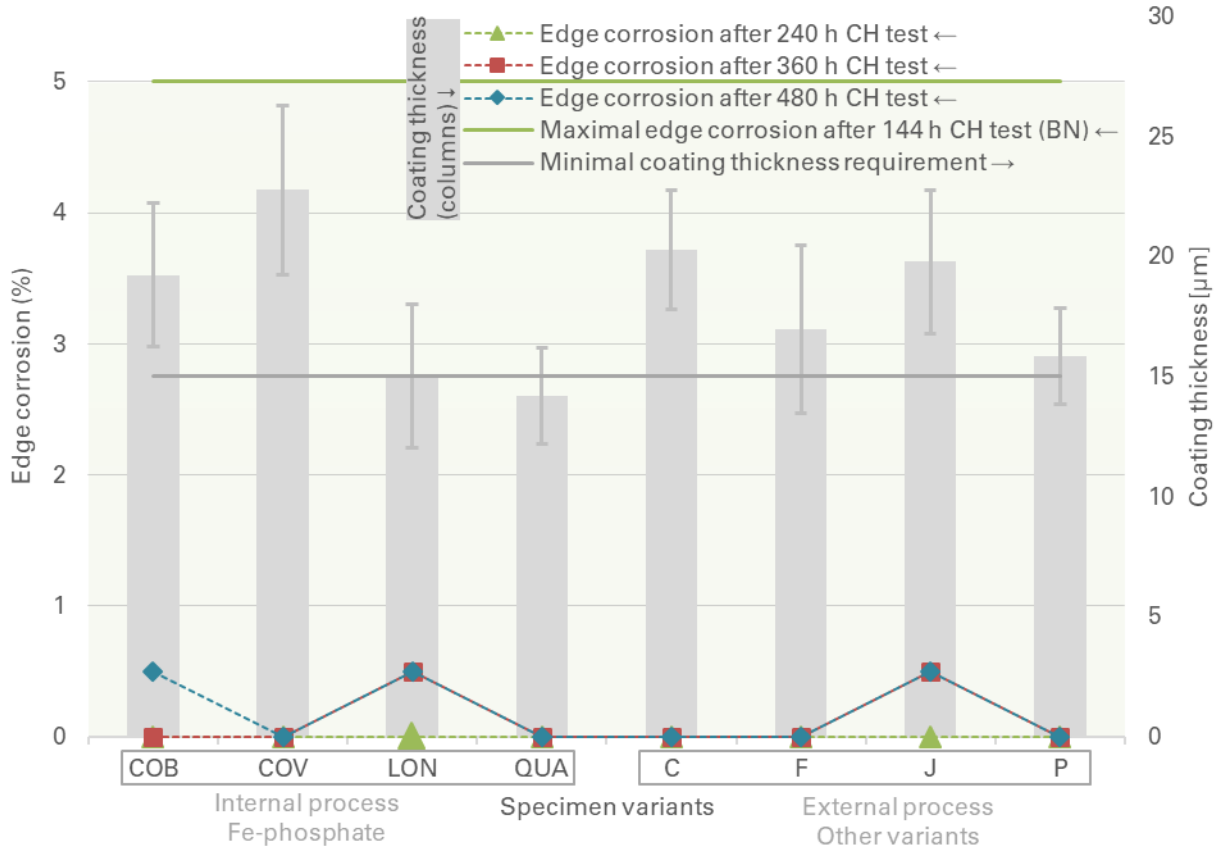

Figure 61. Comparison of edge corrosion results (colored symbols) on CED coated specimens, after 240, 260 and 480 hours of the CH test, in relation to coating thickness (columns) and different pre-treatment variants

6.1.1.2 Degree of corrosion and delamination around a scribe

Figure 62 displays the delamination results on CED coated specimens after 240, 360 and 480 hours of CH test. Marked with green triangles, the degree of corrosion and delamination, even after 240 hours, is below the Brose requirement of 1 mm after 144 hours.

After 360 and 480 hours, dissimilarities in regard to pre-treatment variants can be observed. Specimens with iron phosphate exhibit a higher degree of delamination compared to other variants. Specimens C, J and P exhibit no degree of delamination after all durations, which is most likely connected to their similar pre-treatment process.

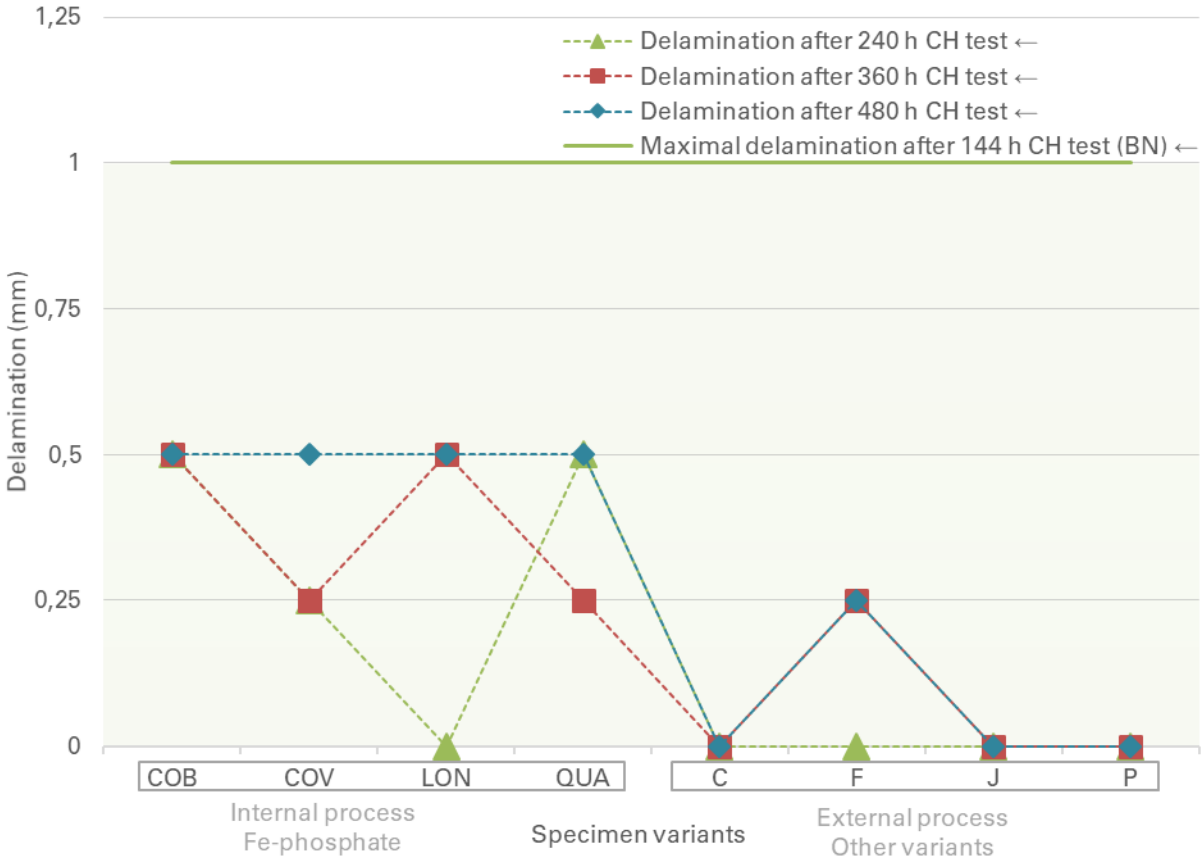

Figure 62. Comparison of delamination results (colored symbols) on CED coated specimens, after 240, 260 and 480 hours of the CH test, in relation to different pre-treatment variants

The delaminated area is circular and intermittent across the whole length of the scribe line. This pattern is unlike any other delamination manifestation caused by other accelerated corrosion tests. From figure 63, it is safe to assume that the delamination was caused by blistering around

the scribe line. Those blistering effects around the scribe line are not found on specimens (C, J, P) with the tricationic phosphate step in the coating process.

Figure 63. Delamination pattern around the scribe line on COB after 480 h of CH test

6.1.1.3. Daimler scratch test

Figure 64 displays the scratch test results on CED coated specimens after 240, 360 and 480 hours of CH test. The green, red and blue bars represent the results after increasing testing times, while the grey bar indicates the initial grade established prior to the test. Consistently, the maximal acceptable grade after any testing time is K2, as defined in the Brose standard.

Specimen QUA is graded with K3 after all durations of the test, which in term means, that coating adhesion is not satisfactory after those testing times.

The CH test does not seem to influence the adhesion of C and J specimens, which continue to demonstrate remarkable results with the grade K0.

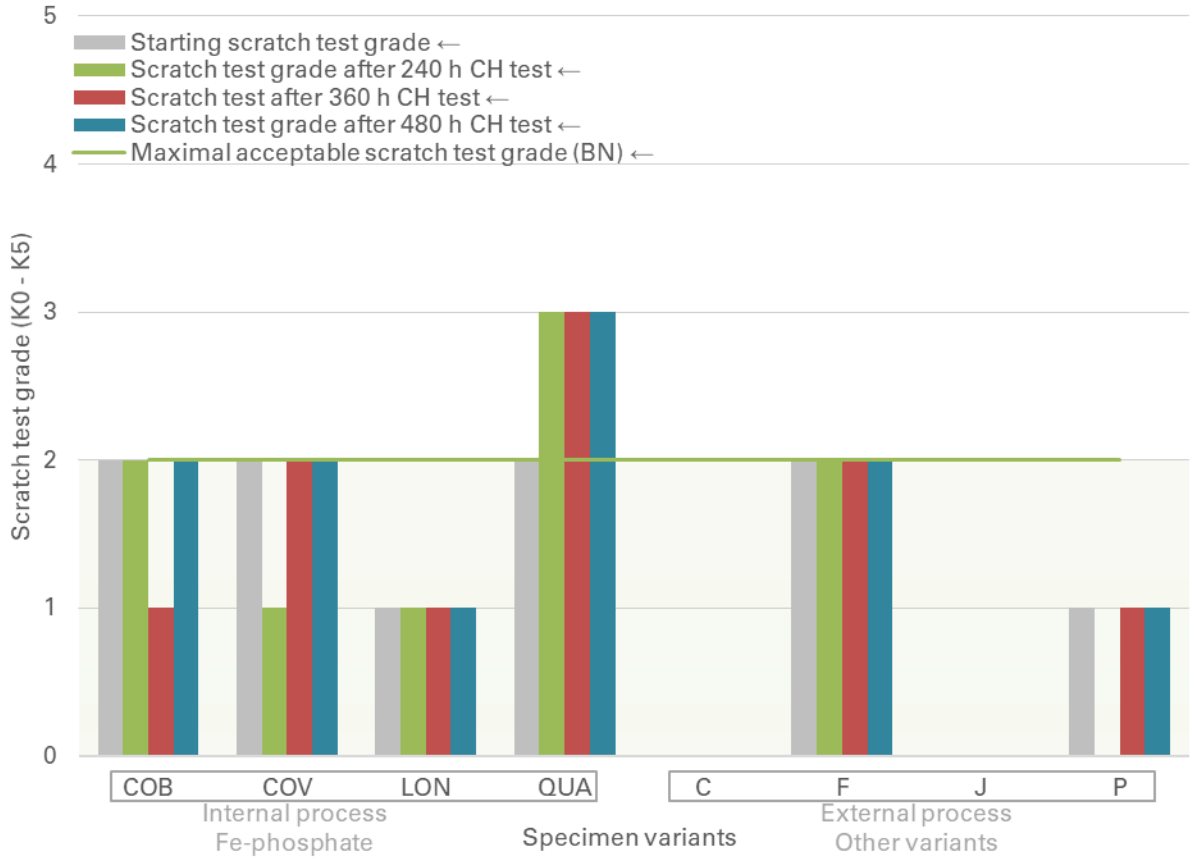

Figure 64. Comparison of scratch test results (colored bars) on CED coated specimens, after 240, 260 and 480 hours of the CH test, in relation to initial values (grey bars) and different pre-treatment variants

6.1.2. CH test – Powder coated specimens

6.1.2.1. Degree of rusting on surface and edges

Powder coated specimens are unphased by the stresses of the CH test regarding surface and edge corrosion. They exhibit no degree of surface nor edge corrosion at all durations of the test. This is most likely due to the high coating thickness and relatively mild degree of straining in the CH test.

6.1.2.2. Degree of delamination and corrosion around a scribe

Figure 65 displays the delamination results on powder coated specimens after 240, 360 and 480 hours of CH test. Marked with green triangles, the degree of corrosion and delamination is below the Brose requirement of 1 mm after 240 hours of testing.

None of the specimens exhibit a significant degree of delamination after all durations of the test. Only after 480 hours, Zn_EP and Zn_EN show a miniscule amount of delamination.

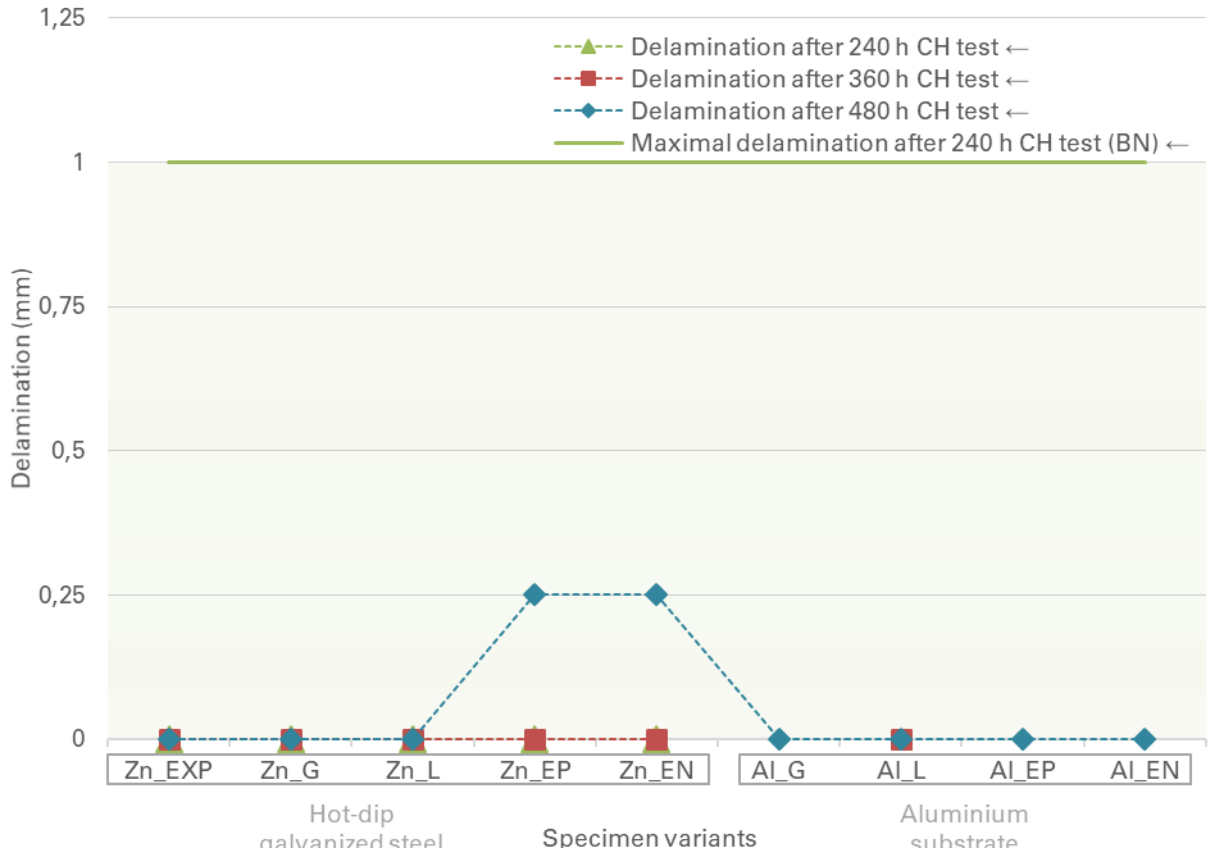

Figure 65. Comparison of delamination results (colored symbols) on powder coated specimens, after 240, 260 and 480 hours of the CH test, in relation to different substrates (the full extent of Zn_EXP delamination not shown in chart)

6.1.3. NSS test – CED specimens

6.1.3.1. Degree of rusting on edges (Edge corrosion)

Figure 66 displays the edge corrosion results on CED specimens after 96, 144 and 240 hours of NSS test. Marked with green triangles, edge corrosion after 96 hours of testing is well below the Brose requirement of 5% on all specimens.

CED coated parts and specimens are usually tested up to 96 hours in the NSS test, meaning that the 144 and 240 hour duration overstrained them to a great extent, thus edge corrosion on most specimens is substantial after 144 and 240 hours. Specimen QUA, with the lowest coating thickness, shows the greatest amount of edge corrosion after 240 hours of testing.

Specimen C, with sufficient coating thickness, tricationic phosphating and subsequent passivation exhibits by far the least amount of edge corrosion.

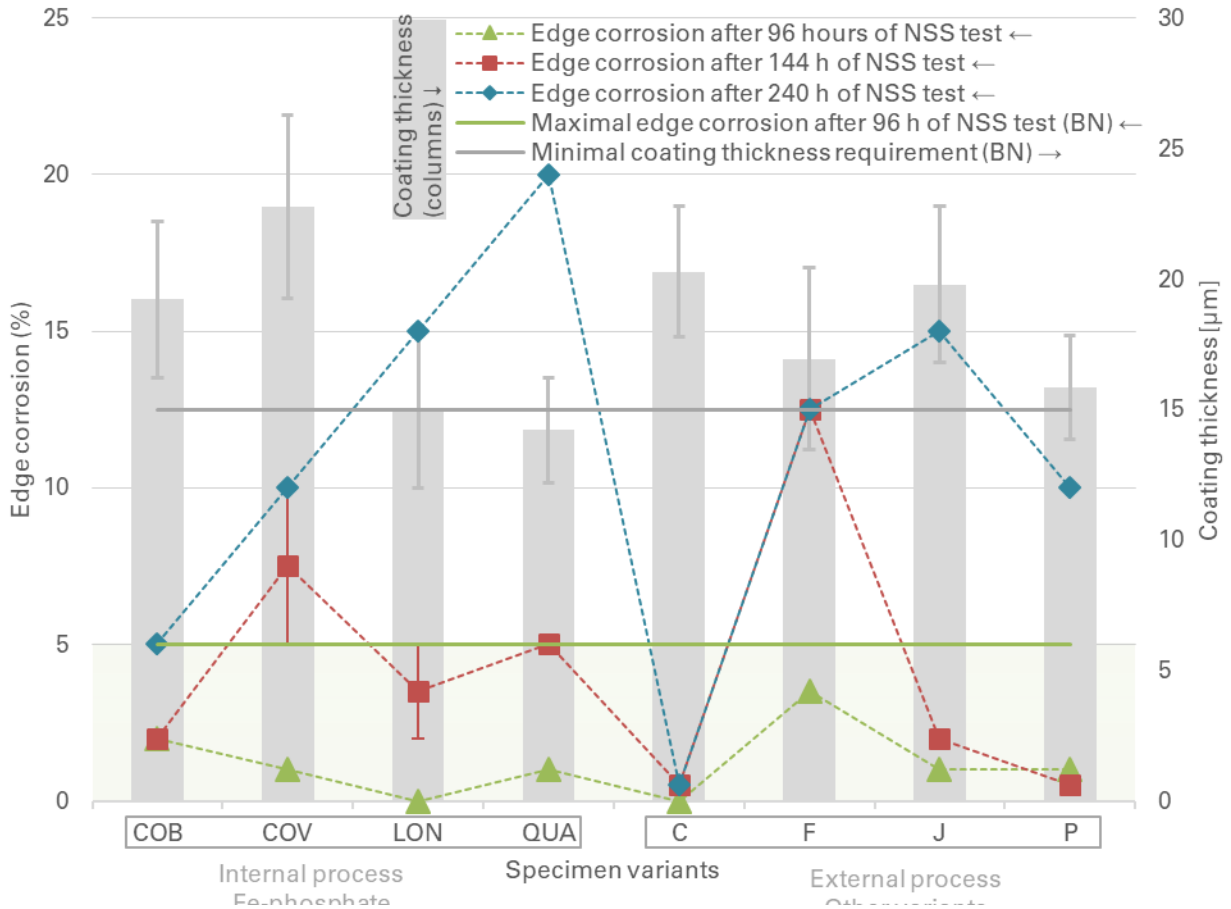

Figure 66. Comparison of edge corrosion results (colored symbols) on CED coated specimens, after 96, 144 and 240 hours of the NSS test, in relation to coating thickness (columns) and different pre-treatment variants

6.1.3.2. Degree of corrosion and delamination around a scribe

Figure 67 displays the delamination results on CED coated specimens after 96, 144 and 240 hours of NSS test. Marked with green triangles, the degree of corrosion and delamination, even after 96 hours, is below the Brose requirement of 1 mm on all specimens.

With increasing duration times, the results start to fluctuate. After 144 and 240 hours, clear differences can be seen with regard to different pre-treatment methods. Specimens C, J and P with the tricationic phosphate show absolutely no delamination, even when strained severely.

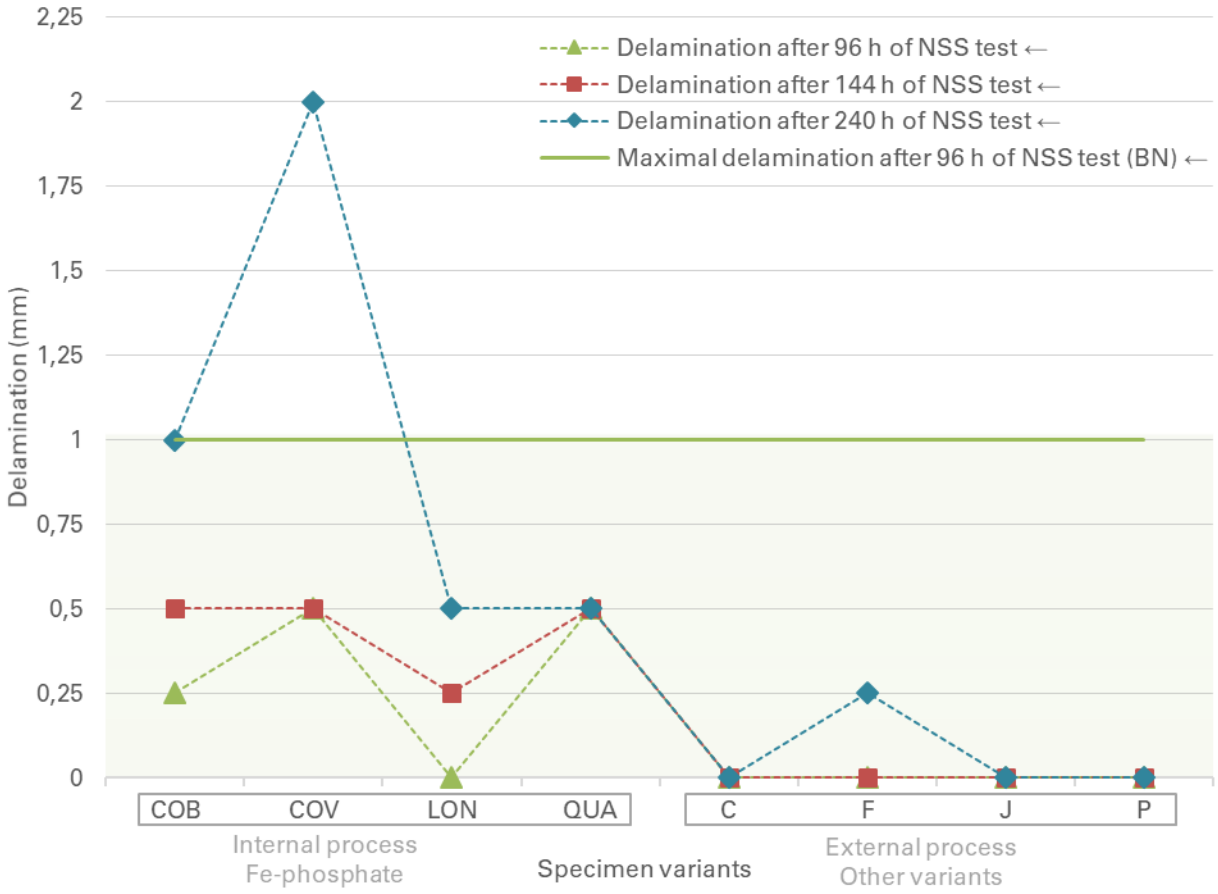

Figure 67. Comparison of delamination results (colored symbols) on CED coated specimens, after 96, 144 and 240 hours of the NSS test, in relation to different pre-treatment variants

6.1.3.3. Daimler scratch test

Figure 68 displays the scratch test results on CED coated specimens after 96, 144 and 240 hours of NSS test. The green, red and blue bars represent the results after increasing testing times, while the grey bar indicates the initial grade established prior to the test. Consistently, the maximal acceptable grade after any testing time is K2, as defined in the Brose standard.

Specimen QUA is graded with K3 after all durations of the test, which in term means, that coating adhesion is not satisfactory after those testing times.

The NSS test does not seem to influence the adhesion of C and J specimens, which continue to demonstrate remarkable results with the grade K0.

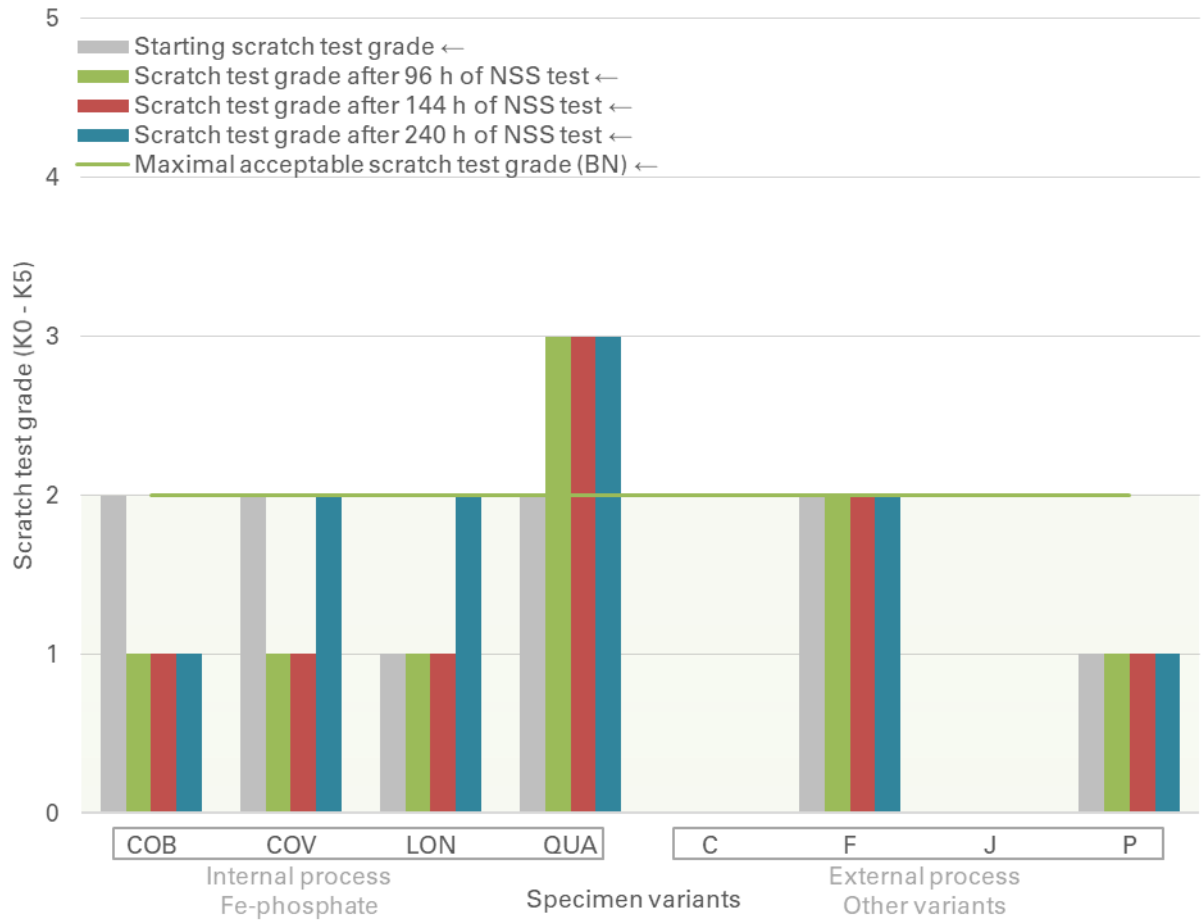

Figure 68. Comparison of scratch test results (colored bars) on CED coated specimens, after 96, 144 and 240 hours of the NSS test, in relation to initial values (grey bars) and different pre-treatment variants

6.1.4. NSS test – Powder coated specimens

6.1.4.1. Degree of rusting on edges (Edge corrosion)

Figure 69 displays the edge corrosion results on powder coated specimens after 240, 360 and 480 hours of NSS test. Marked with green triangles, edge corrosion after 240 hours of testing is above the specified Brose requirement of 0% on specimens Zn_G, Zn_EP and Zn_L. It is important to state, that this requirement is only valid for functional areas of powder coated car parts, which consequently have a bigger coating thickness than the tested specimens

Zn_EP is the only outlier, with edge corrosion up to 30% after 480 hours of testing. This is most likely due to its low coating thickness, which dips under the minimal required coating thickness at some measured points.

Aluminium specimens do not exhibit any edge corrosion throughout the test.

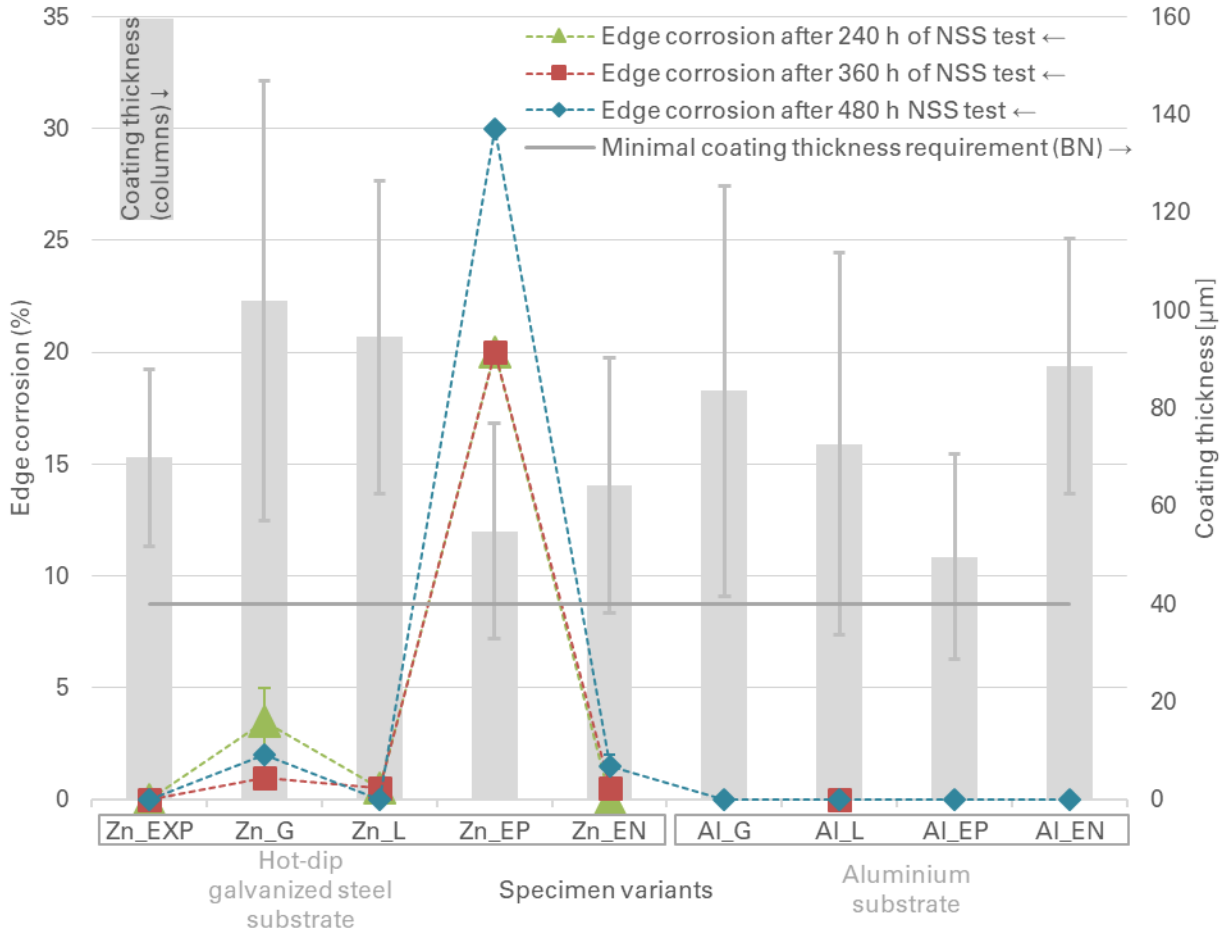

Figure 69. Comparison of edge corrosion results (colored symbols) on powder coated specimens, after 240, 360 and 480 hours of the NSS test, in relation to coating thickness (columns) and different substrates

Strangely, the Zn_G specimen exhibits more edge corrosion after 240 h than after 360 or 480 hours. This anomaly is most likely caused by a faulty individual specimen, the one which was tested for 240 hours.

6.1.4.2. Degree of corrosion and delamination around a scribe

Figure 70 displays the delamination results on powder coated specimens after 240, 360 and 480 hours of NSS test. Marked with green triangles, the degree of corrosion and delamination on Zn_L and Zn_EP is above the Brose requirement of 1 mm after 240 hours, while Zn_EXP, Zn_L and Zn_EN are borderline cases.

Oppositely, the aluminium specimens do not show any degree of delamination, even after 480 hours.

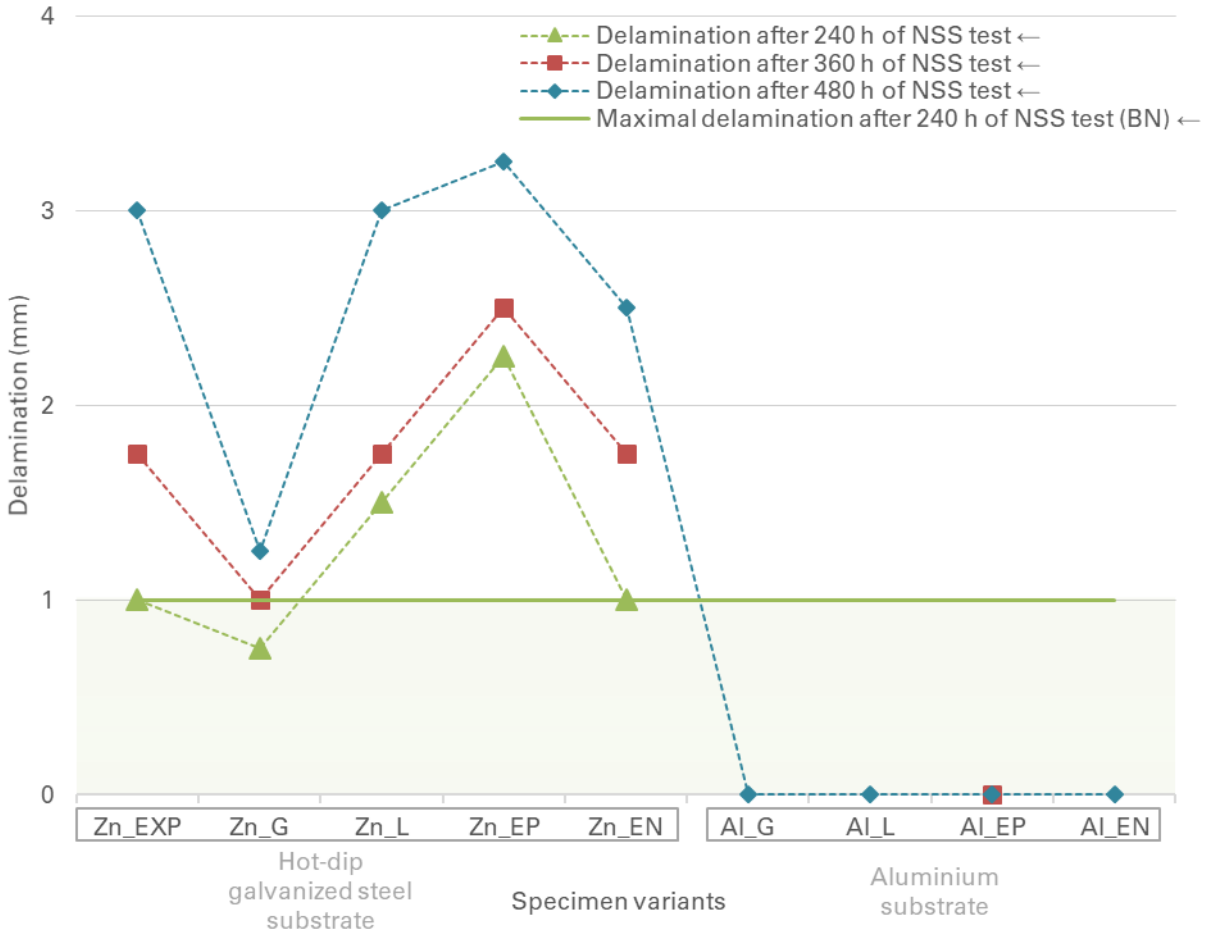

Figure 70. Comparison of delamination results (colored symbols) on powder coated specimens, after 240, 360 and 480 hours of the NSS test, in relation to different substrates (the full extent of Zn_EXP delamination not shown in chart)

6.1.5. Cycle-B test – CED specimens

6.1.5.1. Degree of rusting on edges (Edge corrosion)

Figure 71 displays the edge corrosion results on CED specimens after one, three and six cycles of Cycle-B test. Marked with green triangles, edge corrosion after one cycle of testing is well below the Brose requirement of 30 % on all specimens.

CED coated parts and specimens are usually tested up to one cycle in the Cycle-B test test, meaning that the three and six cycle duration overstrained them to a great extent. At higher durations, differences with regard to pre-treatment methods can be seen. Specimen C, with tricationic phosphating and subsequent passivation has by far the least amount of edge corrosion.

COB exhibits an unusually high amount of edge corrosion after six cycles.

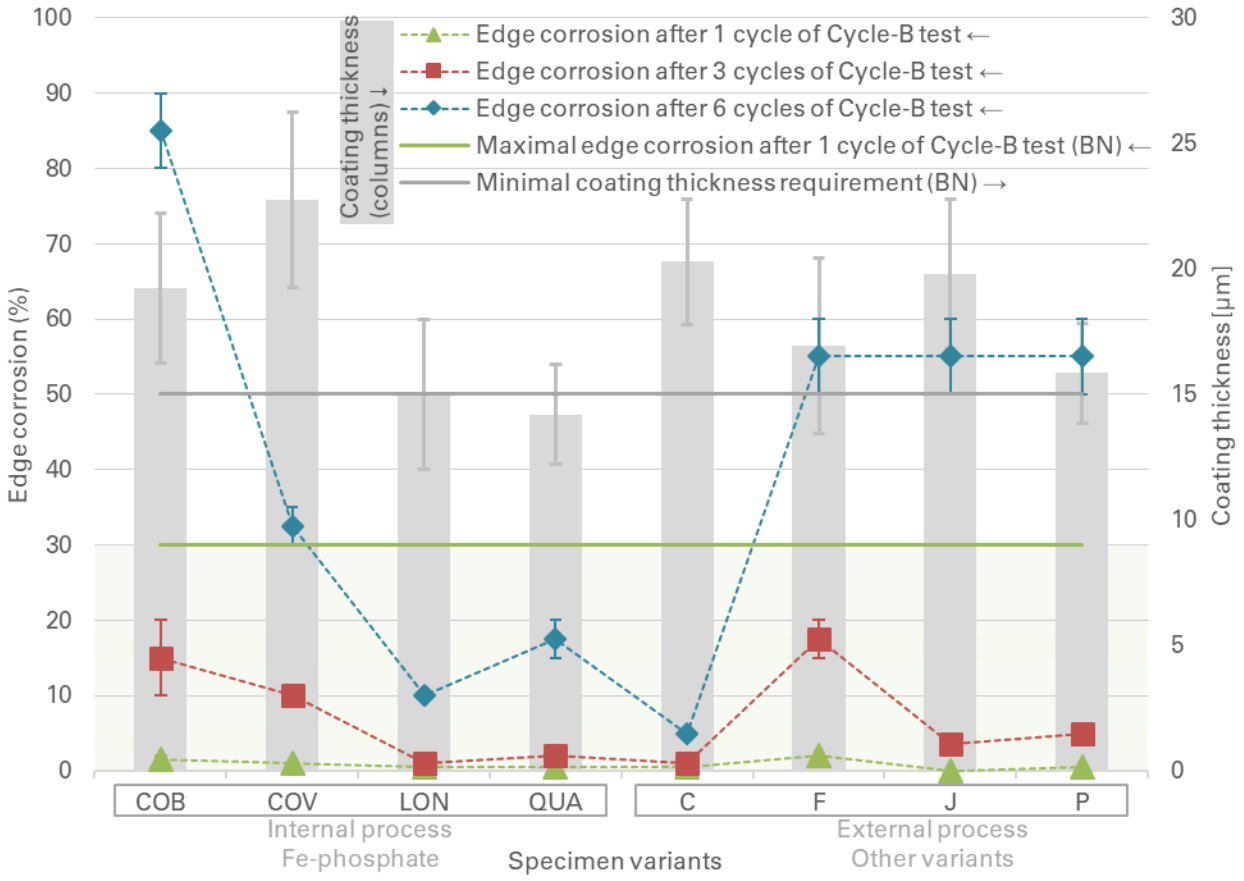

Figure 71. Comparison of edge corrosion results (colored symbols) on CED coated specimens, after one, three and six cycles of the Cycle-B test, in relation to coating thickness (columns) and different pre-treatment variants

6.1.5.2. Degree of corrosion and delamination around a scribe

Figure 72 displays the delamination results on CED coated specimens after one, three and six cycles of Cycle-B test. Marked with green triangles, the degree of corrosion and delamination, after one cycle of testing, is below the Brose requirement of 2 mm on all specimens.

After three and six cycles, clear differences can be seen with regard to different pre-treatment methods. The specimens with tricationic phosphate (C, J, P) display considerably less delamination than specimens with iron phosphate.

The big differences in delamination on specimens with the iron phosphate might stem from used coating systems.

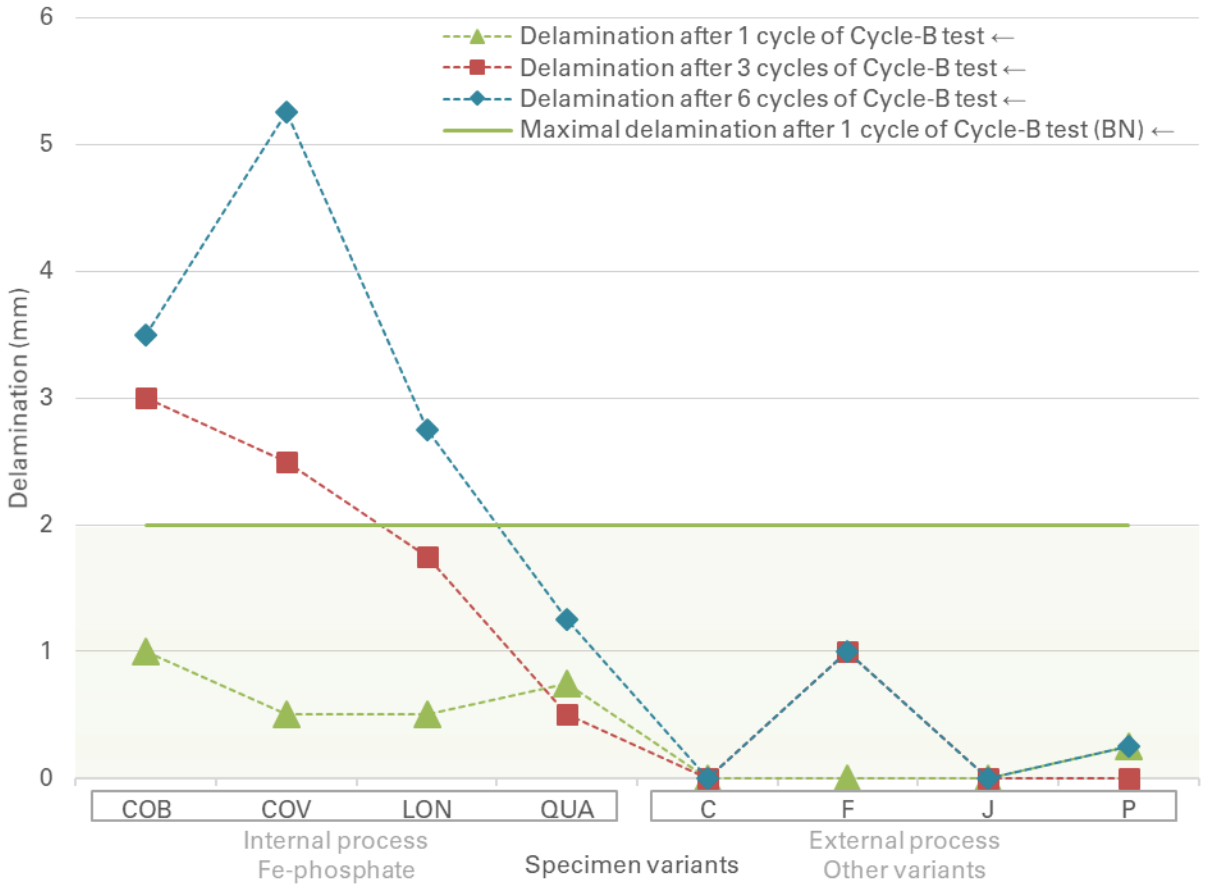

Figure 72. Comparison of delamination results (colored symbols) on CED coated specimens, after one, three and six cycles of the Cycle-B test, in relation to different pre-treatment variants

6.1.5.3. Daimler scratch test

Figure 73 displays the scratch test results on CED coated specimens after one, three and six cycles of Cycle-B test. The green, red and blue bars represent the results after increasing testing times, while the grey bar indicates the initial grade established prior to the test. Consistently, the maximal acceptable grade after any testing time is K2, as defined in the Brose standard.

Specimen COV is graded with K3 after three cycles and F after just one cycle. This would mean, that coating adhesion of those specimens is not satisfactory after the mentioned testing times.

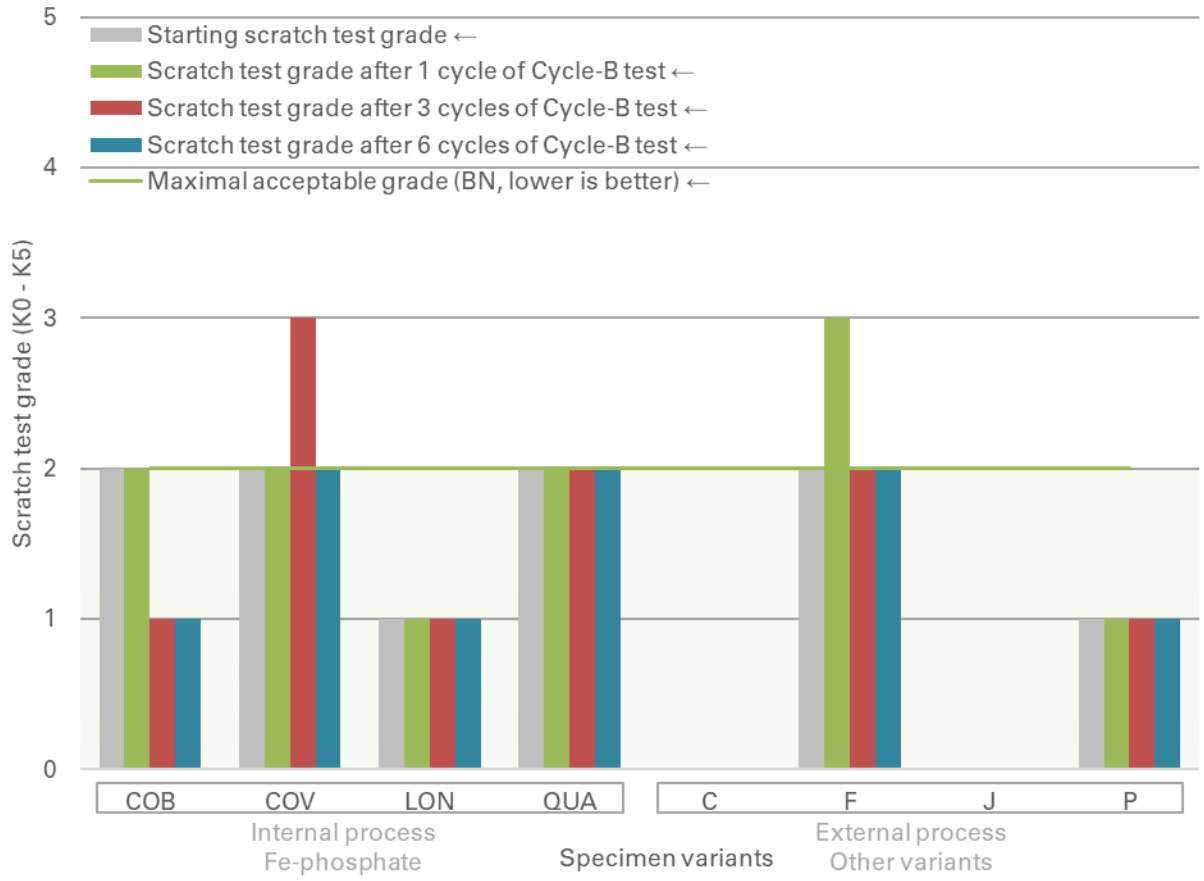

Figure 73. Comparison of scratch test results (colored bars) on CED coated specimens, after one, three and six cycles of the Cycle-B test, in relation to initial values (grey bars) and different pre-treatment variants

6.1.6. Cycle-B test – Powder coated specimens

6.1.6.1. Degree of rusting on edges (Edge corrosion)

Figure 74 displays the edge corrosion results on powder coated specimens after three, six and ten cycles of Cycle-B test. Marked with red squares, edge corrosion after six cycles of testing is below the specified Brose requirement of 30% on all specimens, beside Zn_EP. Moreover, Zn_EP exhibits high degrees of edge corrosion after all durations, which is most likely connected to the low coating thickness.

All aluminium specimens show 0% edge corrosion throughout the whole testing period.

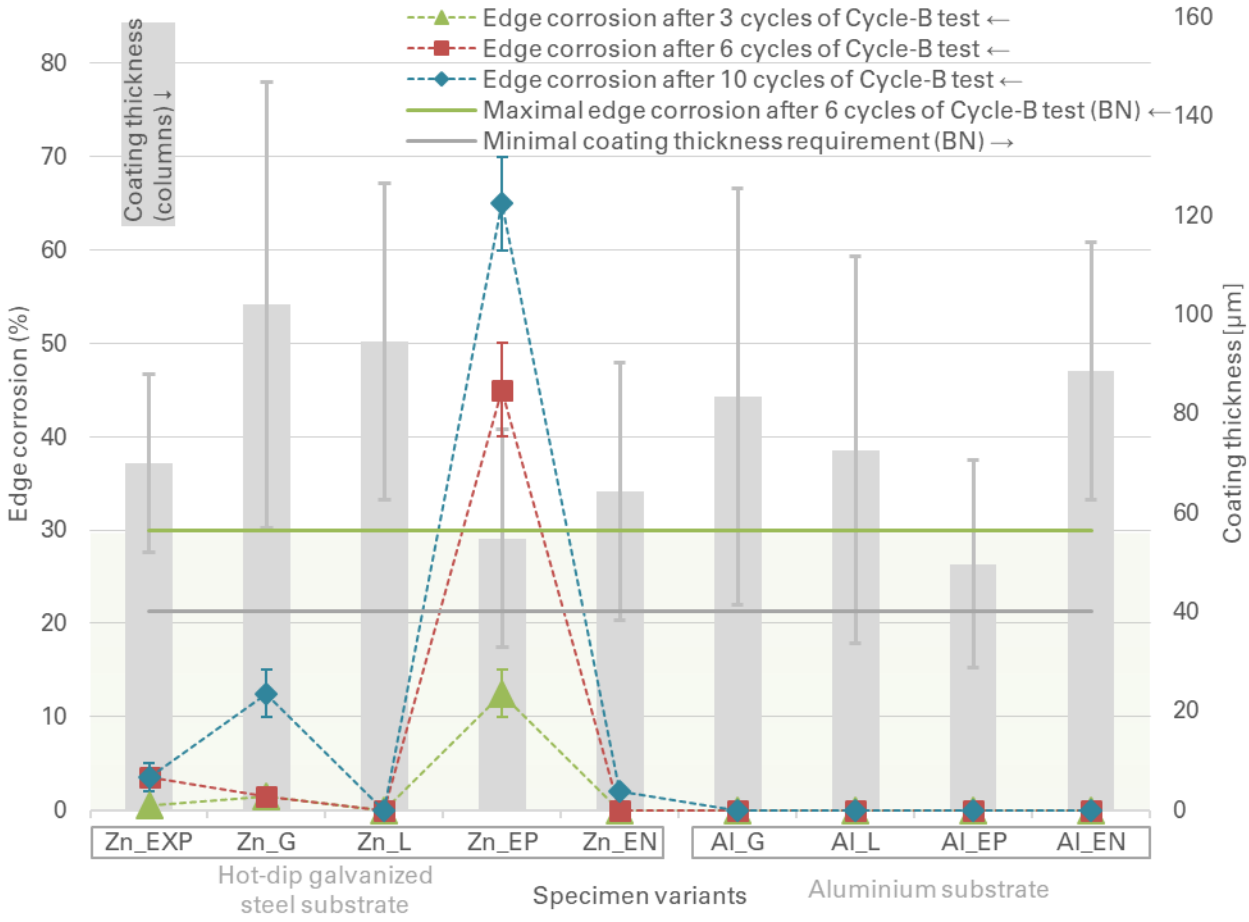

Figure 74. Comparison of edge corrosion results (colored symbols) on powder coated specimens, after three, six and ten cycles of the Cycle-B test, in relation to coating thickness (columns) and different substrates

6.1.6.2. Degree of corrosion and delamination around a scribe

Figure 75 displays the delamination results on powder coated specimens after one, three and six cycles of Cycle-B test. Marked with red squared, the degree of corrosion and delamination on all specimens is well within the Brose requirement of 4 mm after six cycles.

Hot dip galvanized steel specimens exhibit similar degrees of delamination, except for Zn_G, which has the lowest amounts of delamination throughout the test.

Aluminium specimens exhibit virtually no degree of delamination, when compared to hot-dip galvanized steel specimens.

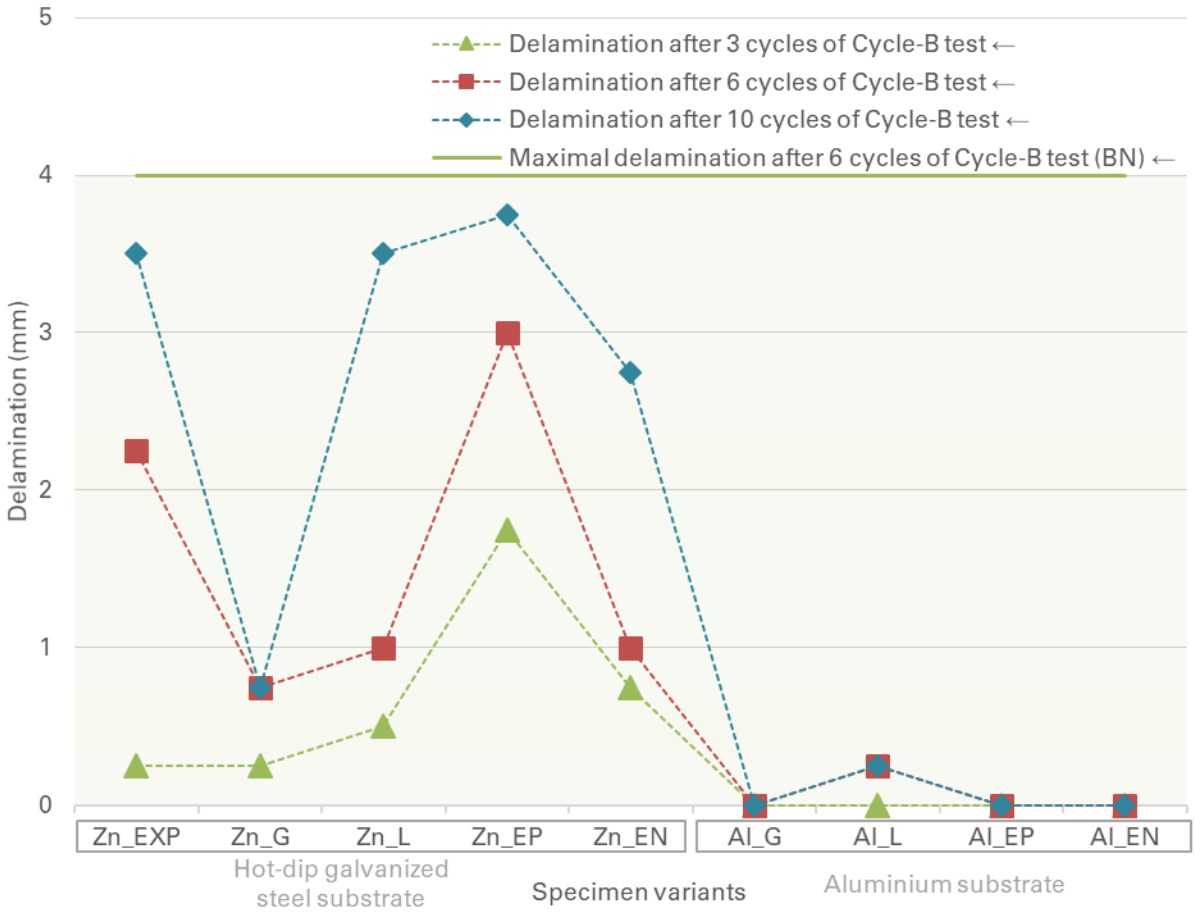

Figure 75. Comparison of delamination results (colored symbols) on powder coated specimens, after three, six and ten cycles of Cycle-B test, in relation to different substrates (the full extent of Zn_EXP delamination not shown in chart)

6.1.7. PV 1210 test – CED specimens

6.1.7.1. Degree of rusting on edges (Edge corrosion)

Figure 76 displays the edge corrosion results on CED specimens after five, ten and fifteen cycles of PV 1210 test. Marked with green triangles, edge corrosion after ten cycles of testing is well below the Volkswagen requirement of 25 % on all specimens. Brose took over this requirement from the Volkswagen standard "TL 162", where the PV 1210 test is prescribed.

With increased testing duration, some clear differences can be observed in relation to coating thickness, which is depicted as grey bars. The specimen QUA, with the lowest coating thickness, displays the biggest degree of rusting on edges, after both ten and fifteen cycles. This is only matched by J, after the longest duration of the test, even though the specimen has adequate coating thickness. Specimen C continues to exhibit the least amount of degradation on the edge, as in all previous tests.

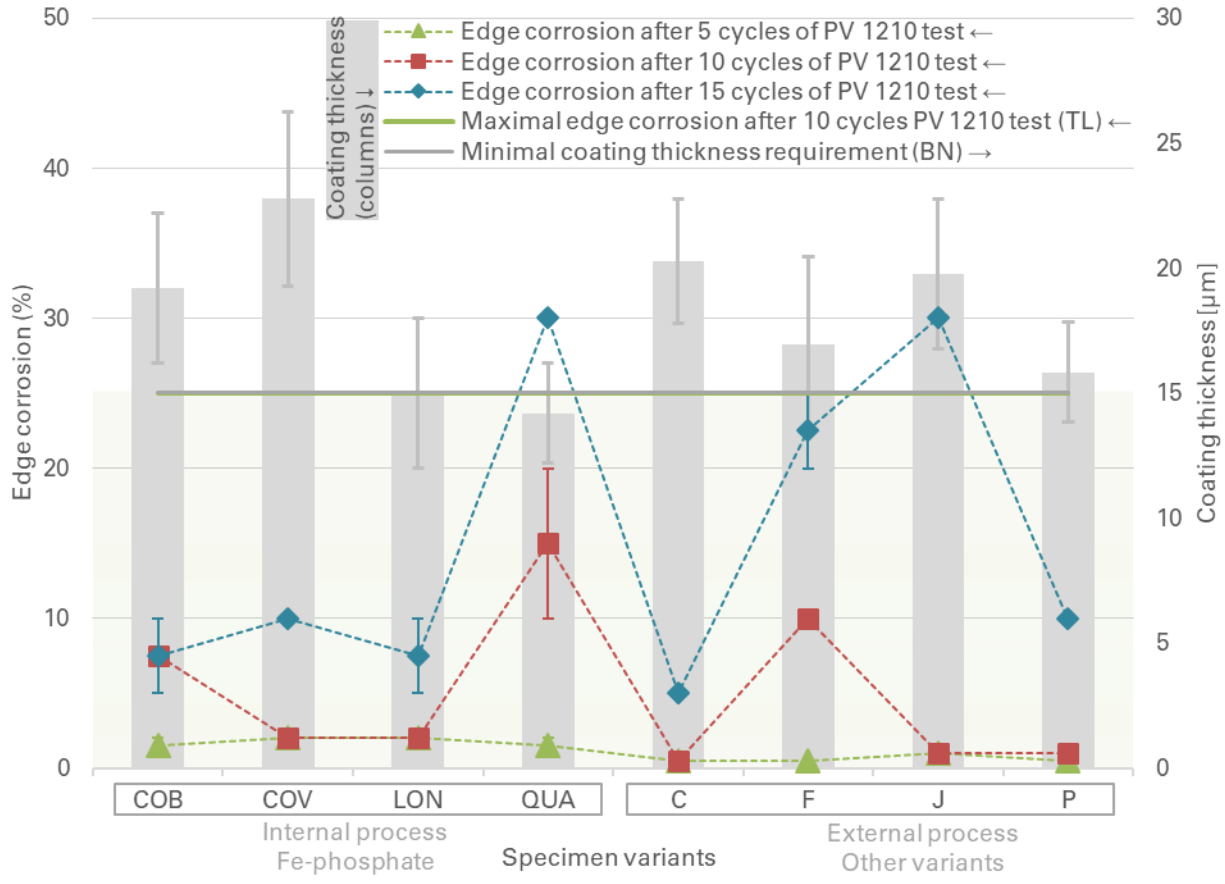

Figure 76. Comparison of edge corrosion results (colored symbols) on CED coated specimens, 5, 10 and 15 cycles of the PV 1210 test, in relation to coating thickness (columns) and different pre-treatment variants

6.1.7.2. Degree of corrosion and delamination around a scribe

Figure 77 displays the delamination results on CED coated specimens after five, ten and fifteen cycles of PV 1210 test. Marked with blue squares, the degree of corrosion and delamination on COV and LON is above the Volkswagen requirement of 2,5 mm after 15 cycles. Same as for edge corrosion, Brose took over this requirement from the Volkswagen standard "TL 162", where the PV 1210 test is originally prescribed.

After only five cycles, dissimilarities in regard to pre-treatment variants can be observed. Specimens with iron phosphate exhibit a higher degree of delamination compared to other variants. The trend continues with increased testing time as the performance of those specimens decreases even further. Specimens C and J exhibit no degree of delamination after all durations, which is most likely connected to their similar pre-treatment process.

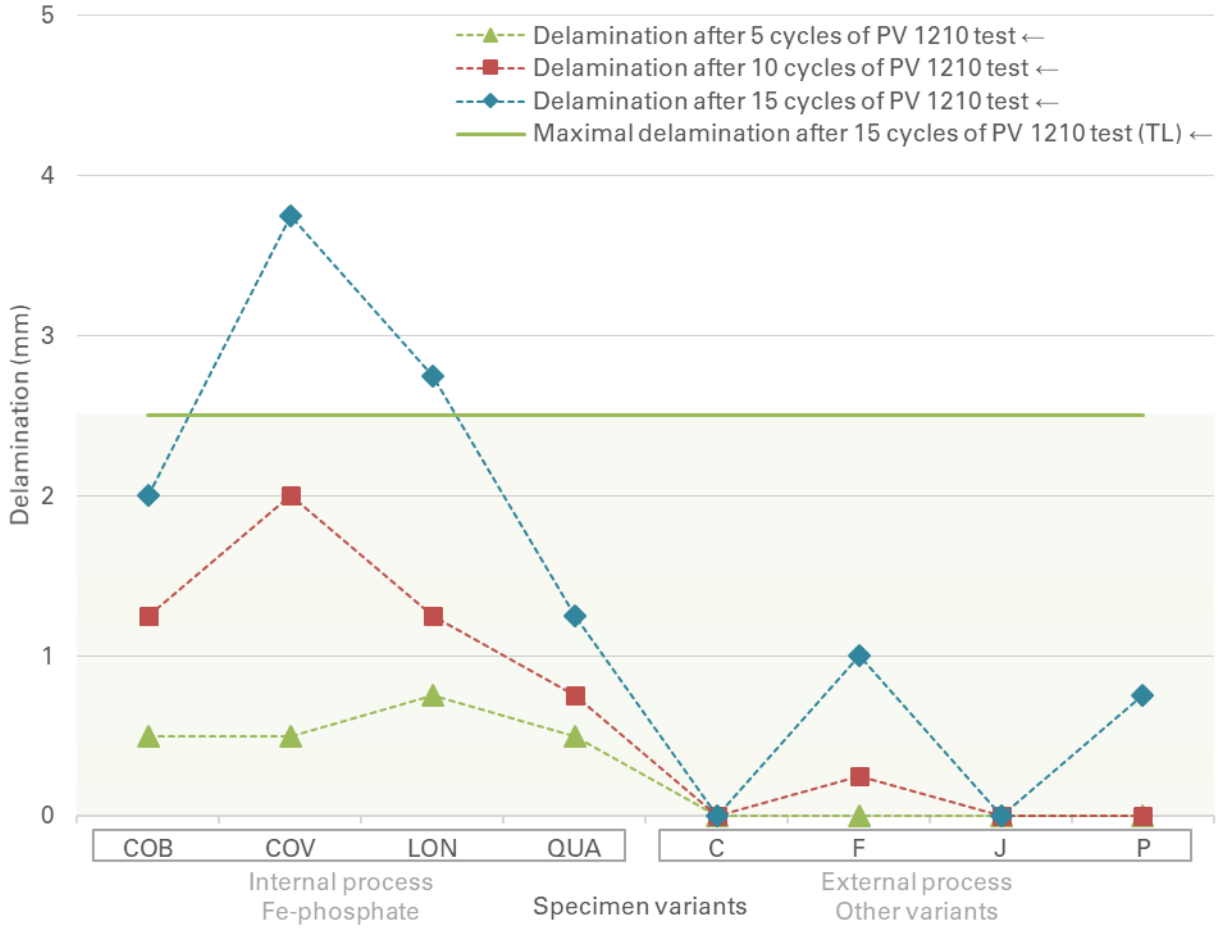

Figure 77. Comparison of delamination results (colored symbols) on CED coated specimens, after 5, 10 and 15 cycles of the PV 1210 test, in relation to different pre-treatment variants

6.1.7.3. Daimler scratch test

Figure 78 displays the scratch test results on CED coated specimens after five, ten and fifteen cycles of PV 1210 test. The green, red and blue bars represent the results after increasing testing times, while the grey bar indicates the initial grade established prior to the test. Consistently, the maximal acceptable grade after any testing time is K2.

The specimen QUA is graded with K3 after ten and fifteen cycles of the test, which in term means, that coating adhesion is not satisfactory after those testing times.

The PV 1210 test does not seem to influence the adhesion of C and J specimens, which continue to demonstrate remarkable results with the grade K0.

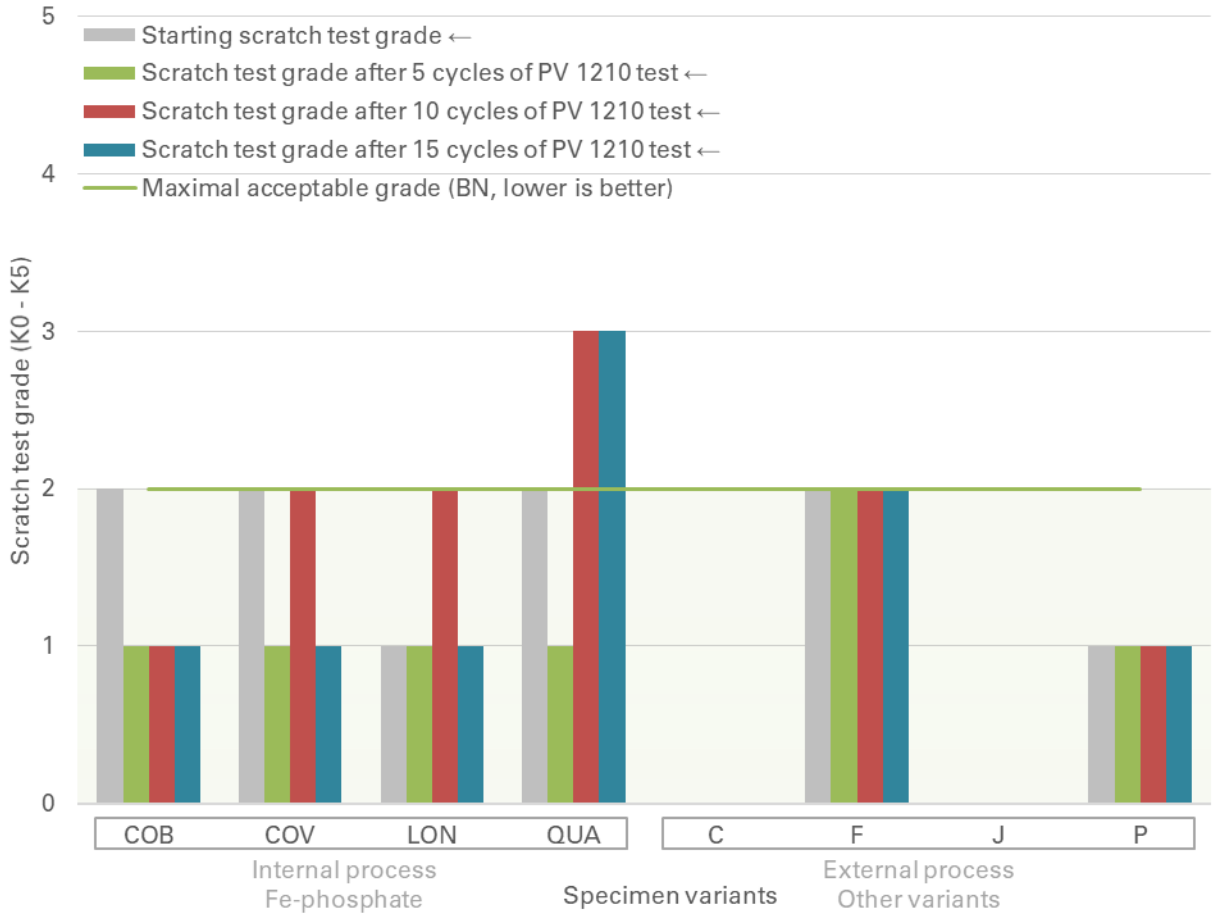

Figure 78. Comparison of scratch test results (colored bars) on CED coated specimens, after 5, 10 and 15 cycles of the PV 1210 test, in relation to initial values (grey bars) and different pre-treatment variants

6.1.8. PV 1210 test – Powder coated specimens

6.1.8.1. Degree of rusting on edges (Edge corrosion)

Figure 79 displays the edge corrosion results on powder coated specimens after 15, 30 and 60 cycles of PV 1210 test. Marked with green triangles, edge corrosion after 15 cycles of testing is above the specified Brose requirement of 0% on some specimens. The Brose standard declares, that this requirement is only valid for functional areas of powder coated parts. In practice, those areas purposefully go through additional coating steps in order to achieve a higher coating thickness and thereby become more corrosion resistant. Accordingly, the Brose requirement is neglected for this particular evaluation.

Specimen Zn_EP is the only outlier in this chart, with edge corrosion values higher than 50% after 60 cycles of testing. This result can be connected to the relatively low coating thickness of Zn_EP, which dips under the minimal requirement of 40 µm.

All aluminium specimens are unaffected regarding edge corrosion.

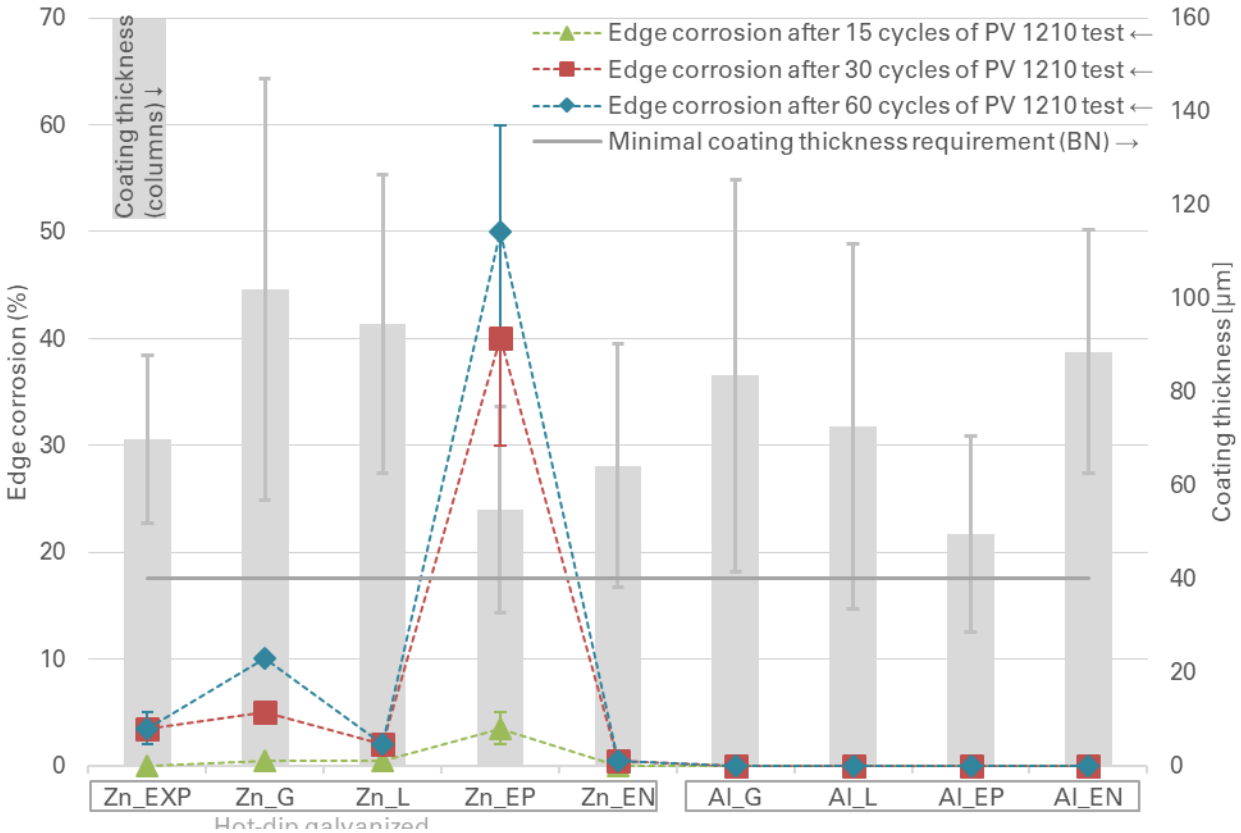

Figure 79. Comparison of edge corrosion results (colored symbols) on powder coated specimens, after 15, 30 and 60 cycles of the PV 1210 test, in relation to coating thickness (columns) and different substrates

6.1.8.2. Degree of corrosion and delamination around a scribe

Figure 80 displays the delamination results on powder coated specimens after 15, 30 and 60 cycles of PV 1210 test. Marked with green triangles, the degree of corrosion and delamination on Zn_EXP and Zn_EP is above the Brose requirement of 1,5 mm after 15 cycles, while Zn_EN is a borderline case.

With increased testing time, the degree of delamination increases exponentially on Zn_L, ZN_EP and Zn_EN. This phenomenon can be explained by taking the pretreatment processes of those specimens into account. Unlike other specimens, Zn_L does not have a passivation step after phosphating. Zn_EP and Zn_EN have an iron phosphate step, while the other specimens have a tricationic phosphate step in the pretreatment. Alumimium specimens continue to exhibit virtually no degree of delamination.

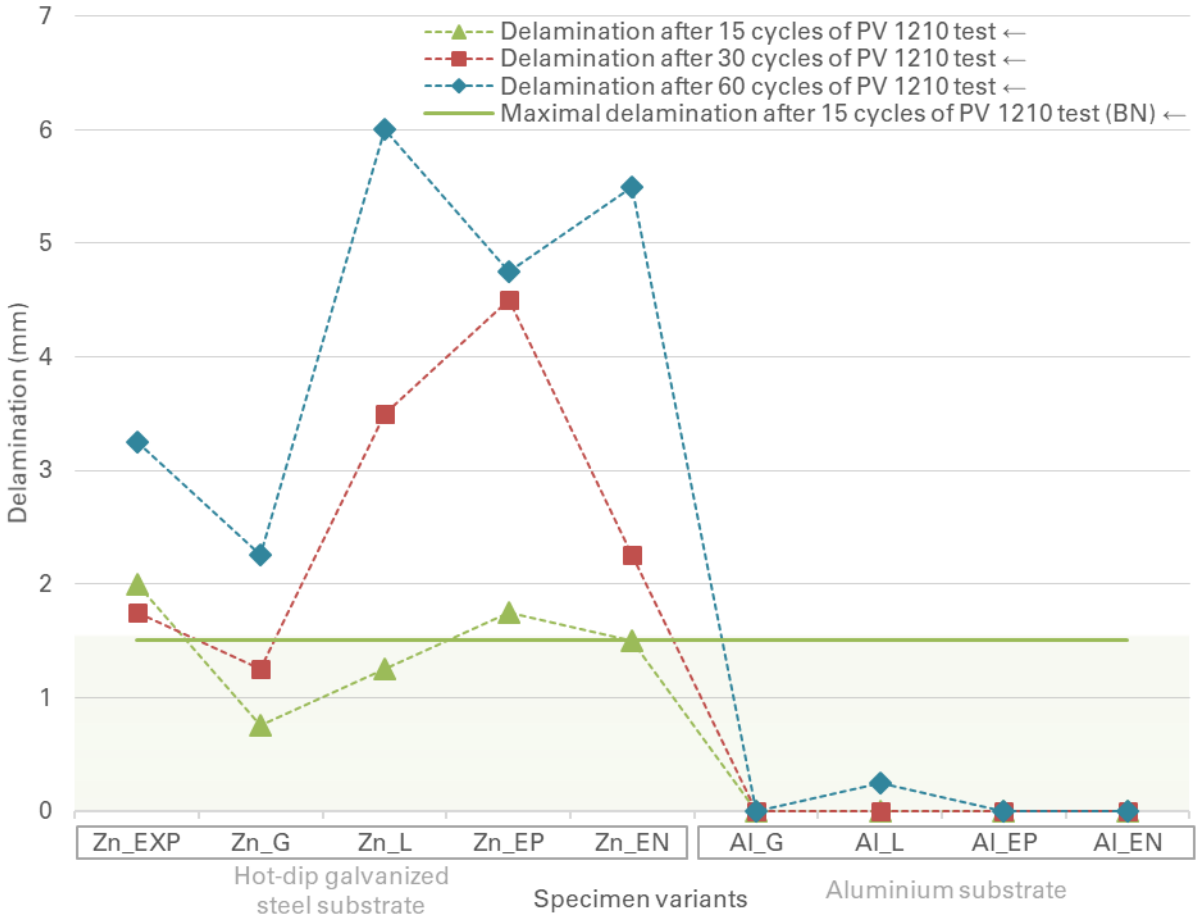

Figure 80. Comparison of edge corrosion results (colored symbols) on powder coated specimens, after 15, 30 and 60 cycles of the PV 1210 test, in relation to different substrates

6.1.9. VDA-new test – CED specimens

6.1.9.1. Degree of rusting on edges (Edge corrosion)

Figure 81 displays the edge corrosion results on CED specimens after one, three and six cycles of VDA-new test. Marked with green triangles, edge corrosion after one cycle of testing is well below the maximal edge corrosion requirement of 30 % on all specimens. This is not an internal Brose requirement, but the test is clearly defined in the DBL 7381 (Daimler standard for coatings in the vehicle exterior). Since the demands for parts in the vehicle exterior are noticeably higher than for parts in the interior, the test durations are adopted from the DBL 7382 (Daimler standard for coatings in the vehicle interior), which has not been updated with the VDA-new test yet. The brose standard does not include this requirement, because it is not yet required for CED parts.

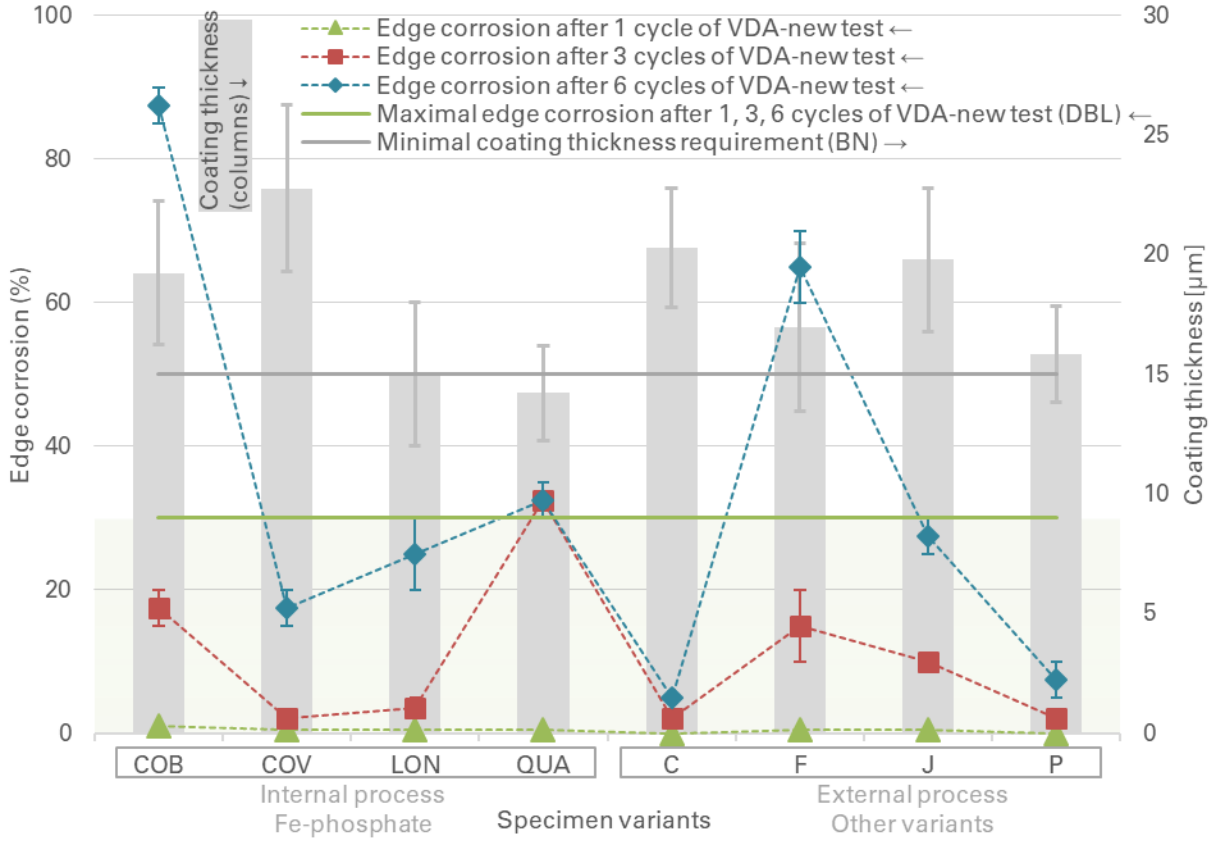

Figure 81. Comparison of edge corrosion results (colored symbols) on CED coated specimens, after one, three and six cycles of the VDA-new test, in relation to coating thickness (columns) and different pre-treatment variants

In contrast, most specimens exhibit a substantial degree of rusting on edges with increased testing durations. After three cycles of testing, QUA is the only outlier with more than 30% edge corrosion. This finding is probably connected to the lacking coating thickness of the specimen.

Specimens C and P consistently show the least degree of edge corrosion throughout the test, while COB and F make an extreme jump after six cycles.

6.1.9.2. Degree of corrosion and delamination around a scribe

Figure 82 displays the delamination results on CED coated specimens after one, three and six cycles of VDA-new test. Marked with green triangles, the degree of corrosion and delamination after one cycle of testing is below the requirement of 2 mm, on all specimens. Just like in the case of edge corrosion, the requirement comes from Daimler's standard DBL 7381. The same procedure for choosing testing times and evaluation criteria as for degree of rusting is applied here.

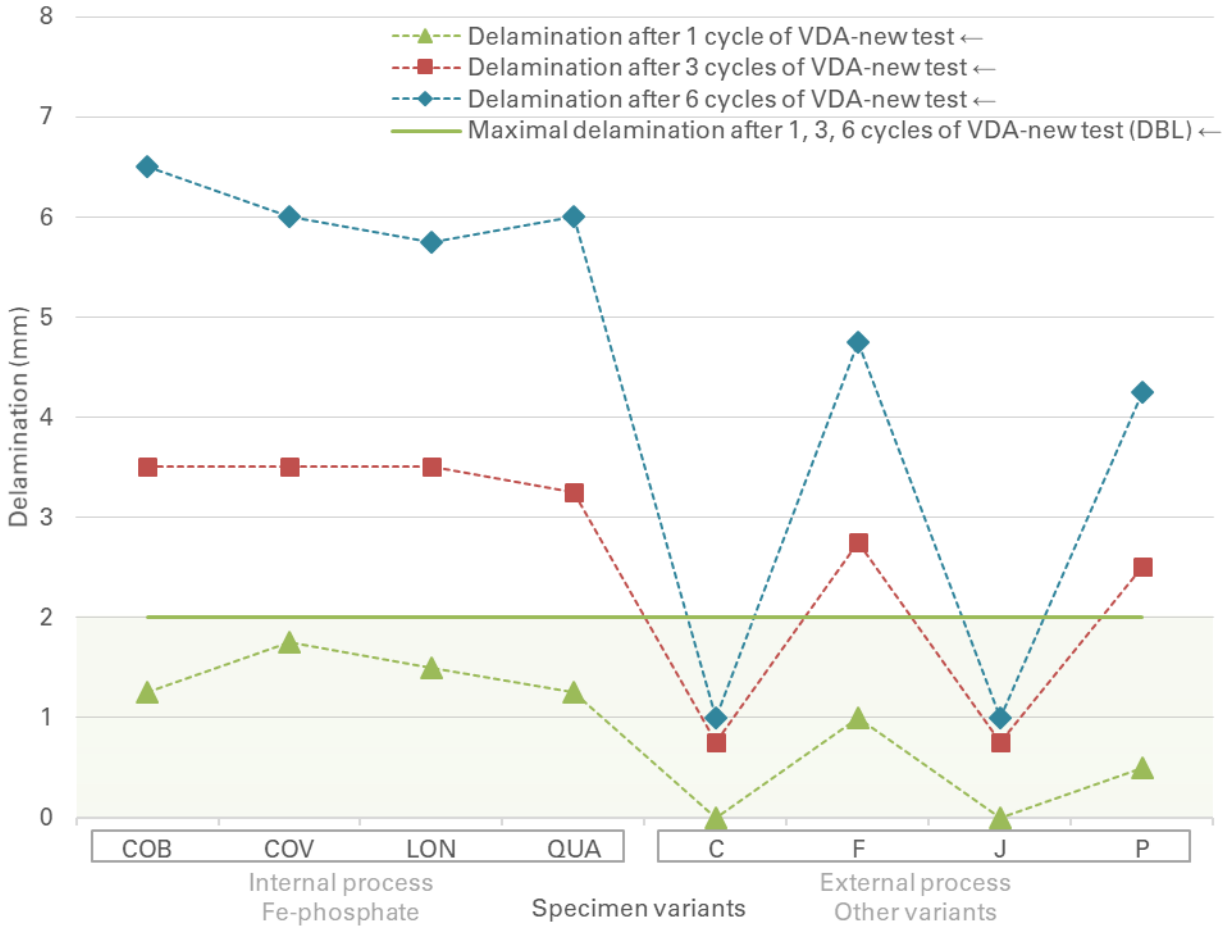

Figure 82. Comparison of delamination results (colored symbols) on CED coated specimens, after one, three and six cycles of the VDA-new test, in relation to different pre-treatment variants

Upon taking a closer look at figure 82, an interesting pattern can be seen. Specimens with the iron phosphate exhibit a higher degree of delamination than specimens with other pre-treatment variants after matching testing times. Furthermore, the degree of delamination seemingly doubles after three and six cycles on those specimens. A similar pattern of increasing delamination can be observed in other specimens too, but with lesser effects. This would indicate that the degree of delamination is greatly connected with the pre-treatment variant of specimens. Specimens C and J continue to exhibit the least amount of delamination.

While on the topic of delamination, another fascinating phenomenon was discovered on CED specimens with iron phosphate pre-treatment. COB, COV, LON and QUA started exhibiting a mild degree of coating delamination at the top and bottom of the specimens after just three cycles of the test. The degree of delamination increased considerably after six cycles of testing, as shown in figure 83. The same phenomenon is not found among any specimens with other pre-treatment variants.

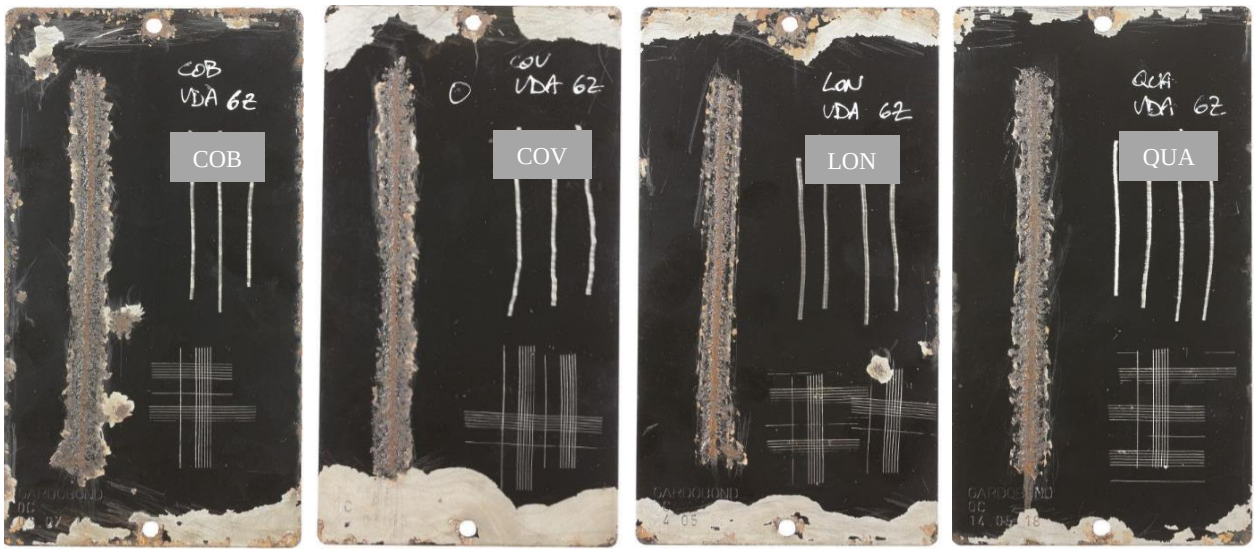

Figure 83. Delaminated edges on specimens with iron phosphate after six cycles of VDA-new test (COB, COV, LON, QUA)

The source of this delamination are seemingly the holes and edges of the specimens, where a wave like discoloration, spreading towards the centre of the specimen is observed (Figure 84).

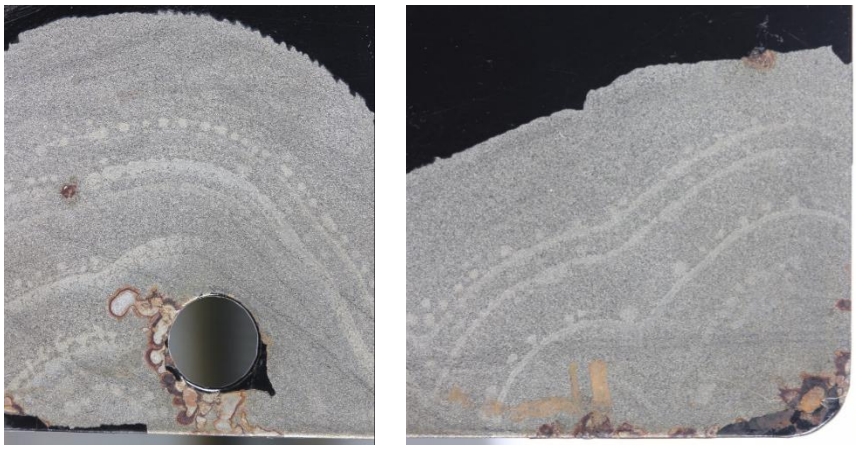

Figure 84. Close up of the delaminated areas around the hole and corned on COV after six cycles of VDA-new test

Interestingly, the corrosion pattern around the scribe lines on CED specimens in the VDA-new test is unlike any other, as seen in figure 85.

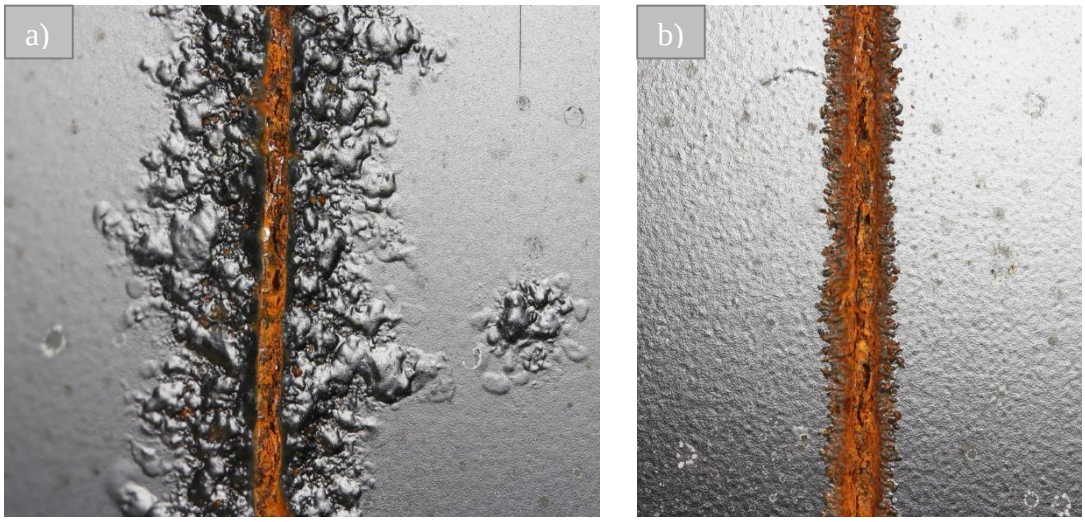

Figure 85. Corrosion pattern around scribe lines on CED coated specimens after six cycles of VDA-new test a) specimen COB b) specimen C

Specimens with the iron phosphate have rigid elevated areas spreading away from the scribe line. The coating itself can not be removed easily from the seemingly swollen area, as it strongly adheres to the underlying corrosion products. The overall course of the corroded area appears more symmetrical and less random than in other climatic tests. Oppositely, specimens with the tricationic phosphate form an elevated trace of corrosion products right above the scribe line. These corrosion products are also hard to remove for the evaluation, but no delamination of the surrounding coating can be detected.

6.1.9.3. Daimler scratch test

Figure 86 displays the scratch test results on CED coated specimens after one, three and six cycles of VDA-new test. The green, red and blue bars represent the results after increasing testing times, while the grey bar indicates the initial grade established prior to the test. Consistently, the maximal acceptable grade after any testing time is K2.

Specimen QUA is the only outlier with K3 after all durations of the test. This means, that coating adhesion is not satisfactory after those testing times.

Specimens C and J are not influenced by the stresses of the VDA-new test and continue to demonstrate a remarkable level of adhesion with the grade K0.

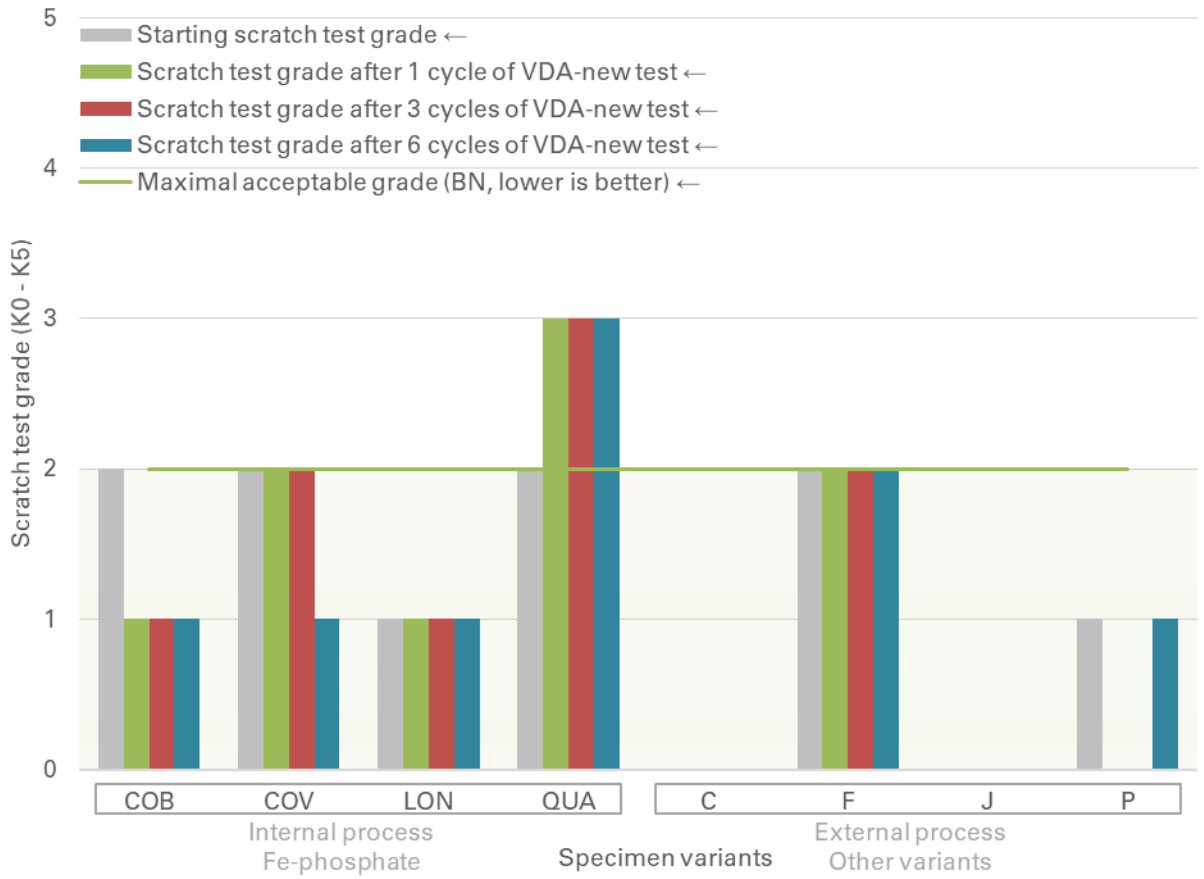

Figure 86. Comparison of scratch test results (colored bars) on CED coated specimens, after one, three and six cycles of the VDA-new test, in relation to initial values (grey bars) and different pre-treatment variants

6.1.10. VDA-new test – Powder coated specimens

6.1.10.1. Degree of rusting on edges (Edge corrosion)

Figure 87 displays the edge corrosion results on powder coated specimens after three, six and nine cycles of VDA-new test. The minimal edge corrosion requirement is defined in the DBL 7381 standard and is not yet integrated in the Brose standard. In this particular DBL standard, the degree of corrosion should be measured only on one edge of a part and not all edges like in this examination. Therefore, the resulting edge corrosion might appear more severe. After three cycles of testing, the edges should not exhibit more than 5% corrosion.

Specimen Zn_EP is the only outlier in this chart, with edge corrosion values higher than 60% after 9 cycles of testing. This result is most likely connected to the relatively low coating thickness of Zn_EP, which dips under the minimal requirement of 40 µm. All aluminium specimens exhibit no degree of rusting on edges.

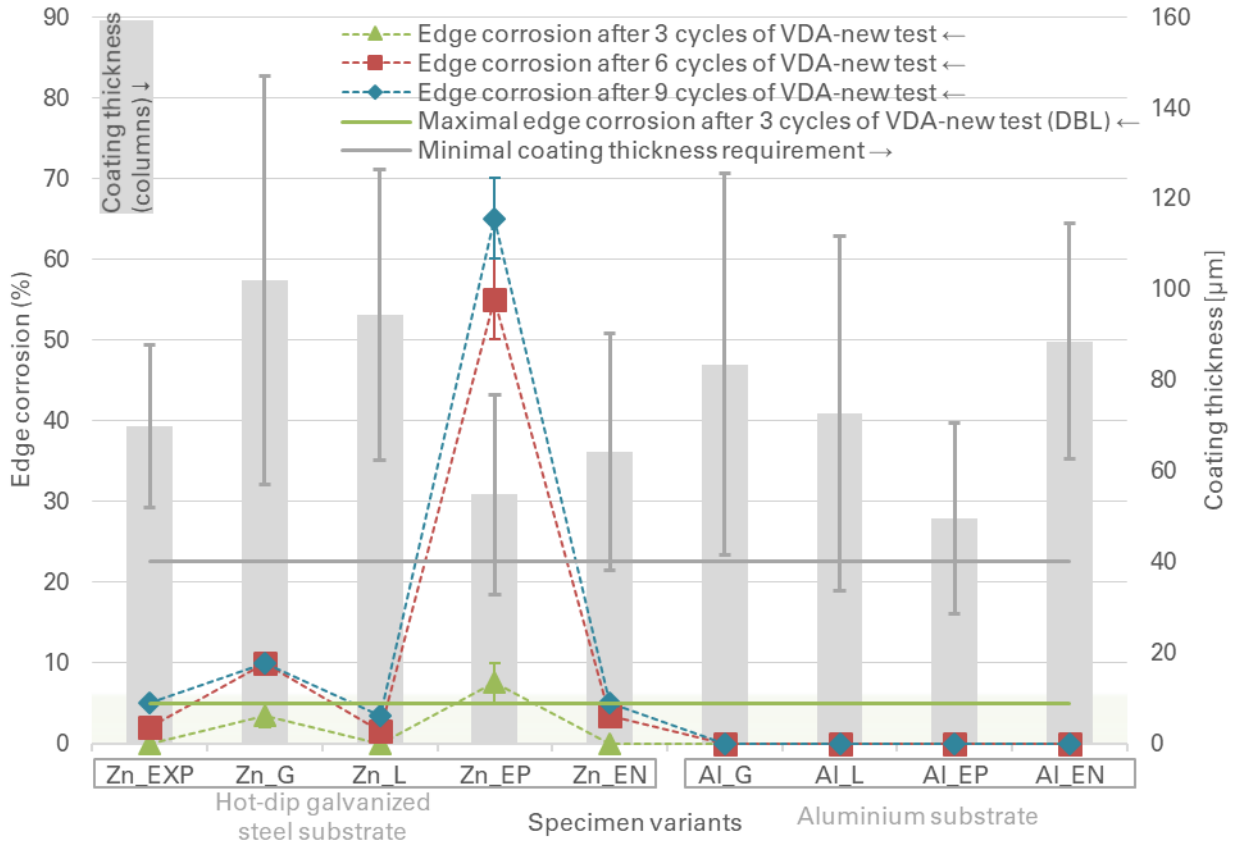

Figure 87. Comparison of edge corrosion results (colored symbols) on powder coated specimens, after three, six and nine cycles of the VDA-new test, in relation to coating thickness (columns) and different substrates

6.1.10.2. Degree of corrosion and delamination around a scribe

Figure 88 displays the delamination results on powder coated specimens after three, six and nine cycles of VDA-new test. The delamination requirement for hot-dip galvanized steel specimens is also defined in the DBL 7381. According to the standard, the specimens should not exhibit more than 4 mm delamination after three, six or ten cycles of the test. Evident form the chart, all specimens comply with this requirement.

The degree of delamination, on all specimens, is fairly low for all durations of the VDA-new test. Moreover, the aluminum specimens also exhibit a small degree of delamination. This finding would confirm that this test is more in line with realistic corrosion propagation pictures (Figure 42), at least on hot-dip galvanized and aluminum substrates with powder coatings.

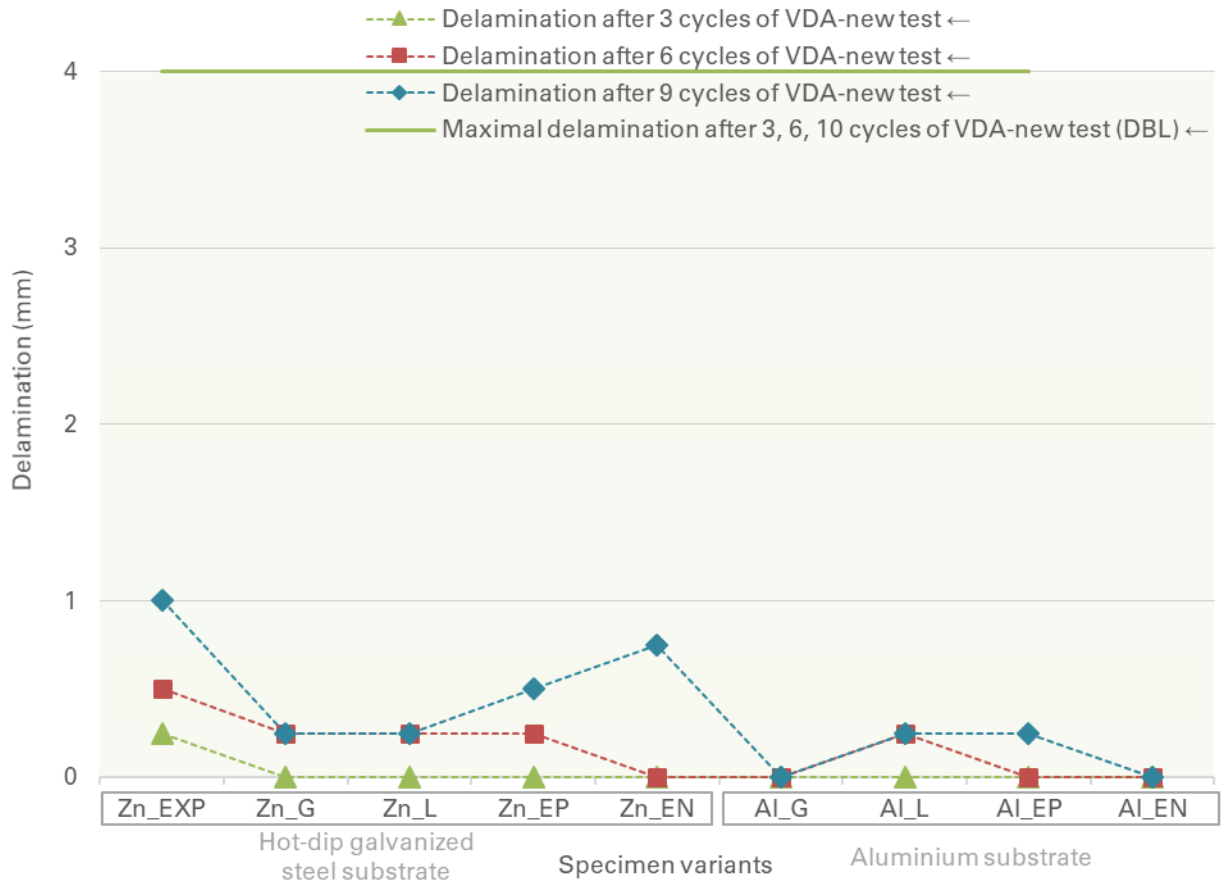

Figure 88. Comparison of edge corrosion results (colored symbols) on powder coated specimens, after three, six and nine cycles of the VDA-new test, in relation to different substrates (the full extent of Zn_EXP delamination not shown in chart)

6.1.11. Comparison test results from Faculty of Mechanical Engineering and Naval Architecture in Zagreb

6.1.11.1. CH test - CED and Powder coated specimens

Both laboratories reproduced virtually identical CH test results for every evaluation criterion, both on CED and powder coated specimens. This would demonstrate that the results of the CH test are constant and reproducible across multiple laboratories. Therefore, graphical demonstration of those results will be omitted in this part to avoid repetitiveness. The comparison CH test results will be shown in appendix A instead.

One noteworthy finding is the degree of blistering on the Al_G specimen, which is identical to the one revealed in the Brose laboratory.

6.1.11.2. NSS test – CED coated specimens

Degree of rusting on edges (Edge corrosion)

Figure 89 displays the edge corrosion results on CED specimens after 96, 144 and 240 hours of NSS test. Marked with a green triangle, specimen LON was the only one tested for 96 hours. After that time, LON exhibits less than 5% edge corrosion, which is in line with the Brose requirement.

Similar to the NSS test at the Brose laboratory, specimen QUA shows the highest degree of rusting on edges after 240 hours, most likely due to the low coating thickness.

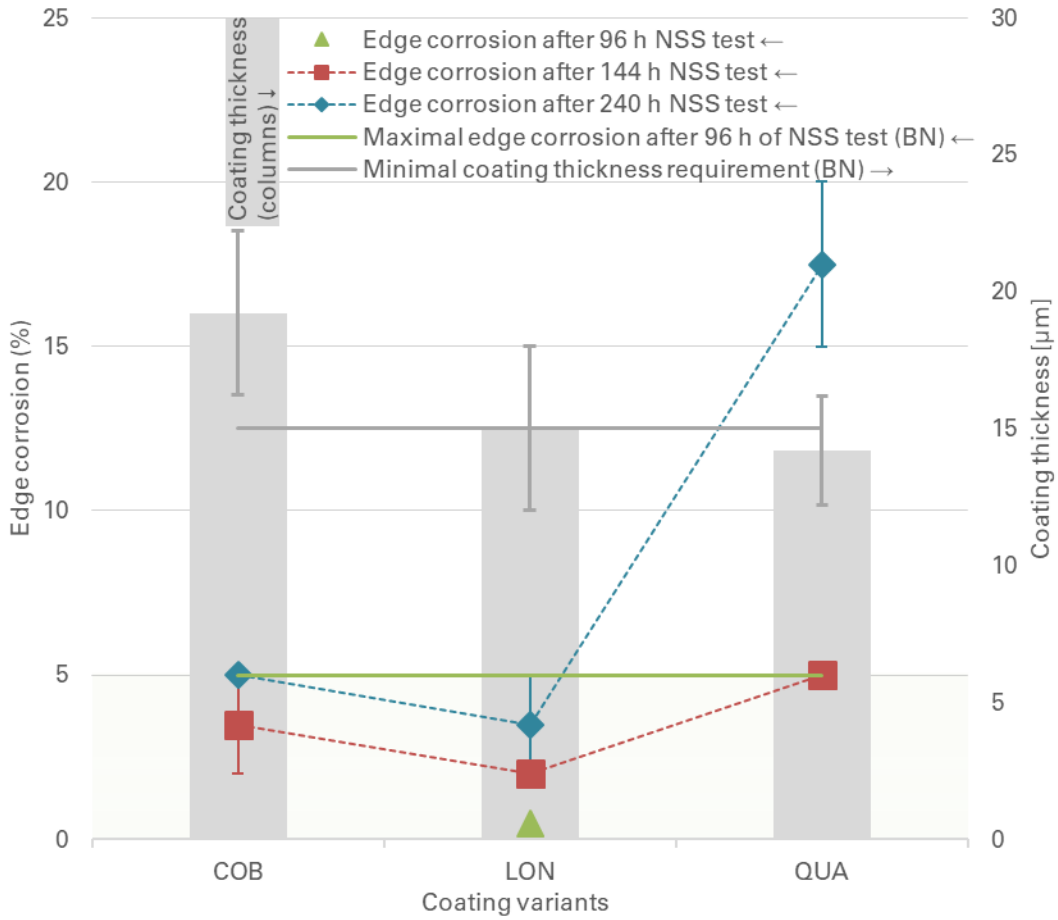

Figure 89. Comparison of edge corrosion results (colored symbols) on CED coated specimens, after 96, 144 and 240 hours of the NSS test in relation to coating thickness (Laboratory for the protection of materials)

Degree of corrosion and delamination around a scribe

Figure 90 displays the delamination results on CED coated specimens after 96, 144 and 240 hours of NSS test. Marked with a green triangle, specimen LON was the only one tested for 96 hours. After that time, LON exhibits less than 1 mm of delamination, which is in line with the Brose requirement. Furthermore, none of the specimens show more than 1 mm of delamination even after 240 hours.

This result is straying a bit from the measured delamination on the specimens tested in the Brose laboratory. This deviation can be explained when taking a look at the running parameters of the tests. For example, the viable pH range for the NSS test is from 6,5 to 7,2 pH, as defined in the standard. Brose materials laboratory tries to keep the pH value close to 6,5 in order to have a stricter test, while the NSS test in Zagreb is usually carried out with pH values closer to 7,2. These variations should be further examined in order to identify all causes for the differences in results.

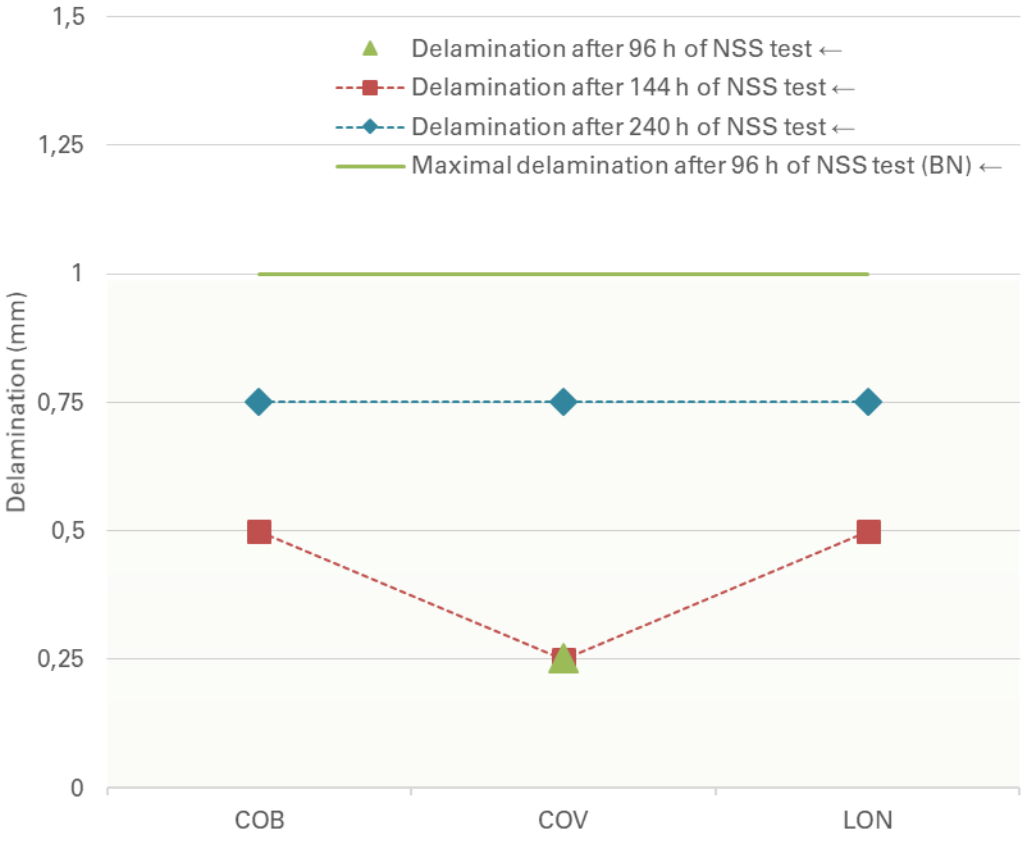

Figure 90. Comparison of delamination results (colored symbols) on CED coated specimens, 96. 144 and 240 hours of the NSS test (Laboratory for the protection of materials)

6.1.11.3. NSS test – Powder coated specimens

Degree of rusting on edges (Edge corrosion)

Figure 91 displays the edge corrosion results on powder coated specimens after 240, 360 and 480 hours of NSS test. The results correlate well with those of the NSS test at the Brose laboratory, except for Zn_G. This specimen exhibits unusually high degree of rusting on edges, compared to all other tests, including the NSS test carried out in the Brose materials laboratory. After further examination, the cause for this unusually high values is found; specimen Zn_G was put in the specimen carrier with the burr side facing upwards. The edge on that side was attacked more aggressively, as the coating thickness is much thinner around the burr. This also confirms

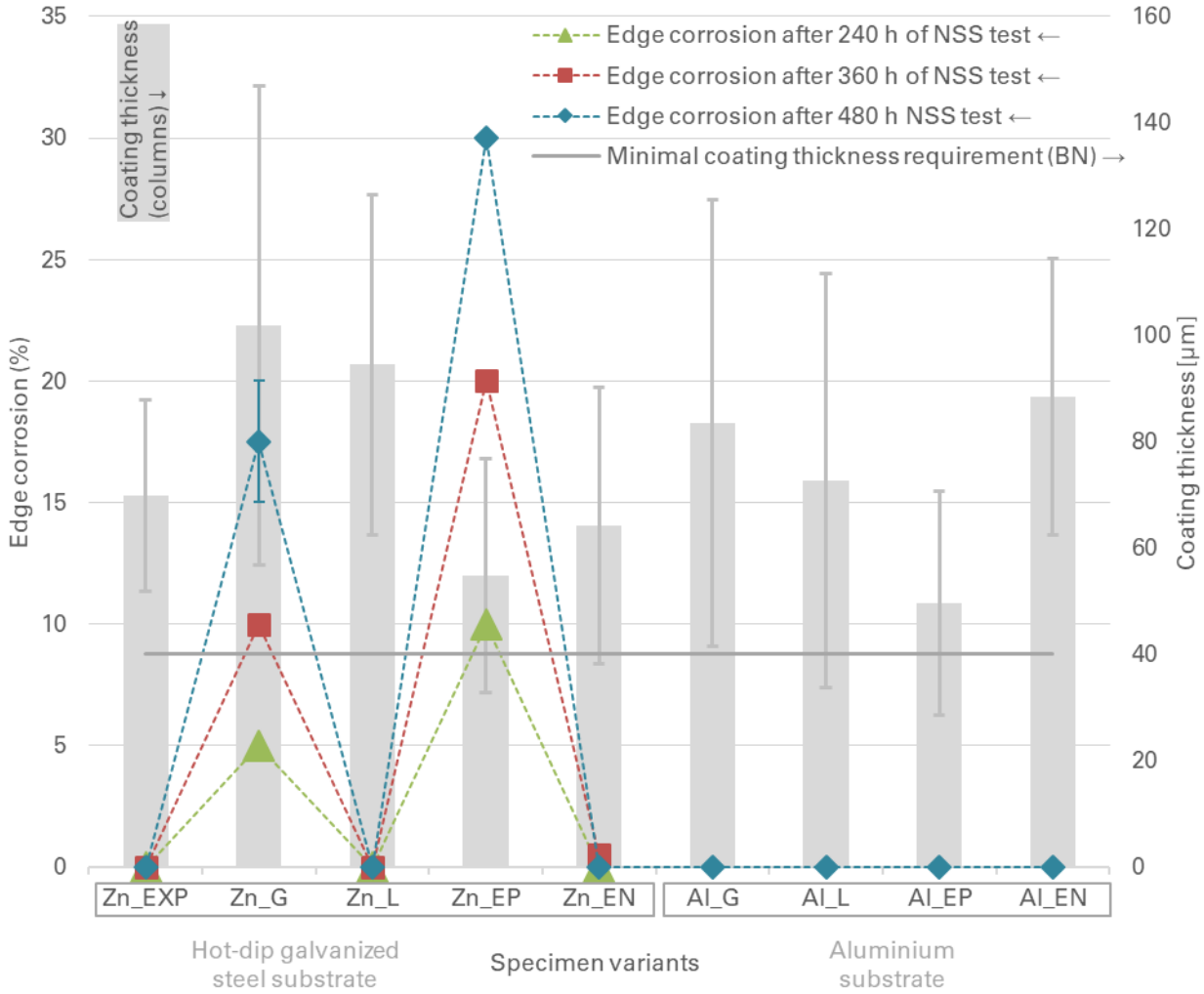

Figure 91. Comparison of edge corrosion results (colored symbols) on powder coated specimens, after 240, 360 and 480 hours of the NSS test, in relation to coating thickness (columns) and different substrates (Laboratory for the protection of materials)

the importance of uniform specimen orientation in the tests, as otherwise, they would exhibit results which could not be compared with each other.

Specimen Zn_EP continues to exhibit the highest degree of edge corrosion, most likely related to low coating thickness, while none of the aluminium specimens show any degree of rusting on edges.

Degree of corrosion and delamination around a scribe

Figure 92 displays the delamination results on powder coated specimens after 240, 360 and 480 hours of NSS test. Marked with green triangles, the degree of corrosion and delamination on all hot-dip galvanized steel specimens is well below the Brose requirement of 1 mm.

The same differences in delamination severity, compared to the NSS test in the Brose laboratory, can be observed on the powder coated specimens. The relatively low degree of

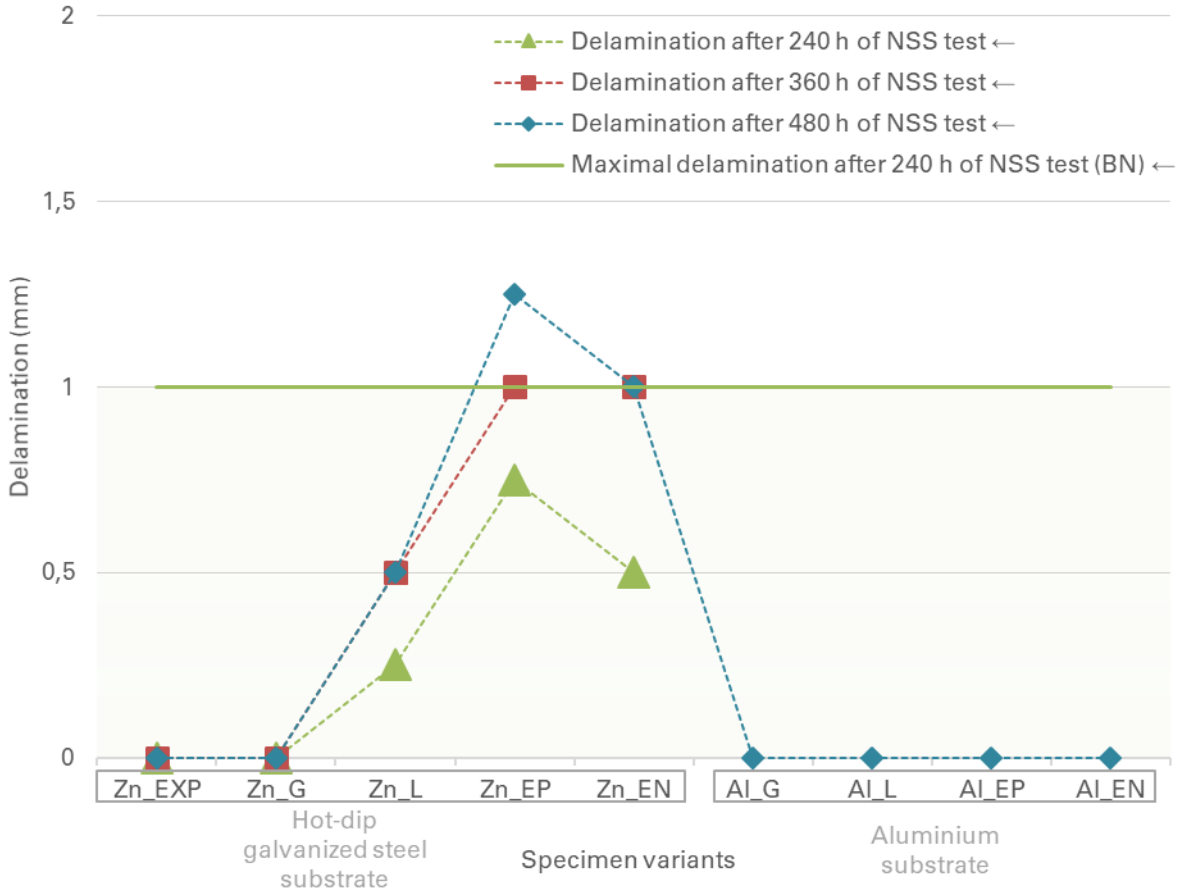

Figure 92. Comparison of edge corrosion results (colored symbols) on powder coated specimens, 240, 360 and 480 hours of the NSS test, in relation to different substrates (Laboratory for the protection of materials)

delamination is most likely connected to the difference in the running parameters of the NSS test. Nevertheless, the results are comparable, but on a slightly lower scale.

6.1.12. Results from evaluation methods not depicted in charts

6.1.12.1. Degree of rusting on surface across all tests

The CED specimens exhibit virtually no degree of rusting on the surface in any of the tests. The only exceptions, which show surface rusting, are small mechanically damaged areas, which were marked upon first visual inspection. These local defects, most likely caused by rough transportation and handling, were prevalent in specimens which were shipped from great distances. Consequently, those areas are excluded from the evaluation. In this regard, all of the CED specimens have 0% of rust on the surface and comply with the Brose standard requirement.

In the same respect, the powder coated specimens also display no degree of surface rusting in any of the tests. Moreover, these specimens do not have local defects which could potentially corrode in the tests and also comply with the Brose standard.

6.1.12.2. Cross-cut test

Both the CED and powder coated specimens do not show any changes in relation to the initial values in the cross cut test. More precisely, all specimens received the best possible grade of zero, while QUA is the only outlier with a grade of one in some tests. Since QUA was graded with zero to one before the tests, the value of one is not considered as a significant change. Thereby, all specimens meet the Brose requirement. The detailed results of the cross-cut test will be displayed in the appendix.

6.1.12.3. Degree of blistering

There is no visible surface blistering on any CED specimens after all durations of the NSS test, with the exception of COB after six cycles of Cycle B test (Figure 93).

All other CED specimens meet the Brose requirement of no degree of blistering on the surface.

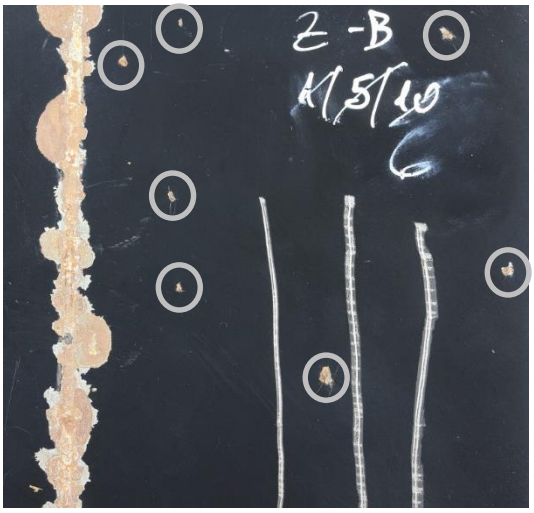

Figure 93. Blistering on the surface of COB after six cycles of Cycle-B test

A similar story is repeated when examining the powder coated specimens. None of the specimens exhibit any blistering, except for Al_G in the CH, PV 1210, Cycle-B and VDA-new test. In the PV 1210, Cycle-B and VDA-new test, the blistering on AL_G is concentrated around the scribe line, as shown in figure 94.

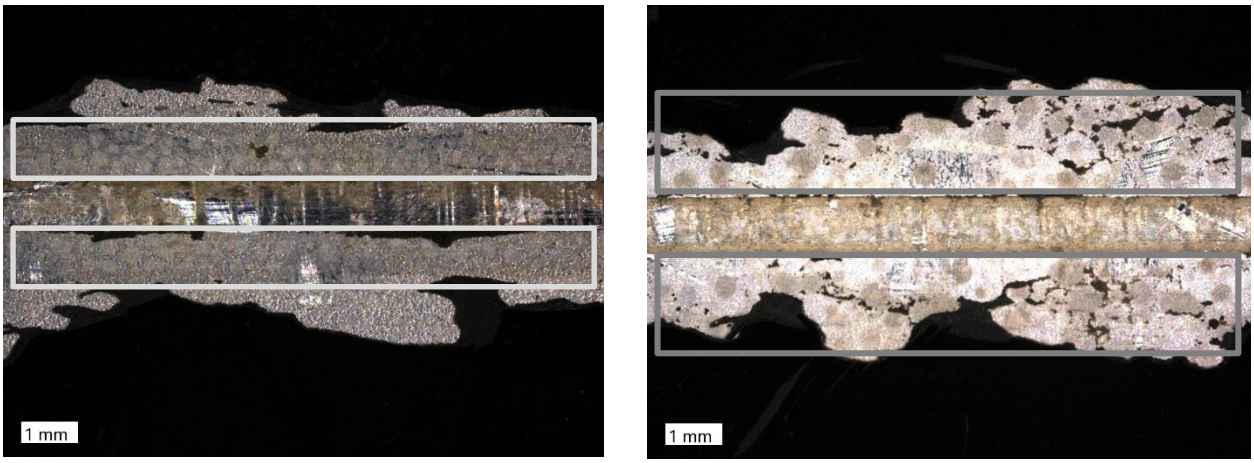

Figure 94. Blistering around the scribe line on the Al_G specimen after nine cycles of VDA-new and six cycles of Cycle-B test

At longer durations of the CH test, the blistering spreads throughout the whole surface while impairing coating adhesion (Figure 95.) The blisters were revealed while attempting to determine the degree of delamination around the scribe line.

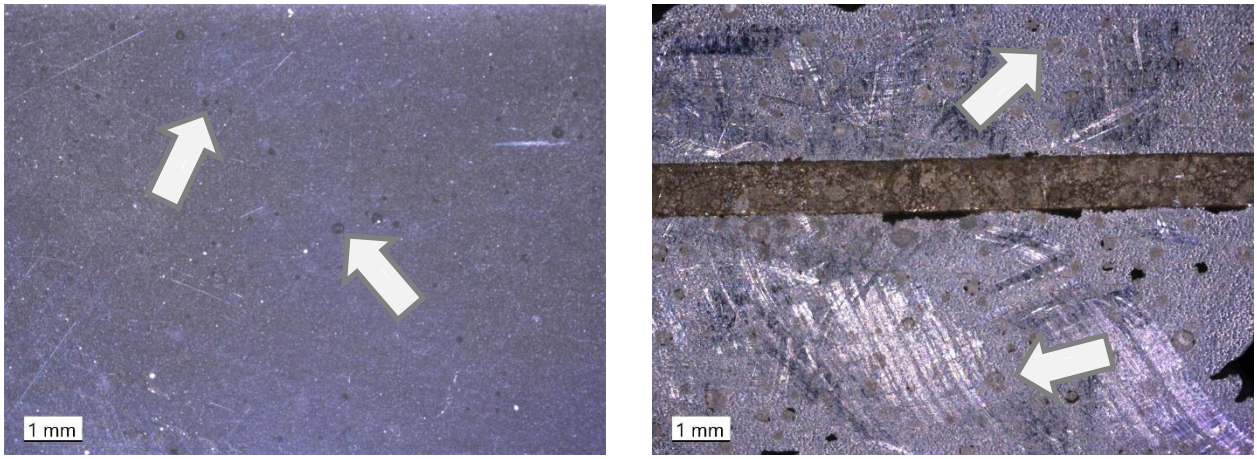

Figure 95. Blistering on the surface of the AL_G specimen, after 480 hours of CH test

During the evaluation, the coating could be pushed aside with relative ease, revealing small discoloured circles on the surface. Precise results of the degree of blistering for all listed tests are available in the evaluation tables in appendix A.

6.1.13. General assessment for individual accelerated corrosion tests

This part will go over some frequent phenomena found during the specimen evaluation, as well as the reasoning behind certain anomalies.

Firstly, the scattered results of the scratch tests have to be discussed. Every Daimler scratch test chart displays at least one specimen where a lower grade is given to a particular specimen after a longer test duration. At first, this appears counter intuitive, since it is expected that the specimens would deteriorate more with increased testing duration. However, after remembering the flaws of the scratch test and the subjective nature of the evaluation, such results can be expected. Moreover, after comparing all results from the test and initial values, it is obvious that not much has changed. This would mean that the accelerated corrosion tests had just a slight effect on the degree of adhesion when tested with this method. The pre-treatment of the specimens is satisfactory, and no problems are detected in that regard with this test.

The specimen QUA seems to be influenced the most by the tests in regard to coating adhesion. This result might stem from the fact that QUA is a relatively new internal coater which did not have the chance of running the plant under full occupation. Without doing so, the coating process cannot be dialled in to the full extent. Resulting is a still relatively instable process subjected to fluctuations that are to be expected from any new coating plant. QUA will start series production in 2019, by that time the coating process should be entirely stable. The latest series monitoring test on CED parts show considerably better results, thereby confirming that the coating process at QUA is now operating at a satisfactory level [17].

In contrast, specimens C and J have the best overall results from all CED coatings in every test, with C surviving even the benchmark durations without any notable signs of corrosion or other alterations. This most likely originates from the pre-treatment differences between the specimens. The tricationic phosphate seems to be superior to the iron phosphate in regard to the extent of edge corrosion, adhesion and delamination. In addition to the tricationic phosphate, C and J have a passivation step in their pre-treatment, unlike any other CED coating. This seems to further increase their corrosion resistance properties across multiple tests. Finally, specimen C, which shows the best overall results of any CED specimen, is coated with compatible products form just one company. It is evident that running a coating process with corresponding products from one supplier yields the best results.

Secondly, the test durations for the CED coated specimens have to be reviewed further. Evident from the results is that the longer durations, like six cycles of VDA-new or Cycle-B test, represent greatly exaggerated stresses for those parts. Most of the specimens start to fluctuate wildly when exposed for such long times. CED coatings are generally not designed to withstand those high stresses, as they are usually tested up to three cycles in climatic tests or just 96 hours in the NSS test. Nevertheless, the idea of overstraining the coatings to their limits was successful, as some clear favourites like C and J emerged.

Lastly, another recommendation can be made regarding the coating thickness of powder coated parts. Specimen Zn_EP exhibits by far the most unfavourable results regarding edge corrosion in all climatic test. This occurrence is at least partly connected to the low coating thickness, which measures less than the required 40 µm at some points of the specimen. Additional influencing factors should also be considered when judging this phenomenon and deciding about future steps to mitigate such results. Altogether, in order for powder coated parts to be more reliable in the future, the minimal coating thickness could be increased. This alone would provide superior protection properties without any immense changes of other parameters in the coating process.

6.2. Comparison among the accelerated corrosion tests

In order to gage any similarities or differences between all utilized accelerated corrosion tests, comparison charts for specific evaluation criteria are made. The specimens are grouped into CED and powder coated categories, just like for the individual results. The CH test has been deliberately excluded from this comparison, as none of the specimens exhibit any significant changes in relation to the chosen criteria, at least not to the extent of other climatic tests. This should not detract from the effectiveness of the CH test but imply that the used coating and pre-treatment processes are on a high technological level.

From the six previously utilized evaluation criteria, the degree of rusting on edges and degree of delamination around a scribe demonstrate distinctive results on both CED and powder coated specimens. Other evaluation criteria exhibit modest changes compared to the initial state of specimen, but still capture individual cases with extreme results, i.e. blistering on Al_G specimens and K3 scratch test grade on specimen QUA. Therefore, the following comparison charts are based on the former two criteria, which best depict specimen behaviour across all specimens, rather than just for a handful of them.

When determining the durations, which should be used for the comparison, the midpoint durations of climatic tests appeared most rational. At the midpoint of the climatic tests, which means, after three weeks of testing for CED and six weeks for powder coated specimens, specimens exhibit plentiful changes in relation to coatings, pre-treatment variants or different substrates. In contrast, after the shortest durations, i.e. one week of any climatic test for CED or three weeks for powder coated specimens, they exhibit minimal changes in relation to the chosen evaluation criteria. Thus, no obvious differences between coatings or pre-treatment variants can be seen. Contrary, the longest durations, six to ten weeks, are subject to high fluctuations, which would make an objective comparison more difficult.

The only exception in the following comparison is the NSS test. In order to compare the results of the NSS test to other climatic tests, the duration of the NSS test, which exhibits the most similar results to the midpoint duration of the climatic tests is chosen. Meaning that CED specimens after 240 hours of NSS test, exhibit similar results as specimens after three weeks of climatic tests. The same is true for powder coated specimens, which, after 480 hours of NSS test exhibit similar results to specimens after six weeks of climatic tests.

6.2.1. CED coated specimens

6.2.1.1. Degree of rusting on the edges

Figure 96 displays the edge corrosion results on CED specimens after three weeks of Cycle-B, PV 1210 and VDA-new test and 240 hours of NSS test.

At the first glance, the results seem to scatter randomly, and the tests do not appear analogues, but upon a second look, some regularities can be observed. Evident from all tests, specimen C exhibits the lowest degree of edge corrosion, compared to all other specimens. Other specimens show more fluctuations from test to test than C. QUA fluctuates from under 5 %, all the way to 35% , similar to J. Unlike QUA and J, specimen F fluctuates at higher percentages of edge corrosion, but in a much tighter distribution. Based on the compared results, a singular influencing factor for the degree of rusting on edges can not be determined.

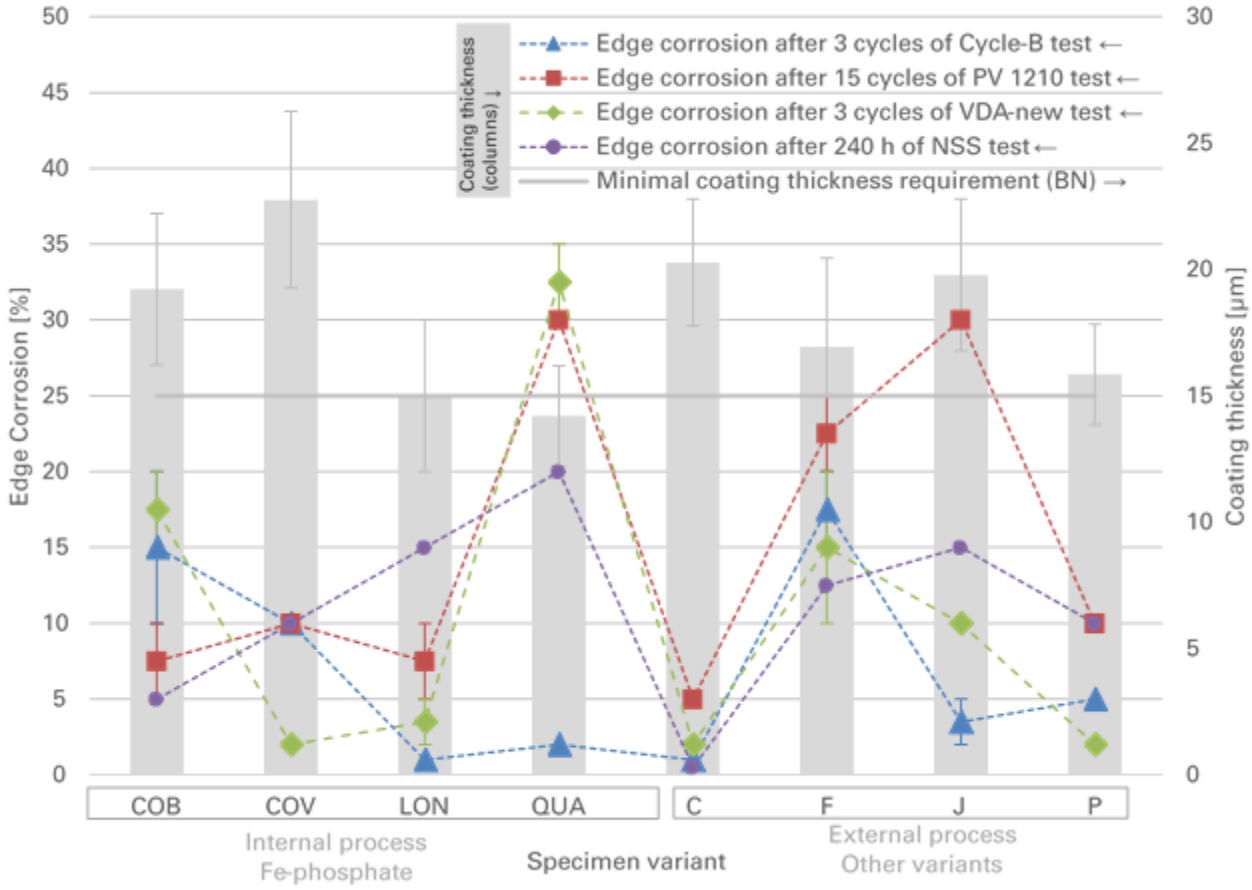

Figure 96. Comparison of edge corrosion results (colored symbols) on CED coated specimens, after 3 cycles of Cycle-B and VDA-new test,15 cycles of PV 1210 test and 240 hours of NSS test in relation to coating thickness (columns) and different pre-treatment variants

6.2.1.2. Degree of corrosion and delamination around a scribe

Figure 97 displays the delamination results on CED specimens after three weeks of Cycle-B, PV 1210 and VDA-new test and 240 hours of NSS test.

As previously described, the NSS test shows the least amount of delamination when compared to cyclic tests. The PV 1210 test exhibits a higher degree of delamination trend, compared to the Cycle-B test. Meaning that the daily intermittent phases of the test (salt spray, humidity and dry phase) have a greater degree of influence on CED coatings.

In the VDA-new test specimens with iron phosphate exhibit a higher degree of delamination than specimens with other phosphate variants in all tests. Particularly, specimens C and J with tricationic phosphate and subsequent passivation continue to exhibit the least amount of delamination. VDA-new seems to mainly show the differences in the pre-treatment, while the results of other climatic tests show other significant influences, like coating variant.

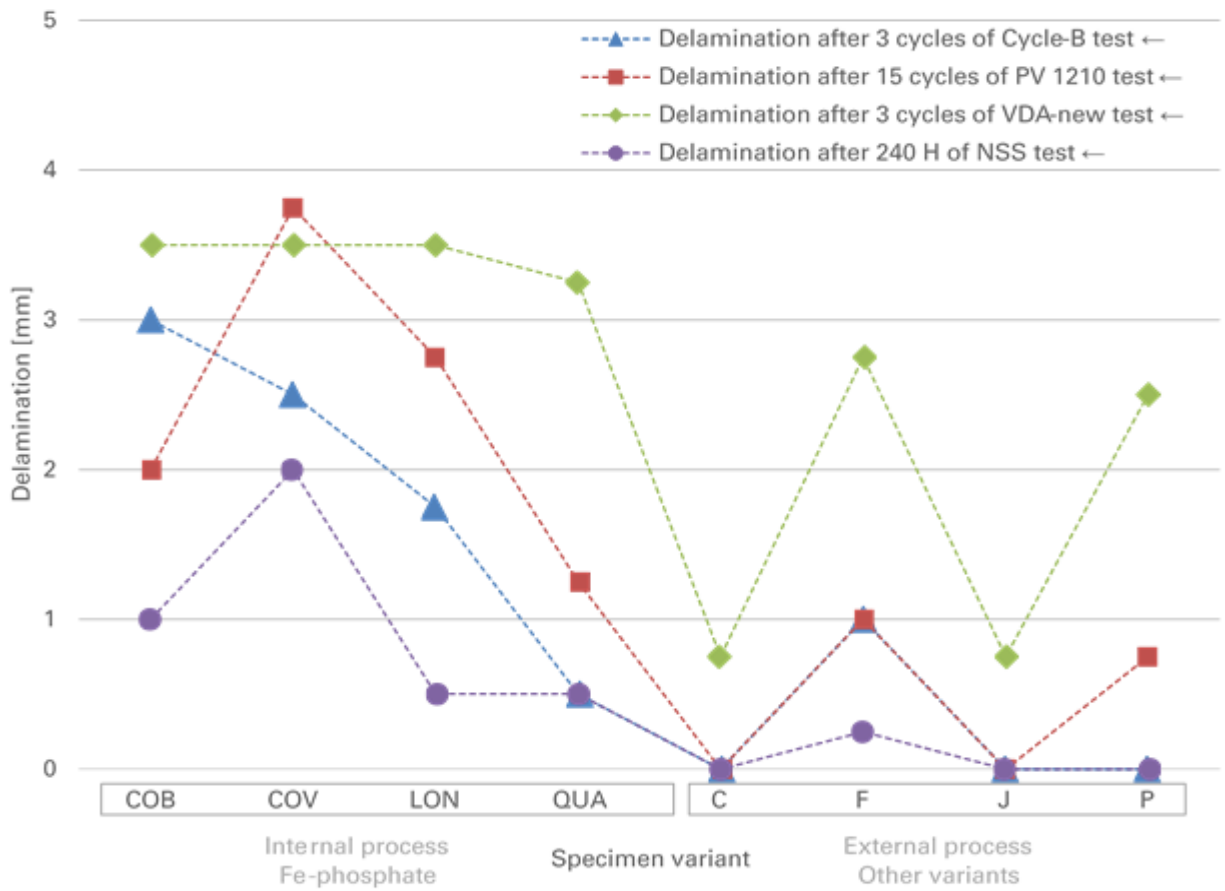

Figure 97. Comparison of delamination results (colored symbols) on CED coated specimens, after 3 cycles of Cycle-B and VDA-new test,15 cycles of PV 1210 test and 240 hours of NSS test in relation to different pre-treatment variants

6.2.2. Powder coated specimens

6.2.2.1. Degree of rusting on the edges

Figure 98 displays the edge corrosion results on powder coated specimens after six weeks of Cycle-B, PV 1210 and VDA-new test and 480 hours of NSS test.

Interestingly, the edge corrosion results from all tests correlate with each other to a great extent. In the focus of the chart is the relation between hot-dip galvanized steel and aluminium substrates. Apparent from the comparison, aluminium specimens exhibit no degree of rusting on edges. This would call for the implementation of other accelerated corrosion tests, designed specifically for aluminium substrates, which are not included in this thesis, i.e. CASS test (copper-accelerated acetic acid salt spray).

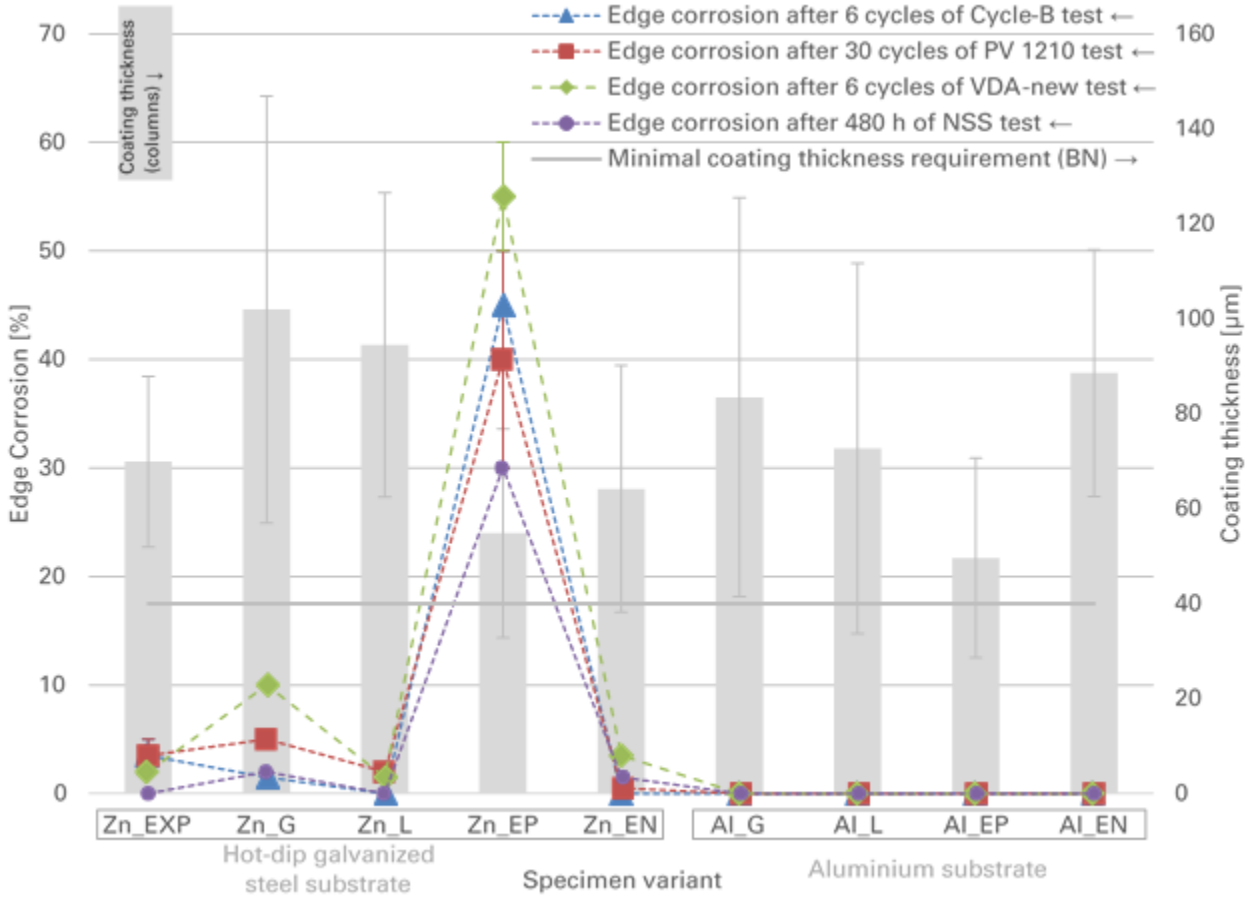

Figure 98. Comparison of edge corrosion results (colored symbols) on powder coated specimens, after 6 cycles of Cycle-B and VDA-new test,30 cycles of PV 1210 test and 480 hours of NSS test in relation to coating thickness (columns) and different substrates

Hot-dip galvanized steel specimens with the relatively high coating thickness on the edges, show sufficient protection regarding edge corrosion across all tests. The only major outlier is Zn_EP with high degrees of edge corrosion. Zn_EP has the lowest coating thickness, but all influencing factors on the unfavourable edge corrosion results should be further exanimated.

6.2.2.2. Degree of corrosion and delamination around a scribe

Figure 99 displays the delamination results on powder coated specimens after six weeks of Cycle-B, PV 1210 and VDA-new test and 480 hours of NSS test.

Similar to the previous chart, aluminium specimens exhibit almost no degree of corrosion and delamination around a scribe. Even the VDA-new test shows minimal delamination on aluminium specimens. Based on the results, aluminium specimens show remarkable properties in all tests, which would mean that the powder coating processes on aluminium substrates are high quality. In order to make clearer distinctions between coatings on aluminium parts or specimens, those should be further examined in specialized accelerated corrosion tests for aluminium.

On hot-dip galvanized steel specimens, NSS, Cycle-B and PV 1210 tests exhibit comparable delamination results. Similar to the CED specimens, PV 1210 test exhibits a higher degree of delamination trend, compared to the Cycle-B test. Meaning that the daily intermittent phases of the test (salt spray, humidity and dry phase) have a greater influence on powder coatings.

VDA-new test exhibits noticeably lower degrees of delamination on hot-dip galvanized steel specimens in comparison to other tests. Even when taking the different pre-treatment variations into account (iron and tricationic phosphate) the specimens do not exhibit the same differences as CED specimens with analogue pre-treatment variants. This phenomenon could be connected to the composition of the phases in the VDA-new test and the distinct stresses, the most obvious being the 1% sodium chloride solution and the freezing phase.

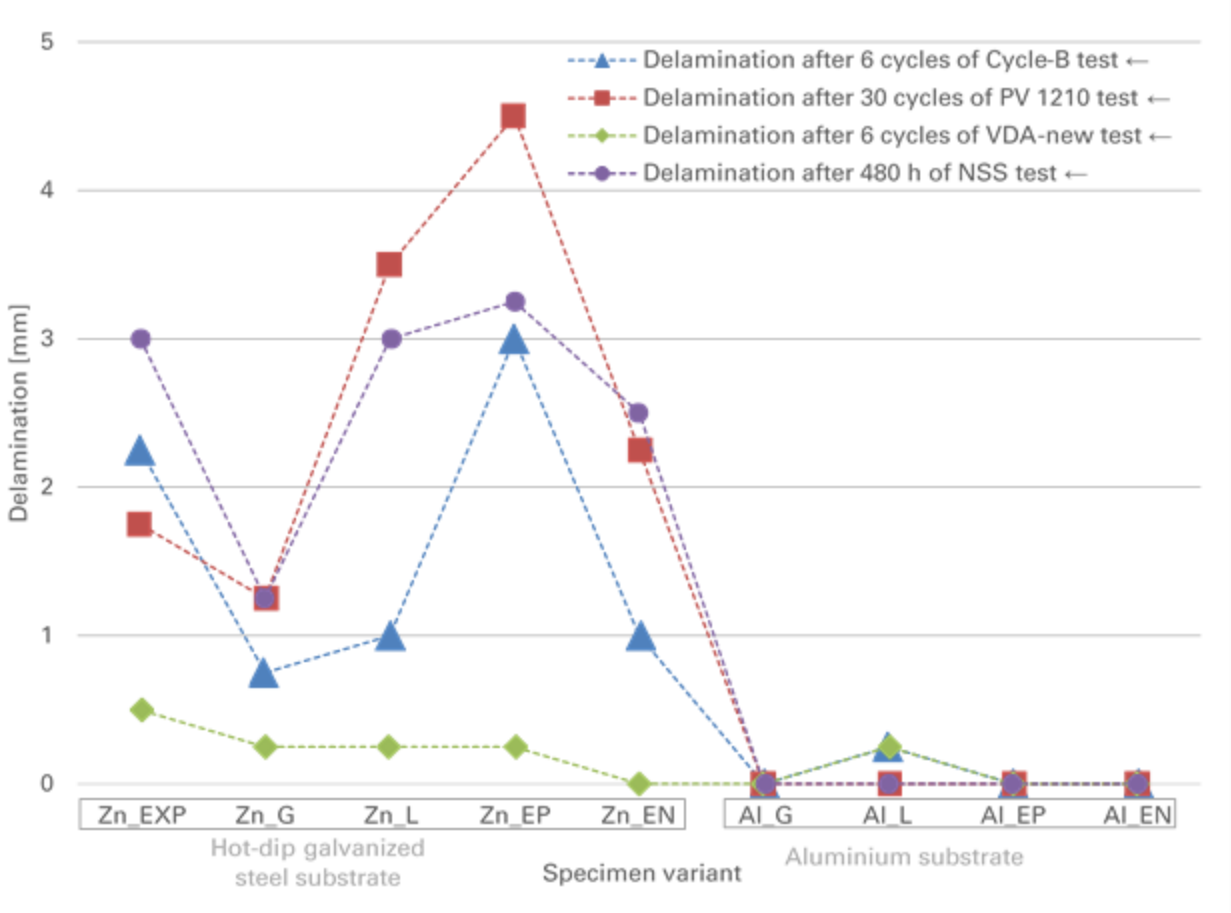

Figure 99. Comparison of delamination results (colored symbols) on powder coated specimens, after 6 cycles of Cycle-B and VDA-new test,30 cycles of PV 1210 test and 480 hours of NSS test in relation to different substrates

6.3. Electrochemical methods results

The results of the electrochemical methods are divided into two parts. First, the corrosion rate of the three substrates is determined with the help of Tafel and polarisation resistance plots. Secondly, the protection properties of the coatings are displayed in Bode plots with associated phase plots.

6.3.1. Corrosion rate results

Figure 100 displays the Tafel plot measured on the steel substrate in 5% sodium chloride solution at room temperature. The blue marked area indicates the portion of the chart, which is used for the numerical fit of the curve.

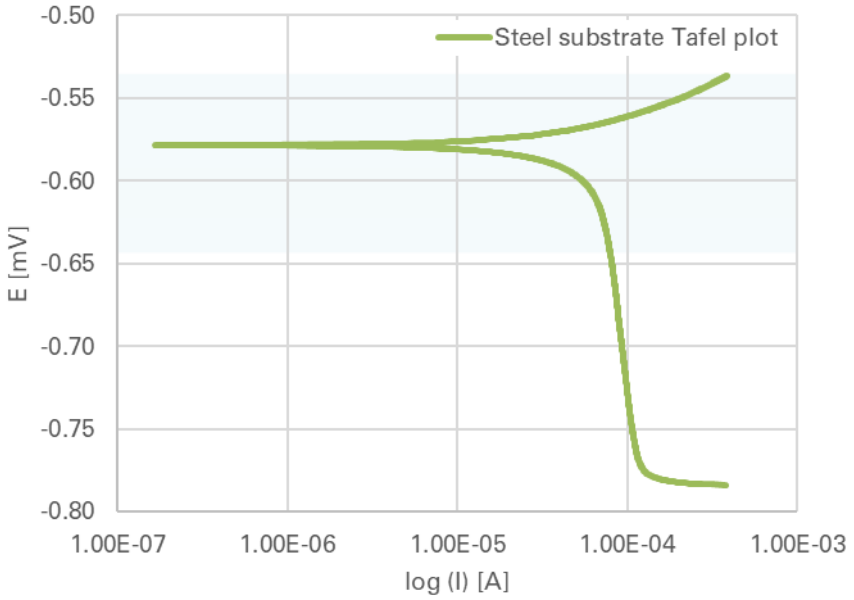

Figure 100. Steel substrate Tafel plot, measured with „Gamry Paracell“ in 5% sodium chloride solution

By using the “Gamry Echem Analyst” software, the curve is evaluated with the “Tafel” function. This function automatically calculates the E_{oc} and I_{corr} of the substrate using the selected area of the plot. Additionally, the software calculates the expected corrosion rate of the tested substrate. The remaining Tafel plots, for hot-dip galvanized steel and aluminium substrate, can be found in appendix B.

Figure 101 displays the polarisation resistance curve measured on the steel substrate in 5% sodium chloride solution at room temperature. Similar to the Tafel plot chart, the blue marked area indicates the portion of the chart, which is used for the numerical fit of the curve.

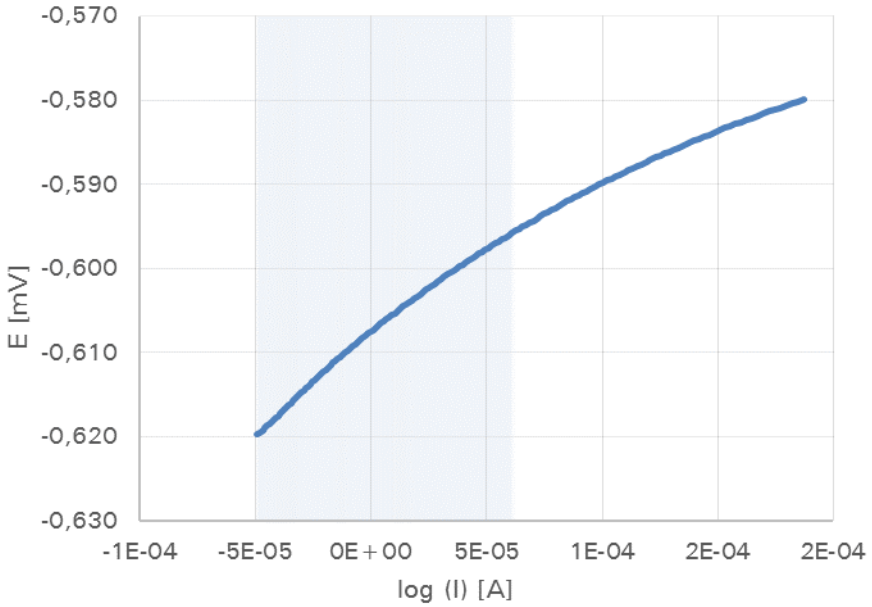

Figure 101. Steel substrate polarization resistance plot, measured with „Gamry Paracell“ in 5% sodium chloride solution

In this case, the curve is also evaluated by using “Gamry Echem Analyst” software with the “Polarisation Resistance” function. As seen from the marked area on figure 101, the section of the curve used for the numerical fit is near 0 [A] current values. The remaining polarisation resistance curves, for hot-dip galvanized steel and aluminium substrate, can be found in appendix B. The final results for E_{oc}, I_{corr}, R_p and corrosion rates are displayed in table 12.

Table 12. Resulting E_{oc}, I_{corr} and R_p as well as corrosion rates for all substrates

Substrates	E_{oc}	I_{corr}	R_p	Corrosion rate
Steel	-578,0 mV	84,20 µA	229,8 Ω	0,977 mmpy
Hot-dip galvanized steel	-1,150 V	30,40 µA	98,2 kΩ	0,299 mmpy
Aluminium	-965,0 mV	968,0 nA	131,5 kΩ	0,014 mmpy

Table 12 shows that the steel substrate has the highest corrosion rate with almost 1 mm per year in 5% sodium chloride solution. Hot dip galvanized steel is about three times more corrosion resistant in the same medium with a corrosion rate of about 0,3 mm per year. Aluminium exhibits by far the lowest corrosion rate of 0,014 mm per year.

6.3.2. Electrochemical impedance spectroscopy results

Results for the EIS measurements are displayed in Bode plots with respective phase curves. Since only a handful of specimens showed changes in impedance after the aging process, only those charts are displayed in this portion of the results. The rest of the Bode plots is available in appendix B.

The Bode plot is generated from right to left, meaning that the reading, as well as the applied current from the potentiostat, starts from higher frequencies and gradually transitions to lower frequencies. The coatings exhibit less impedance at higher frequency currents than at low ones, thus the plot builds upwards slowly as the applied frequency form the potentiostat is reduced.

In an ideal, intact organic coating, the Bode plot would be a straight line, angled upwards towards higher impedance values. The corresponding phase curve would also be a straight line at -90°. If the coating is damaged in any way, or the protective barrier bypassed by the surrounding medium, the curve starts to bend downward after a certain frequency has been applied. This shows how the impedance of the system decreases under those stresses. Simultaneously, the phase curve rises upwards, closing to 0° phase, at which point the impedance of the system is purely ohmic in character. From the equivalent electric circuit (Figure 55), if there is no capacitive resistance from the coating, the resistance becomes purely ohmic, meaning that the coating does not impede the flow of electrons between the substrate and surrounding medium [34].

As suggested by the company “InnCoa”, the impedance of the coatings is evaluated at a frequency of 0,1 Hz. This is a value determined by long-term experience of EIS testing on organic coatings. Simplified, this means that the coatings are expected to retain their protective properties if they do not exhibit any changes or reduced impedance at that frequency value. To simplify the evaluation of EIS data, the value of 0,1 Hz is used to draw conclusions about the impedance of examined coatings [34].

Figures 102 to 105 display Bode plots with the matching phase plots for specimen COB, Zn_G, Al_EN and Al_EP, measured in saturated sodium chloride solution, before and after aging. The green lines show the results before aging, while the red lines show results after aging, measured on the same spot of the specimen. The red area of the chart indicates typical frequencies at which organic coatings are expected to show impedance fluctuations.

6.3.2.1. CED coated specimens

Specimen COB exhibits a nearly ideal impedance curve, when tested in its initial state. The Bode plot is almost a straight line until it reaches a frequency of 0,001 Hz. At that point, the impedance of the coating starts to fluctuate, and the phase starts rising towards 0°, as shown in figure 102. This would indicate that the protective properties of the coating started failing.

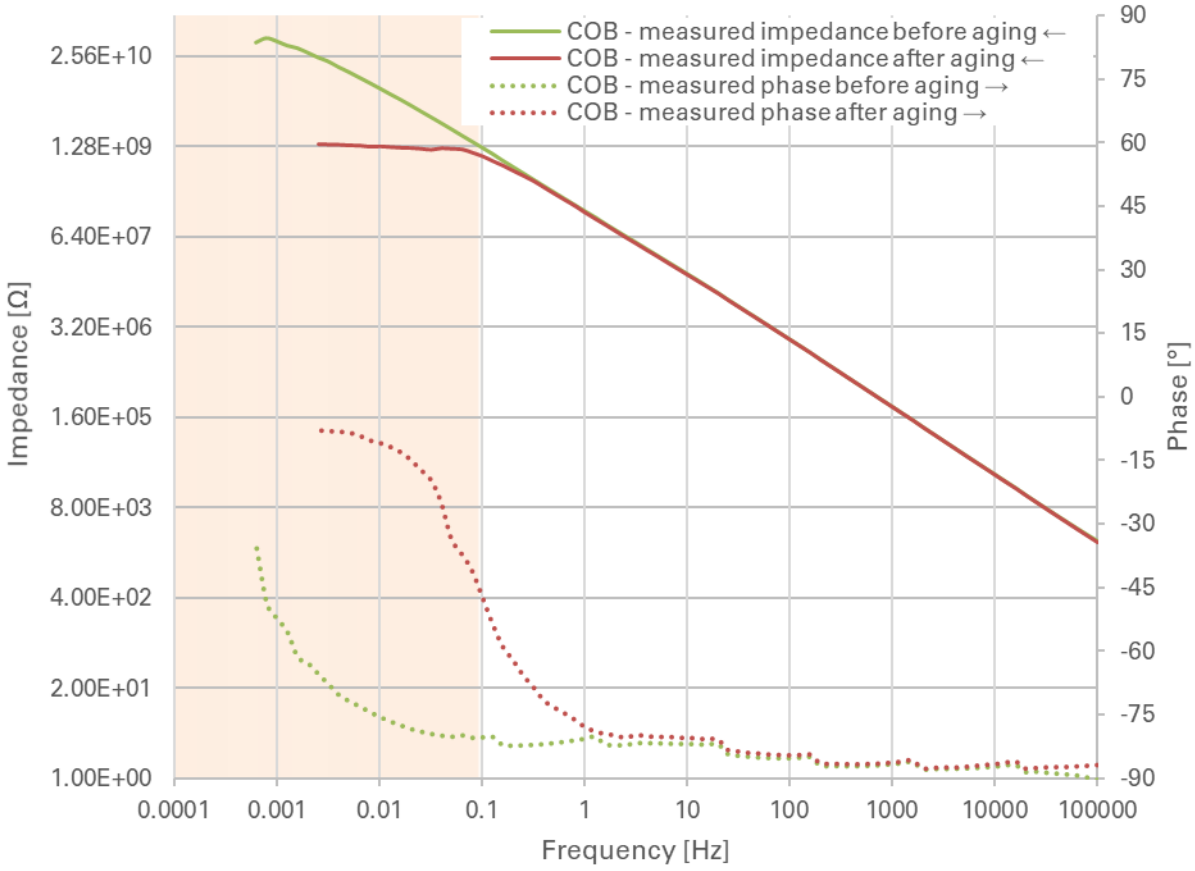

Figure 102. Bode plot with matching phase plot for specimen COB, measured in saturated sodium chloride solution, before (green lines) and after (red lines) 24 days of aging in 5% sodium chloride solution

Evident from the chart is that the impedance of the coating changes minimally at the 0,1 Hz mark after aging. Therefore, the coating is still successfully protecting the substrate at this point but has reduced protection properties as the frequency becomes smaller.

This is the only CED coated specimen that showed any notable change in coating impedance after aging. Since this change is considered minor, with respect to the chosen evaluation criteria, a statement can be made, that the protection properties of CED coatings did not suffer noticeably after aging.

6.3.2.2. Powder coated specimens

Specimen Zn_G also shows a nearly ideal Bode plot when tested in its initial state, without any striking fluctuations throughout the measured frequency range. The same is true for the measured phase, which stays close to -90° (Figure 103).

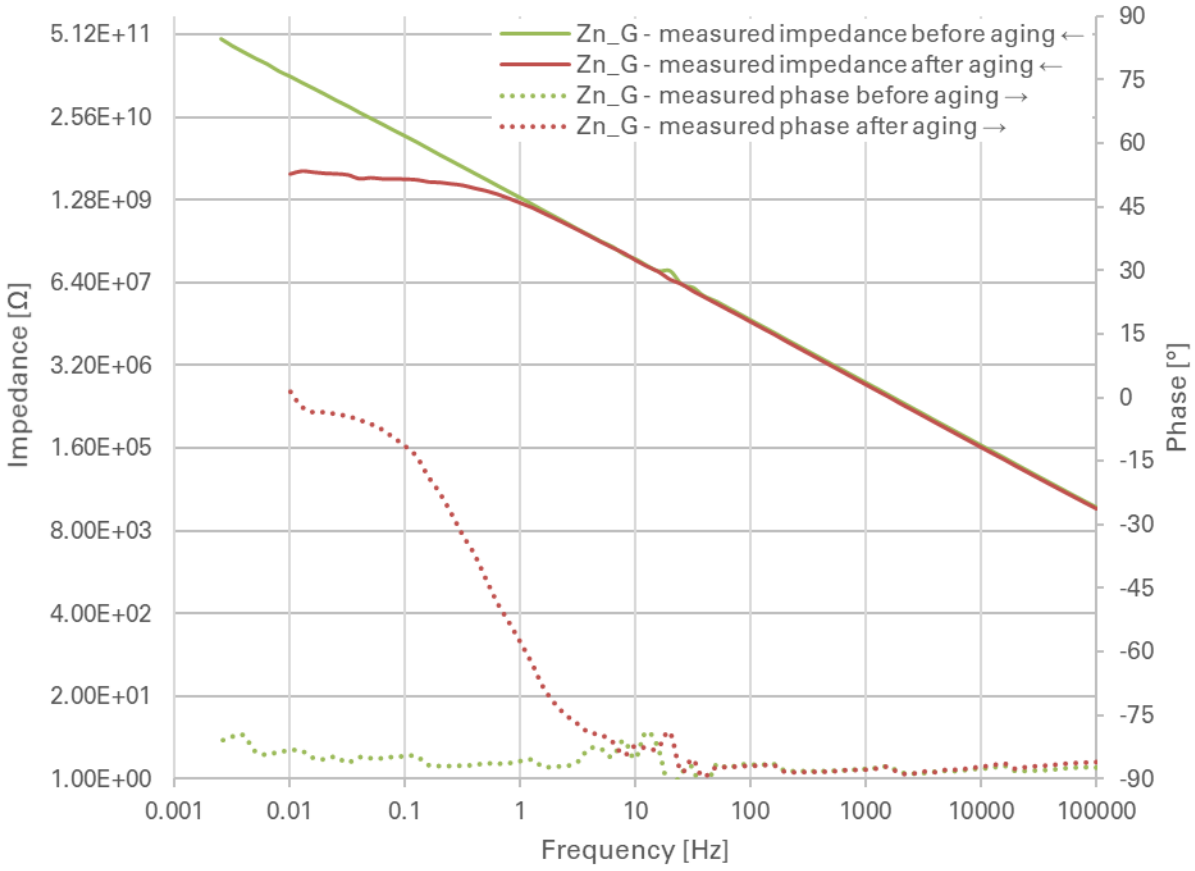

Figure 103. Bode plot with matching phase plot for specimen Zn_G, measured in saturated sodium chloride solution, before (green lines) and after (red lines) 25 days of aging in 5% sodium chloride solution

After aging, the impedance of the coating starts to decrease at the frequency of 1 Hz. This signifies a decline in corrosion resistance properties of the coating, even before the predetermined frequency value of 0,1 Hz. Clearly, the aging process negatively affected the impedance of the coating, which would not have satisfactory protection properties after aging.

Similar to Zn_G, the specimen Al_EP exhibits a nearly ideal bode plot when examined before aging. Correspondingly, the recorded phase is also near -90°, indicating no electron flow through the coating (Figure 104).

The impedance of the coating starts decreasing at the frequency of 100 Hz, when measured on the aged specimen. The decline in protective properties is more severe and occurs earlier than on Zn_G.

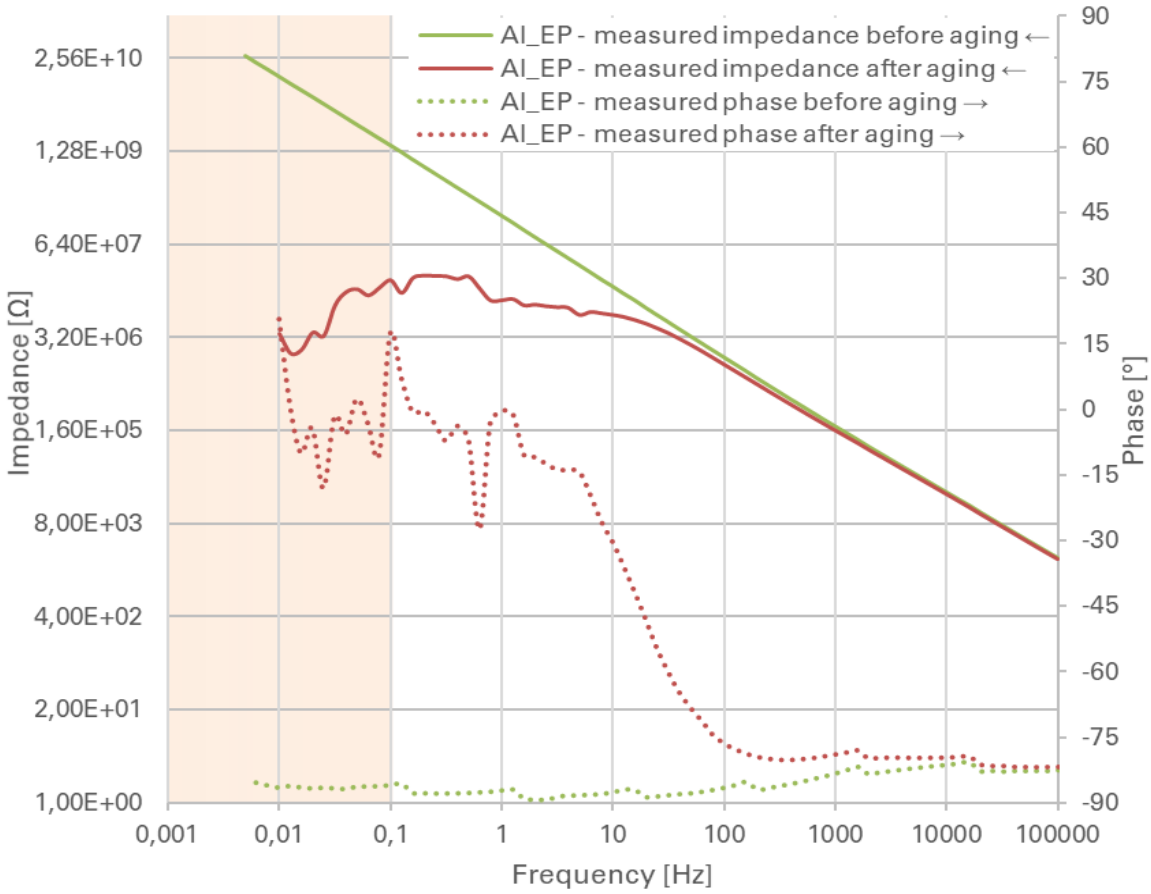

Figure 104. Bode plot with matching phase plot for specimen Al_EP, measured in saturated sodium chloride solution, before (green lines) and after (red lines) 25 days of aging in 5% sodium chloride solution

Specimen Al_EN exhibits similar behaviour to Al_EP. In the initial state, the Bode plot is nearly ideal, as well as the corresponding phase values (Figure 105).

When taking a look at the results after aging, the impedance of the coating starts to decline noticeably at the frequency of 10000 Hz, the same point at which the phase starts to approach 0°. At 10 Hz the phase exhibits a purely ohmic character, which means that the coating does not hinder the exchange of electrons between the medium and the substrate. Clearly, the aging process negatively affected the impedance of the coating, even to a greater degree than observed on Zn_G and Al_EP.

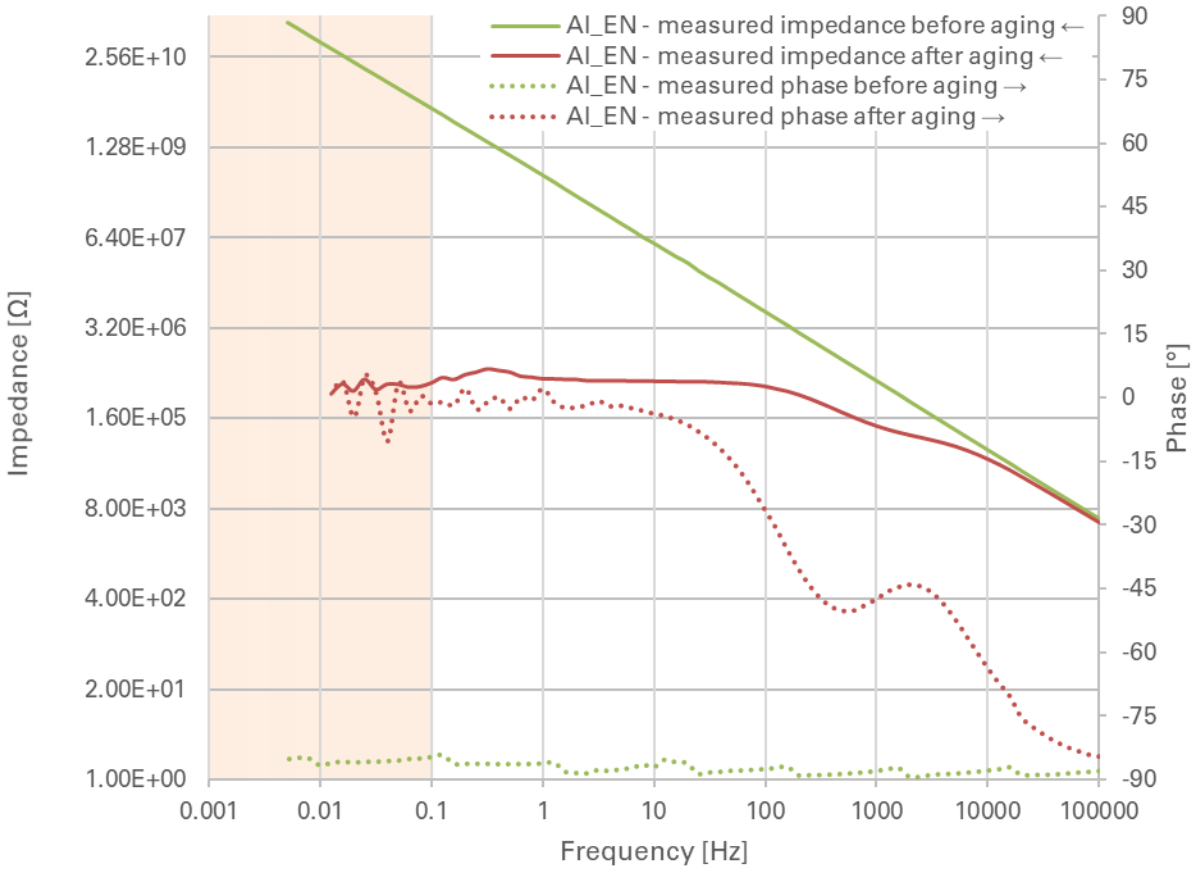

Figure 105. Bode plot with matching phase plot for specimen Al_EN, measured in saturated sodium chloride solution, before (green lines) and after (red lines) 25 days of aging in 5% sodium chloride solution

Conclusively, most powder coated specimens exhibit a noticeable decrease in impedance after aging (Table 13). Since the Bode plots of the specimens were nearly ideal in their initial state, the change undeniably comes from the aging process.

Most apparent changes in coating impedance occurred on powder coated specimens with the lowest coating thickness (Al_EP, Al_EN).

Table 13. Impedance and phase values of powder coated specimens, measured the frequency of 0,1 Hz in saturated sodium chloride solution with average coating thickness at measured points

Specimen	**Before aging**		**After aging**		**Average coating thickness [µm]**
	Impedance [GΩ]	Phase [°]	Impedance [GΩ]	Phase [°]	
Zn_EXP	5,26	-85,6	3,83	-78,0	123,8
Zn_G	12,80	-84,7	2,72	-11,5	198,8
Zn_L	9,24	-86,1	2,97	-79,3	69,5
Al_L	4,15	-84,8	3,00	-73,9	70,2
Al_EP	1,56	-86,0	0,02	17,3	46,1
Al_EN	4,51	-84,6	0,0005	-1,5	38,3

7. Conclusion and outlook

This thesis set out to find key differences between contemporary accelerated corrosion tests used in the automobile industry, as well as to characterize the climatic test according to VDA 233-102. Seventeen varying types of specimens, coated with both CED and powder coatings were utilized in order to capture each and any effect of those tests. Simultaneously, the protection properties of the same specimens were compared with each other to detect key features that distinguish state of the art coating processes. Furthermore, electrochemical methods, such as electrochemical impedance spectroscopy were employed to establish corrosion resistance properties of said organic coatings.

Every accelerated corrosion test has its place in the evaluation of corrosion resistance properties of organic coated car parts or specimens in the automotive industry. Just as before this research, Brose will have to continue to test their parts in all tests, which are prescribed by the customers. The customer and market trend to test parts in climatic tests, rather than in conventional tests, like the salt spray test is reinforced in this thesis. Organic coatings exhibit more effects regarding coating variant and pre-treatment methods in climatic tests with intermittent phases.

While comparing the results from accelerated corrosion tests, an observation can be made, that the composition of individual tests influences the stresses on the tested parts or specimens. Moreover, the undeniable differences and possibilities of the new climatic test according to VDA 233-102 have been verified with the experimental research of the thesis. Apparent from the results, steel substrates exhibit the highest degree of strain in the new test when compared to equivalent durations other climatic tests. Oppositely, hot-dip galvanized steel substrates show the least amount of degradation in comparison to the other tests, while aluminium substrates remain relatively nondescript throughout all tests. This finding would confirm the fact that the new climatic test realistically portrays real life cases of corrosion on different substrates, protected by identical organic coatings, after just a few weeks of testing.

Regarding CED specimens, the impact of pre-treatment, or phosphating variant more precisely, is most obviously displayed with the new VDA test in comparison to other climatic tests. Specimens with iron phosphate display more severe degradation than those with tricationic phosphate after equivalent testing times.

On a similar note, the effects of the Cycle-B and PV 1210 test on hot-dip galvanized specimens and parts are seemingly too severe within prescribed test durations. Brose materials laboratory witnessed those effects only in said tests, where in actuality, the same parts remained unscathed far longer than equivalent aluminium parts. Oppositely, the new VDA test demonstrates that the performance of hot-dip galvanized specimens is not poor at all, but almost on par with aluminium specimens with the same coatings. Consequently, all powder-coated specimens could meet far more demanding requests, when examined in appropriate climatic tests. Brose can take advantage of this fact by establishing new standards of corrosion testing for their parts.

Taking all results into account, both internal and external Brose coaters produce quality products with more than adequate corrosion resistance properties. Only with the intentional overstressing of those coatings, certain effects are shown, mainly regarding the degree of rusting on edges and corrosion and delamination around a scribe. While, the specimens represent an ideal surface for the deposition of coatings, this is not the case with actual production parts. Varying geometrical shapes, holes and welds on car parts would show more fluctuations in results after identical accelerated corrosion tests and testing times. Therefore, as one of the most important factors against the onset of corrosion, coating thickness should not be kept near the lowest acceptable values. Although economic and construction aspects must be taken into account, coated parts would benefit greatly, regarding edge corrosion. with an overall increase in coating thickness. In the same note, better results regarding corrosion and delamination around a scribe could be achieved by pre-treatment optimization, i.e. using tricationic phosphate rather than iron phosphate.

The results of the electrochemical analysis give additional insight in the behaviour of certain specimens in respect to substrate and coating variations. As expected, the steel substrate corrodes at the highest rate, followed by hot-dip galvanized steel, while aluminium displays the slowest corrosion rate in 5% sodium chloride solution. While measuring the impedance of coatings, powder coated specimens exhibited a greater degree of degradation after the aging period. This would mean that in order to preserve the protective properties of powder coatings, they should not be allowed to be in contact with an electrolyte, like sodium chloride solution. Another important finding is that coating thickness seems to greatly affect the impedance of powder coatings after aging, as powder coatings with the lowest coating thickness exhibited the highest degree of change.

REFERENCES

[1] IHS Markit - https://news.ihsmarkit.com/press-release/automotive/vehicles-getting-older-average-age-light-cars-and-trucks-us-rises-again-201 (25. 10 2018)

[2] I. Juraga, A. Vesna, I. Stojanović, *Korozija i zaštita premazima,* Zagreb, Fakultet strojarstva i brodogradnje, 2014

[3] P. A. Schweitzer, *Fundamentals of corrosion: mechanisms, causes, and preventative methods,* Boca Ranton, CRC Press, 2010

[4] Chemistry LibreTexts - https://chem.libretexts.org/Bookshelves/Inorganic_Chemistry/Book%3A_Inorganic_Chemistry_(Wikibook)/Chapter_04%3A_Redox_Stability_and_Redox_Reactions/4.2%3A_Electrochemical_potentials (14. 11 2018)

[5] Chemistry LibreTexts - https://chem.libretexts.org/Bookshelves/General_Chemistry/Book%3A_Chem1_(Lower)/16%3A_Electrochemistry/24.08%3A_Electrochemical_Corrosion (17. 11 2018)

[6] WOTECH - https://www.wotech-technical-media.de/womag/ausgabe/2013/04/21_w_pinger_stueckverzinken_04j2013/21_w_pinger_stueckverzinken_04j2013.php?we_webUser_logout=1 (27. 11 2018)

[7] I. Jurić, Elektroforeza, Seminarski rad iz kolegija mehanizmi zaštite od korozije. Zagreb, 2015

[8] J. Novak, Galvansko nanošenje metalnih prevlaka, Zagreb, 2018

[9] Products finishing - https://www.pfonline.com/articles/pretreatment-for-painting (5. 12 2018)

[10] Wikipedia. *Phosphate conversion coating* - https://en.wikipedia.org/wiki/Phosphate_conversion_coating (22. 12 2018)

[11] K. H. Trostmann, *Korrosion, Ursachen und Vermeidung.* 2001

[12] J. Pietschmann, *Industrielle Pulverbeschichtung* Solothurn, Springer Vieweg, 2013

[13] W. Hellwig, M. Kolbe. *Spanlose Fertigung Stanzen,* Wiesbaden, Springer Vieweg, 2012

[14] Fraunhofer - https://www.ifam.fraunhofer.de/en/Profile/Locations/Bremen/Shaping_Functional_Materials/Materialography_Analytics/Materialography.html (29. 12 2018)

[15] P. D. Rack, *Optical Microscopy,* Tennesee

[16] nanoScience - https://www.nanoscience.com/techniques/scanning-electron-microscopy/ (29. 12 2018)
[17] M. Kwiczala, Personal statement, Brose materials laboratory
[18] N. N., DIN EN ISO 17872: Beschichtungsstoffe - Leitfaden zum Anbringen von Ritzen durcheine Beschichtung auf Metallplatten für Korrosionsprüfungen, 2007
[19] N. N., DIN EN ISO 4628-3: Beschichtungsstoffe – Beurteilung von Beschichtungsschäden – Bewertung der Menge und der Größe von Schäden und der Intensität von gleichmäßigen Veränderungen im Aussehen – Teil 3: Bewertung des Rostgrades, 2016
[20] N. N., DIN EN ISO 4628-8: Beschichtungsstoffe - Beurteilung von Beschichtungsschäden - Beurteilung der Menge und der Größe von Schäden und der Intensität von gleichmäßigen Veränderungen im Aussehen - Teil 8, 2013
[21] N.N., Beschichtungsstoffe - Gitterschnittprüfung, 2013
[22] N.N., DIN EN ISO 4628-2: Beschichtungsstoffe - Beurteilung von Beschichtungsschäden - Bewertung der Menge und der Größe von Schäden und der Intensität von gleichmäßigen Veränderungen im Aussehen - Teil 2: Bewertung des Blasengrades, 2016
[23] N.N., DBL 7382: Liefervorschrift Beschichtung/Lackierung für metallische Teile im Fahrzeuginnenraum, 2010
[24] N.N., DIN EN ISO 6270-2: Beschichtungsstoffe – Bestimmung der Beständigkeit gegen Feuchtigkeit – Teil 2: Kondensation, 2018
[25] N.N., DIN EN ISO 9227: Korrosionsprüfungen in künstlichen Atmosphären – Salzsprühnebelprüfungen, 2017
[26] N.N., DIN EN ISO 11997-1: Beschichtungsstoffe – Bestimmung der Beständigkeit bei zyklischen Korrosionsbedingungen - Teil 1: Nass (Salzsprühnebel)/trocken/feucht, 2018
[27] N.N., PV 1210: Karosserie und Anbauteile Korrosionsprüfung, 2016
[28] N.N., *Moderne Prüfmethoden für Lacke und Beschichtungen*, Stuttgard, Stuttgarder Produktionsakademie, 2015
[29] N.N., VDA 233-102: Zyklische Korrosionsprüfung von Werkstoffen und Bauteilen im Automobilbau, 2013
[30] N.N., Getting Started with Electrochemical Corrosion Measurement, 2012

[31] N.N., Polarization Resistance - https://www.gamry.com/Framework%20Help/HTML5%20-%20Tripane%20-%20Audience%20A/Content/EIS/Theory/Physical%20Electrochemistry%20and%20Circuit%20Elements/Polarization%20Resistance.htm (02. 1 2019)
[32] H. Cesiulis, N. Tsyntsaru, A. Romanavicius, G. Ragoisha, Chapter 1: The Study of Thin Films By Electrochemical Impedance Spectroscopy, Springer International Publishing
[33] D. Loveday, P. Peterson, B. Rodgers, Evaluation of Organic Coatings with Electrochemical Impedance Spectroscopy, Part 1: Fundamentals of Electrochemical Impedance Spectroscopy, Gamry instruments, 2004
[34] I. Sieber, Personal statement, InnCoa Surface and Substrate Engineering
[35] Alibaba - https://www.alibaba.com/product-detail/Thermosetting-electrostatic-powder-paint-for-metal_60428579511.html (22. 12 2018)
[36] custompart.net. https://www.custompartnet.com/wu/sheet-metal-shearing (29. 12 2018)
[37] Jayasuriya, A. ReasearchGate - https://www.researchgate.net/post/Can_we_make_a_Linear_Polarization_Measurement_device_experimentally (02. 1 2019)
[38] N., N. Basics of Electrochemical Impedance Spectroscopy, Gamry Instruments, 2006
[39] D. Loveday, P. Peterson, B. Rodgers. Evaluation of Organic Coatings with Electrochemical Impedance Spectroscopy, Part 2: Application of EIS to Coatings, Gamry Instruments, 2004
[40] N. N., Gamry instruments - https://www.gamry.com/support/legacy-devices/reference-600-legacy/ (5. 1 2019)

APPENDIX A

Accelerated corrosion test results

CH test

Appendix 1. CED coated specimens CH test results

CH test	240 h					
CED specimens	Degree of rusting on surface [%]	Degree of rusting on edges [%]	Daimler scratch test	Cross cut test	Degree of blistering	Delamination [mm]
COB	0	0	2	0	0	0,5
COV	0	0	1	0	0	0,25
LON	0	0	1	0	0	0
QUA	0	0	3	1	0	0,5
C	0	0	0	0	0	0
F	0	0	2	0	0	0
J	0	0	0	0	0	0
P	0	0	0	0	0	0

CH test	360 h					
CED specimens	Degree of rusting on surface [%]	Degree of rusting on edges [%]	Daimler scratch test	Cross cut test	Degree of blistering	Delamination [mm]
COB	0	0	1	0	0	0,5
COV	0	0	2	0	0	0,25
LON	0	0,5	1	0	0	0,5
QUA	0	0	3	1	0	0,25
C	0	0	0	0	0	0
F	0	0	2	0	0	0,25
J	0	0,5	0	0	0	0
P	0	0	1	0	0	0

CH test	480 h					
CED specimens	Degree of rusting on surface [%]	Degree of rusting on edges [%]	Daimler scratch test	Cross cut test	Degree of blistering	Delamination [mm]
COB	0	0,5	2	0	0	0,5
COV	0	0	2	0	0	0,5
LON	0	0,5	1	0	0	0,5
QUA	0	0	3	1	0	0,5
C	0	0	0	0	0	0
F	0	0	2	0	0	0,25
J	0	0,5	0	0	0	0
P	0	0	1	0	0	0

Appendix 2. Powder coated specimens CH test results

CH test	240 h				
Powder coated specimens	Degree of rusting on surface [%]	Degree of rusting on edges [%]	Cross cut test	Degree of blistering	Delamination [mm]
Zn_EXP	0	0	0	0	0
Zn_G	0	0	0	0	0
Zn_L	0	0	0	0	0
Zn_EP	0	0	0	0	0
Zn_EN	0	0	0	0	0
Al_G	-	-	-	-	-
Al_L	-	-	-	-	-
Al_EP	-	-	-	-	-
Al_EN	-	-	-	-	-

CH test	360 h				
Powder coated specimens	Degree of rusting on surface [%]	Degree of rusting on edges [%]	Cross cut test	Degree of blistering	Delamination [mm]
Zn_EXP	0	0	0	0	0
Zn_G	0	0	0	0	0
Zn_L	0	0	0	0	0
Zn_EP	0	0	0	0	0
Zn_EN	0	0	0	0	0
Al_G	-	-	-	-	-
Al_L	0	0	0	0	0
Al_EP	-	-	-	-	-
Al_EN	-	-	-	-	-

CH test	480 h				
Powder coated specimens	Degree of rusting on surface [%]	Degree of rusting on edges [%]	Cross cut test	Degree of blistering	Delamination [mm]
Zn_EXP	0	0	0	0	0
Zn_G	0	0	0	0	0
Zn_L	0	0	0	0	0
Zn_EP	0	0	0	0	0,25
Zn_EN	0	0	0	0	0,25
Al_G	0	0	0	3 (S3)	0
Al_L	0	0	0	0	0
Al_EP	0	0	0	0	0
Al_EN	0	0	0	0	0

NSS test

Appendix 3. CED coated specimens NSS test results

NSS test	96 h					
CED specimens	Degree of rusting on surface [%]	Degree of rusting on edges [%]	Daimler scratch test	Cross cut test	Degree of blistering	Delamination [mm]
COB	0	2	1	0	0	0,25
COV	0	1	1	0	0	0,5
LON	0	0	1	0	0	0
QUA	0	1	3	0	0	0,5
C	0	0	0	0	0	0
F	0	3,5	2	0	0	0
J	0	1	0	0	0	0
P	0	1	1	0	0	0

NSS test	144 h					
CED specimens	Degree of rusting on surface [%]	Degree of rusting on edges [%]	Daimler scratch test	Cross cut test	Degree of blistering	Delamination [mm]
COB	0	2	1	0	0	0,5
COV	0	7,5	1	0	0	0,5
LON	0	3,5	1	0	0	0,25
QUA	0	5	3	1	0	0,5
C	0	0,5	0	0	0	0
F	0	12,5	2	0	0	0
J	0	2	0	0	0	0
P	0	0,5	1	0	0	0

NSS test	240 h					
CED specimens	Degree of rusting on surface [%]	Degree of rusting on edges [%]	Daimler scratch test	Cross cut test	Degree of blistering	Delamination [mm]
COB	0	5	1	0	0	1
COV	0	10	2	0	0	2
LON	0	15	2	0	0	0,5
QUA	0	20	3	1	0	0,5
C	0	0,5	0	0	0	0
F	0	12,5	2	0	0	0,25
J	0	15	0	0	0	0
P	0	10	1	0	0	0

Appendix 4. Powder coated specimens NSS test results

NSS test	240 h				
Powder coated specimens	Degree of rusting on surface [%]	Degree of rusting on edges [%]	Cross cut test	Degree of blistering	Delamination [mm]
Zn_EXP	0	0	0	0	1
Zn_G	0	3,5	0	0	0,75
Zn_L	0	0,5	0	0	1,5
Zn_EP	0	20	0	0	2,25
Zn_EN	0	0	0	0	1
Al_G	-	-	-	-	-
Al_L	-	-	-	-	-
Al_EP	-	-	-	-	-
Al_EN	-	-	-	-	-

NSS test	360 h				
Powder coated specimens	Degree of rusting on surface [%]	Degree of rusting on edges [%]	Cross cut test	Degree of blistering	Delamination [mm]
Zn_EXP	0	0	0	0	1,75
Zn_G	0	1	0	0	1
Zn_L	0	0,5	0	0	1,75
Zn_EP	0	20	0	0	2,5
Zn_EN	0	0,5	0	0	1,75
Al_G	-	-	-	-	-
Al_L	-	0	0	0	0
Al_EP	-	-	-	-	-
Al_EN	-	-	-	-	-

NSS test	480 h				
Powder coated specimens	Degree of rusting on surface [%]	Degree of rusting on edges [%]	Cross cut test	Degree of blistering	Delamination [mm]
Zn_EXP	0	0	0	0	3
Zn_G	0	2	0	0	1,25
Zn_L	0	0	0	0	3
Zn_EP	0	30	0	0	3,25
Zn_EN	0	1,5	0	0	2,5
Al_G	0	0	0	0	0
Al_L	0	0	0	0	0
Al_EP	0	0	0	0	0
Al_EN	0	0	0	0	0

Cycle-B test

Appendix 5. CED coated specimens Cycle-B test results

Cycle-B test	1 cycle					
CED specimens	Degree of rusting on surface [%]	Degree of rusting on edges [%]	Daimler scratch test	Cross cut test	Degree of blistering	Delamination [mm]
COB	0	1,5	2	0	0	1
COV	0	1	2	0	0	0,5
LON	0	0,5	1	0	0	0,5
QUA	0	0,5	2	0	0	0,75
C	0	0,5	0	0	0	0
F	0	2	3	0	0	0
J	0	0	0	0	0	0
P	0	0,5	1	0	0	0,25

Cycle-B test	3 cycles					
CED specimens	Degree of rusting on surface [%]	Degree of rusting on edges [%]	Daimler scratch test	Cross cut test	Degree of blistering	Delamination [mm]
COB	0	15	1	0	0	3
COV	0	10	3	0	0	2,5
LON	0	1	1	0	0	1,75
QUA	0	2	2	1	0	0,5
C	0	1	0	0	0	0
F	0	17,5	2	0	0	1
J	0	3,5	0	0	0	0
P	0	5	1	0	0	0

Cycle-B test	6 cycles					
CED specimens	Degree of rusting on surface [%]	Degree of rusting on edges [%]	Daimler scratch test	Cross cut test	Degree of blistering	Delamination [mm]
COB	0	85	1	0	2 (S3)	3,5
COV	0	32,5	2	0	0	5,25
LON	0	10	1	0	0	2,75
QUA	0	17,5	2	1	0	1,25
C	0	5	0	0	0	0
F	0	55	2	0	0	1
J	0	55	0	0	0	0
P	0	55	1	0	0	0,25

Appendix 6. Powder coated specimens Cycle-B test results

Cycle-B test	3 cycles				
Powder coated specimens	Degree of rusting on surface [%]	Degree of rusting on edges [%]	Cross cut test	Degree of blistering	Delamination [mm]
Zn_EXP	0	0,5	0	0	0,25
Zn_G	0	1,5	0	0	0,25
Zn_L	0	0	0	0	0,5
Zn_EP	0	12,5	0	0	1,75
Zn_EN	0	0	0	0	0,75
Al_G	0	0	0	0	0
Al_L	0	0	0	0	0
Al_EP	0	0	0	0	0
Al_EN	0	0	0	0	0

Cycle-B test	6 cycles				
Powder coated specimens	Degree of rusting on surface [%]	Degree of rusting on edges [%]	Cross cut test	Degree of blistering	Delamination [mm]
Zn_EXP	0	3,5	0	0	2,25
Zn_G	0	1,5	0	0	0,75
Zn_L	0	0	0	0	1
Zn_EP	0	45	0	0	3
Zn_EN	0	0	0	0	1
Al_G	0	0	0	2 (S2)	0
Al_L	0	0	0	0	0,25
Al_EP	0	0	0	0	0
Al_EN	0	0	0	0	0

Cycle-B test	10 cycles				
Powder coated specimens	Degree of rusting on surface [%]	Degree of rusting on edges [%]	Cross cut test	Degree of blistering	Delamination [mm]
Zn_EXP	0	3,5	0	0	3,5
Zn_G	0	12,5	0	0	0,75
Zn_L	0	0	0	0	3,5
Zn_EP	0	65	0	0	3,75
Zn_EN	0	2	0	0	2,75
Al_G	0	0	0	3 (S3)	0
Al_L	0	0	0	0	0,25
Al_EP	0	0	0	0	0
Al_EN	0	0	0	0	0

PV 1210 test

Appendix 7. CED coated specimens PV 1210 test results

PV 1210 test	5 cycles					
CED specimens	Degree of rusting on surface [%]	Degree of rusting on edges [%]	Daimler scratch test	Cross cut test	Degree of blistering	Delamination [mm]
COB	0	1,5	1	0	0	0,5
COV	0	2	1	0	0	0,5
LON	0	2	1	0	0	0,75
QUA	0	1,5	1	0	0	0,5
C	0	0,5	0	0	0	0
F	0	0,5	2	0	0	0
J	0	1	0	0	0	0
P	0	0,5	1	0	0	0

PV 1210 test	10 cycles					
CED specimens	Degree of rusting on surface [%]	Degree of rusting on edges [%]	Daimler scratch test	Cross cut test	Degree of blistering	Delamination [mm]
COB	0	7,5	1	0	0	1,25
COV	0	2	2	0	0	2
LON	0	2	2	0	0	1,25
QUA	0	15	3	1	0	0,75
C	0	0,5	0	0	0	0
F	0	10	2	0	0	0,25
J	0	1	0	0	0	0
P	0	1	1	0	0	0

PV 1210 test	15 cycles					
CED specimens	Degree of rusting on surface [%]	Degree of rusting on edges [%]	Daimler scratch test	Cross cut test	Degree of blistering	Delamination [mm]
COB	0	7,5	1	0	0	2
COV	0	10	1	0	0	3,75
LON	0	7,5	1	0	0	2,75
QUA	0	30	3	1	0	1,25
C	0	5	0	0	0	0
F	0	22,5	2	0	0	1
J	0	30	0	0	0	0
P	0	10	1	0	0	0,75

Appendix 8. Powder coated specimens PV 1210 test results

PV 1210 test	15 cycles				
Powder coated specimens	Degree of rusting on surface [%]	Degree of rusting on edges [%]	Cross cut test	Degree of blistering	Delamination [mm]
Zn_EXP	0	0	0	0	2
Zn_G	0	0,5	0	0	0,75
Zn_L	0	0,5	0	0	1,25
Zn_EP	0	3,5	0	0	1,75
Zn_EN	0	0	0	0	1,5
Al_G	0	0	0	0	0
Al_L	0	0	0	0	0
Al_EP	0	0	0	0	0
Al_EN	0	0	0	0	0

PV 1210 test	30 cycles				
Powder coated specimens	Degree of rusting on surface [%]	Degree of rusting on edges [%]	Cross cut test	Degree of blistering	Delamination [mm]
Zn_EXP	0	3,5	0	0	1,75
Zn_G	0	5	0	0	1,25
Zn_L	0	2	0	0	3,5
Zn_EP	0	40	0	0	4,5
Zn_EN	0	0,5	0	0	2,25
Al_G	0	0	0	0	0
Al_L	0	0	0	0	0
Al_EP	0	0	0	0	0
Al_EN	0	0	0	0	0

PV 1210 test	60 cycles				
Powder coated specimens	Degree of rusting on surface [%]	Degree of rusting on edges [%]	Cross cut test	Degree of blistering	Delamination [mm]
Zn_EXP	0	3,5	0	0	3,25
Zn_G	0	10	0	0	2,25
Zn_L	0	2	0	0	6
Zn_EP	0	50	0	0	4,75
Zn_EN	0	0,5	0	0	5,5
Al_G	0	0	0	3 (S3)	0
Al_L	0	0	0	0	0,25
Al_EP	0	0	0	0	0
Al_EN	0	0	0	0	0

VDA-new test

Appendix 9. CED coated specimens VDA-new test results

VDA-new test	1 cycle					
CED specimens	Degree of rusting on surface [%]	Degree of rusting on edges [%]	Daimler scratch test	Cross cut test	Degree of blistering	Delamination [mm]
COB	0	1	1	0	0	1,25
COV	0	0,5	2	0	0	1,75
LON	0	0,5	1	0	0	1,5
QUA	0	0,5	3	1	0	1,25
C	0	0	0	0	0	0
F	0	0,5	2	0	0	1
J	0	0,5	0	0	0	0
P	0	0	0	0	0	0,5

VDA-new test	3 cycles					
CED specimens	Degree of rusting on surface [%]	Degree of rusting on edges [%]	Daimler scratch test	Cross cut test	Degree of blistering	Delamination [mm]
COB	0	17,5	1	0	0	3,5
COV	0	2	2	0	0	3,5
LON	0	3,5	1	0	0	3,5
QUA	0	32,5	3	1	0	3,25
C	0	2	0	0	0	0,75
F	0	15	2	0	0	2,75
J	0	10	0	0	0	0,75
P	0	2	0	0	0	2,5

VDA-new test	6 cycles					
CED specimens	Degree of rusting on surface [%]	Degree of rusting on edges [%]	Daimler scratch test	Cross cut test	Degree of blistering	Delamination [mm]
COB	0	87,5	1	0	0	6,5
COV	0	17,5	1	0	0	6
LON	0	25	1	0	0	5,75
QUA	0	32,5	3	1	0	6
C	0	5	0	0	0	1
F	0	65	2	0	0	4,75
J	0	27,5	0	0	0	1
P	0	7,5	1	0	0	4,25

Appendix 10. Powder coated specimens VDA-new test results

VDA-new test	3 cycles				
Powder coated specimens	Degree of rusting on surface [%]	Degree of rusting on edges [%]	Cross cut test	Degree of blistering	Delamination [mm]
Zn_EXP	0	0	0	0	0,25
Zn_G	0	3,5	0	0	0
Zn_L	0	0	0	0	0
Zn_EP	0	7,5	0	0	0
Zn_EN	0	0	0	0	0
Al_G	0	0	0	0	0
Al_L	0	0	0	0	0
Al_EP	0	0	0	0	0
Al_EN	0	0	0	0	0

VDA-new test	6 cycles				
Powder coated specimens	Degree of rusting on surface [%]	Degree of rusting on edges [%]	Cross cut test	Degree of blistering	Delamination [mm]
Zn_EXP	0	2	0	0	0,5
Zn_G	0	10	0	0	0,25
Zn_L	0	1,5	0	0	0,25
Zn_EP	0	55	0	0	0,25
Zn_EN	0	3,5	0	0	0
Al_G	0	0	0	0	0
Al_L	0	0	0	0	0,25
Al_EP	0	0	0	0	0
Al_EN	0	0	0	0	0

VDA-new test	9 cycles				
Powder coated specimens	Degree of rusting on surface [%]	Degree of rusting on edges [%]	Cross cut test	Degree of blistering	Delamination [mm]
Zn_EXP	0	5	0	0	1
Zn_G	0	10	0	0	0,25
Zn_L	0	3,5	0	0	0,25
Zn_EP	0	65	0	0	0,5
Zn_EN	0	5	0	0	0,75
Al_G	0	0	0	3 (S3)	0
Al_L	0	0	0	0	0,25
Al_EP	0	0	0	0	0,25
Al_EN	0	0	0	0	0

FSB Zagreb test results

Appendix 11. FSB Zagreb CED coated specimens CH and NSS test results

CH test	240 h					
CED specimens	Degree of rusting on surface [%]	Degree of rusting on edges [%]	Daimler scratch test	Cross cut test	Degree of blistering	Delamination [mm]
COB	0	0	1	0	0	0
LON	0	0	0	0	0	0
QUA	0	0	3	1	0	0,25

CH test	360 h					
CED specimens	Degree of rusting on surface [%]	Degree of rusting on edges [%]	Daimler scratch test	Cross cut test	Degree of blistering	Delamination [mm]
COB	0	0	1	0	0	0
LON	0	0	0	0	0	0
QUA	0	0	3	1	0	0

NSS test	96 h					
CED specimens	Degree of rusting on surface [%]	Degree of rusting on edges [%]	Daimler scratch test	Cross cut test	Degree of blistering	Delamination [mm]
COB	-	-	-	-	-	-
LON	0	0,5	0	0	0	0,25
QUA	-	-	-	-	-	-

NSS test	144 h					
CED specimens	Degree of rusting on surface [%]	Degree of rusting on edges [%]	Daimler scratch test	Cross cut test	Degree of blistering	Delamination [mm]
COB	0	3,5	2	0	0	0,5
LON	0	2	1	0	0	0,25
QUA	0	5	2	1	0	0,5

NSS test	240 h					
CED specimens	Degree of rusting on surface [%]	Degree of rusting on edges [%]	Daimler scratch test	Cross cut test	Degree of blistering	Delamination [mm]
COB	0	5	2	0	0	0,75
LON	0	3,5	1	0	0	0,75
QUA	0	17,5	2	1	0	0,75

Appendix 12. FSB Zagreb powder coated specimens CH and NSS test results

CH test	480 h				
Powder coated specimens	Degree of rusting on surface [%]	Degree of rusting on edges [%]	Cross cut test	Degree of blistering	Delamination [mm]
Zn_EXP	0	0	0	0	0
Zn_G	0	0	0	0	0
Zn_L	0	0	0	0	0
Zn_EP	0	0	0	0	0
Zn_EN	0	0	0	0	0
Al_G	0	0	0	3 (S3)	0
Al_L	0	0	0	0	0
Al_EP	0	0	0	0	0
Al_EN	0	0	0	0	0

NSS test	240 h				
Powder coated specimens	Degree of rusting on surface [%]	Degree of rusting on edges [%]	Cross cut test	Degree of blistering	Delamination [mm]
Zn_EXP	0	0	0	0	0
Zn_G	0	5	0	0	0
Zn_L	0	0	0	0	0,25
Zn_EP	0	10	0	0	0,75
Zn_EN	0	0	0	0	0,5
Al_G	-	-	-	-	-
Al_L	-	-	-	-	-
Al_EP	-	-	-	-	-
Al_EN	-	-	-	-	-

NSS test	360 h				
Powder coated specimens	Degree of rusting on surface [%]	Degree of rusting on edges [%]	Cross cut test	Degree of blistering	Delamination [mm]
Zn_EXP	0	0	0	0	0
Zn_G	0	10	0	0	0
Zn_L	0	0	0	0	0,5
Zn_EP	0	20	0	0	1
Zn_EN	0	0,5	0	0	1
Al_G	-	-	-	-	-
Al_L	-	-	-	-	-
Al_EP	-	-	-	-	-
Al_EN	-	-	-	-	-

NSS test	480 h				
Powder coated specimens	Degree of rusting on surface [%]	Degree of rusting on edges [%]	Cross cut test	Degree of blistering	Delamination [mm]
Zn_EXP	0	0	0	0	0
Zn_G	0	17,5	0	0	0
Zn_L	0	0	0	0	0,5
Zn_EP	0	30	0	0	1,25
Zn_EN	0	0	0	0	1
Al_G	0	0	0	0	0
Al_L	0	0	0	0	0
Al_EP	0	0	0	0	0
Al_EN	0	0	0	0	0

APPENDIX B

Electrochemical examination results

Corrosion rate

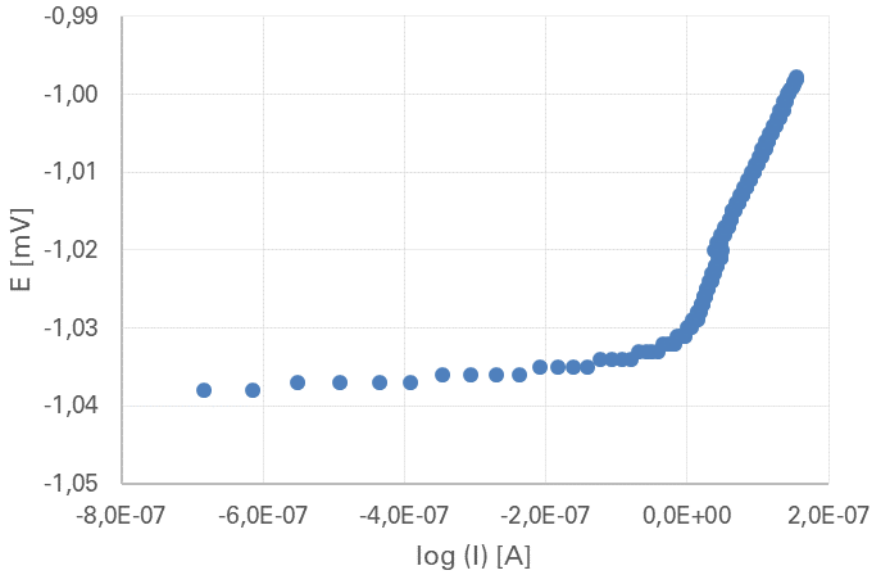

Appendix 13. Aluminium substrate polarization resistance plot, measured with "Gamry Paracell" in 5% sodium chloride solution

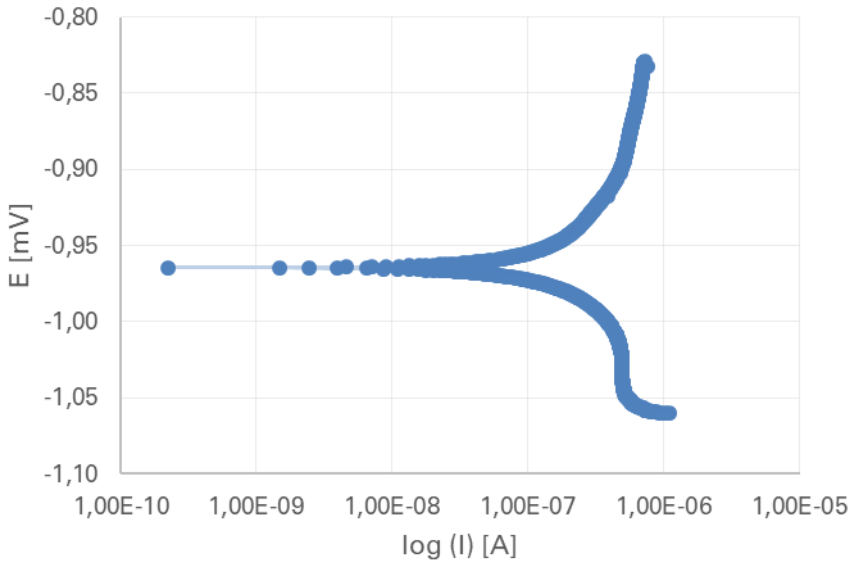

Appendix 14. Aluminium substrate Tafel plot, measured with "Gamry Paracell" in 5% sodium chloride solution

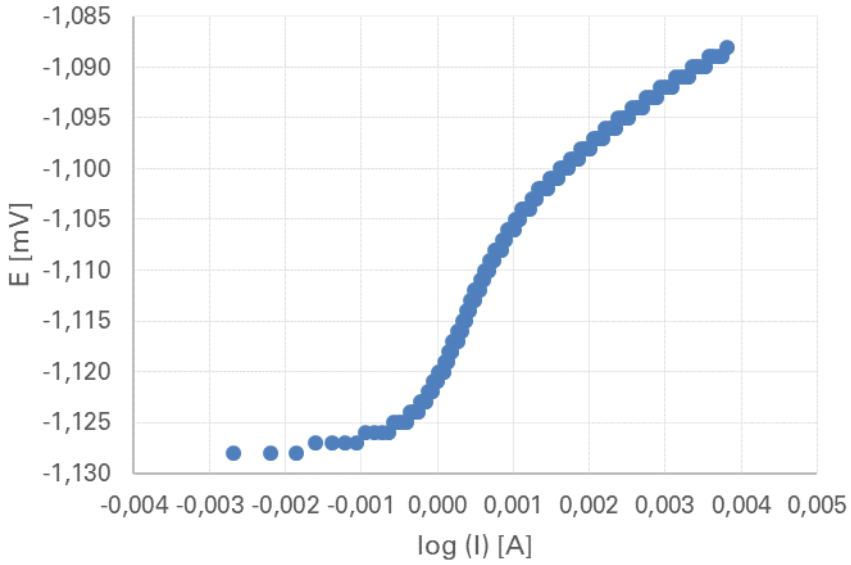

Appendix 15. Hot-dip galvanized steel substrate polarization resistance plot, measured with „Gamry Paracell“ in 5% sodium chloride solution

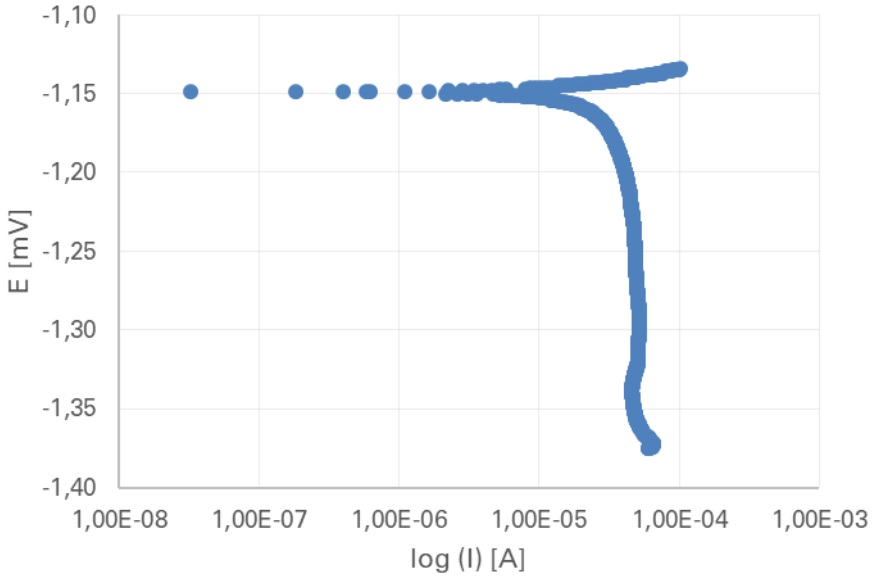

Appendix 16. Hot-dip galvanized steel substrate Tafel plot, measured with „Gamry Paracell“ in 5% sodium chloride solution

Electrochemical impedance spectroscopy results

CED coated specimens

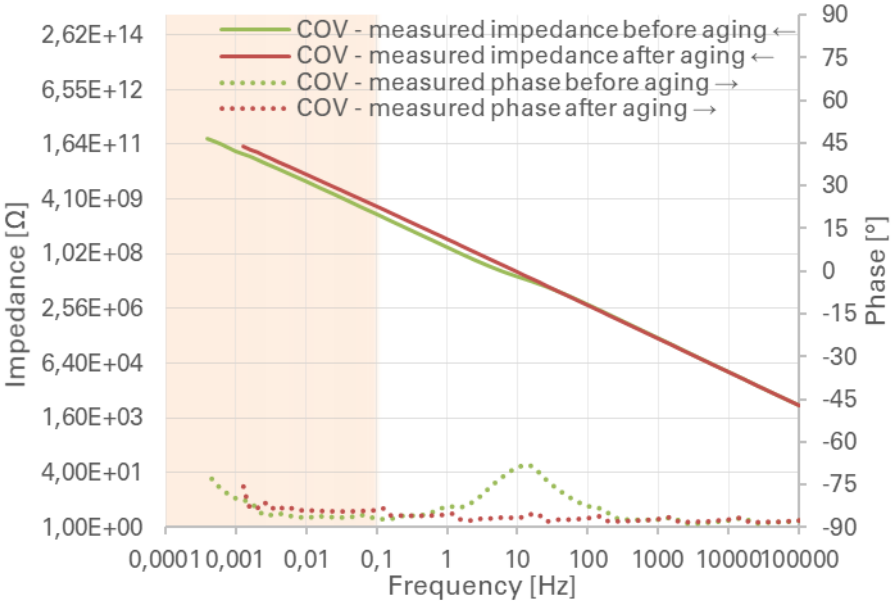

Appendix 17. Bode plot with matching phase plot for specimen COV, measured in saturated sodium chloride solution, before (green lines) and after (red lines) 24 days of aging in 5% sodium chloride solution

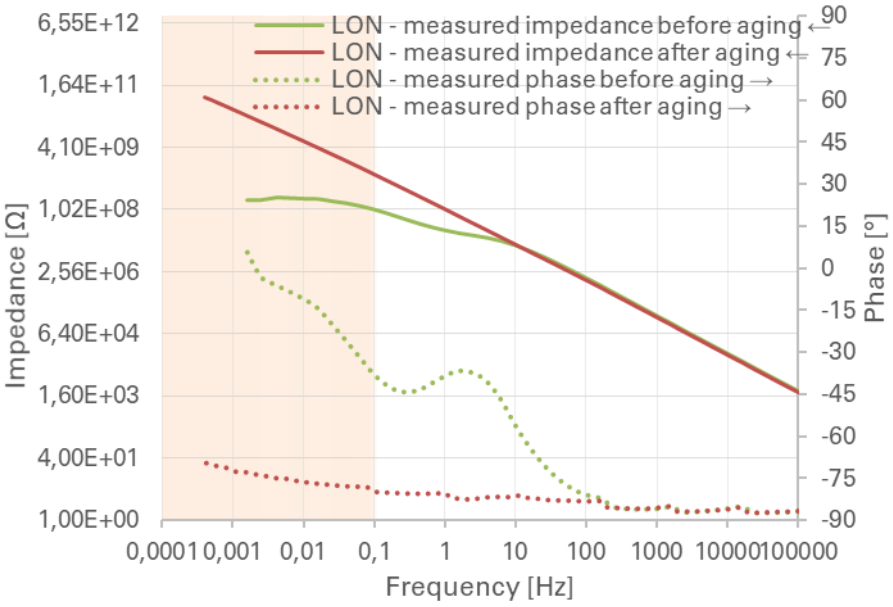

Appendix 18. Bode plot with matching phase plot for specimen LON, measured in saturated sodium chloride solution, before (green lines) and after (red lines) 24 days of aging in 5% sodium chloride solution

Note: The low impedance on specimen LON before aging is a failed measurement. The measurement after aging exhibits values more in line with other CED specimens.

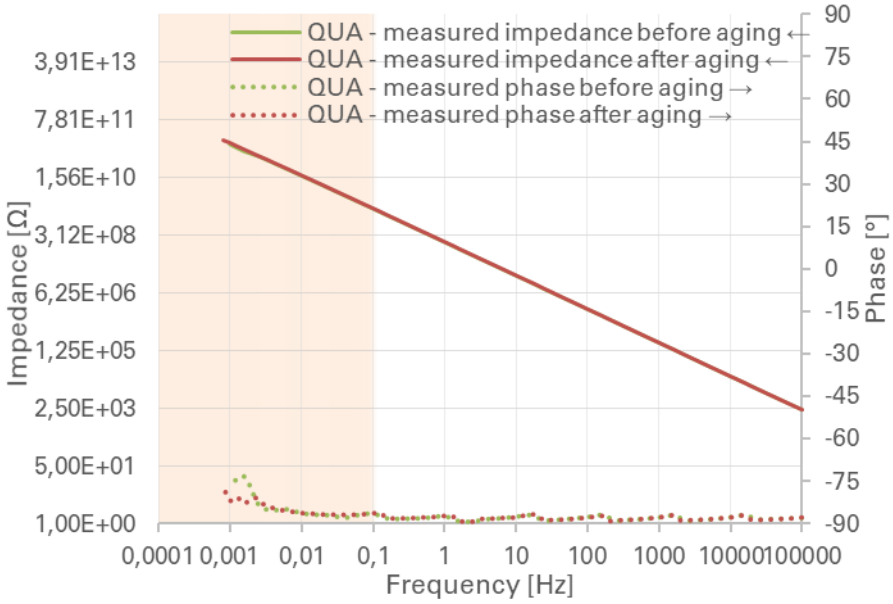

Appendix 19. Bode plot with matching phase plot for specimen QUA, measured in saturated sodium chloride solution, before (green lines) and after (red lines) 25 days of aging in 5% sodium chloride solution

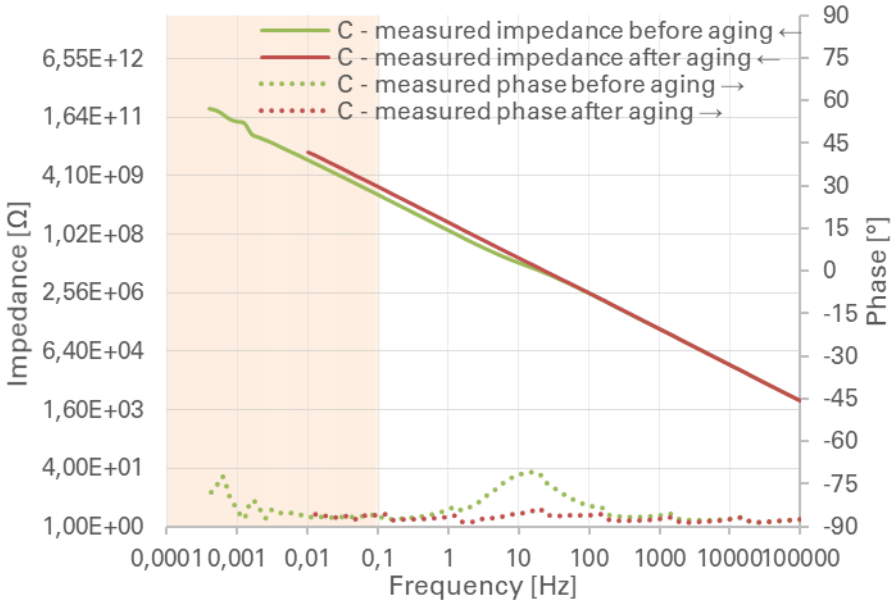

Appendix 20. Bode plot with matching phase plot for specimen C, measured in saturated sodium chloride solution, before (green lines) and after (red lines) 27 days of aging in 5% sodium chloride solution

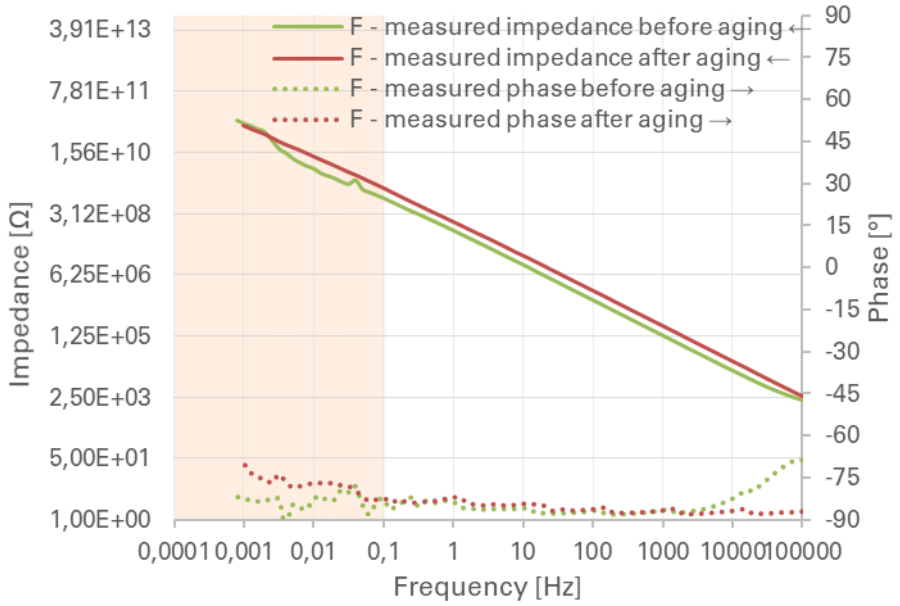

Appendix 21. Bode plot with matching phase plot for specimen F, measured in saturated sodium chloride solution, before (green lines) and after (red lines) 27 days of aging in 5% sodium chloride solution

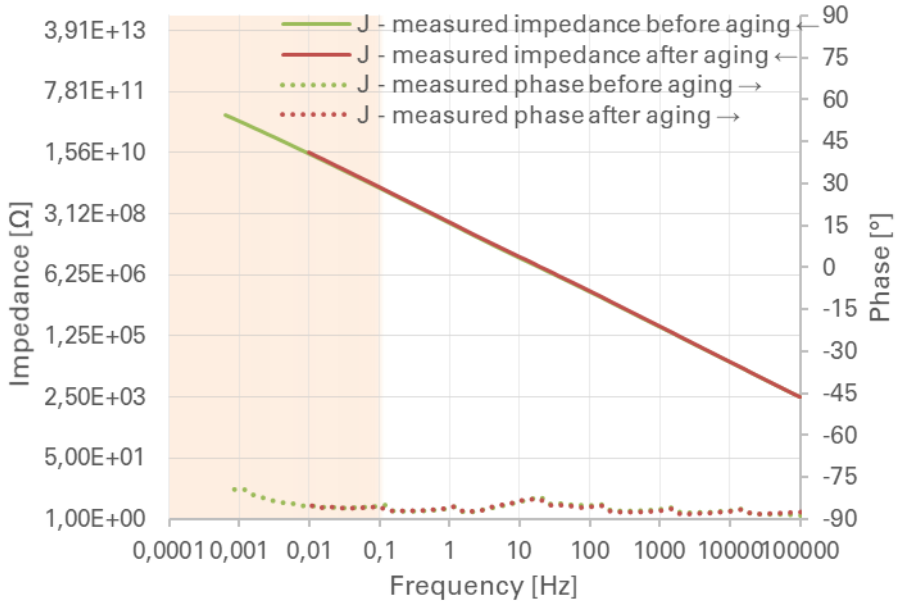

Appendix 22. Bode plot with matching phase plot for specimen J, measured in saturated sodium chloride solution, before (green lines) and after (red lines) 25 days of aging in 5% sodium chloride solution

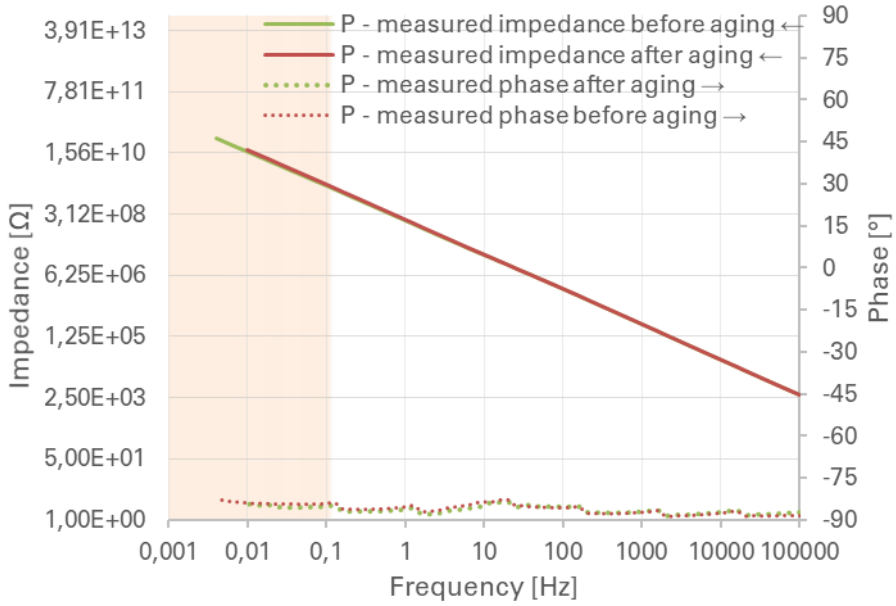

Appendix 23. Bode plot with matching phase plot for specimen P, measured in saturated sodium chloride solution, before (green lines) and after (red lines) 25 days of aging in 5% sodium chloride solution

Powder coated specimens

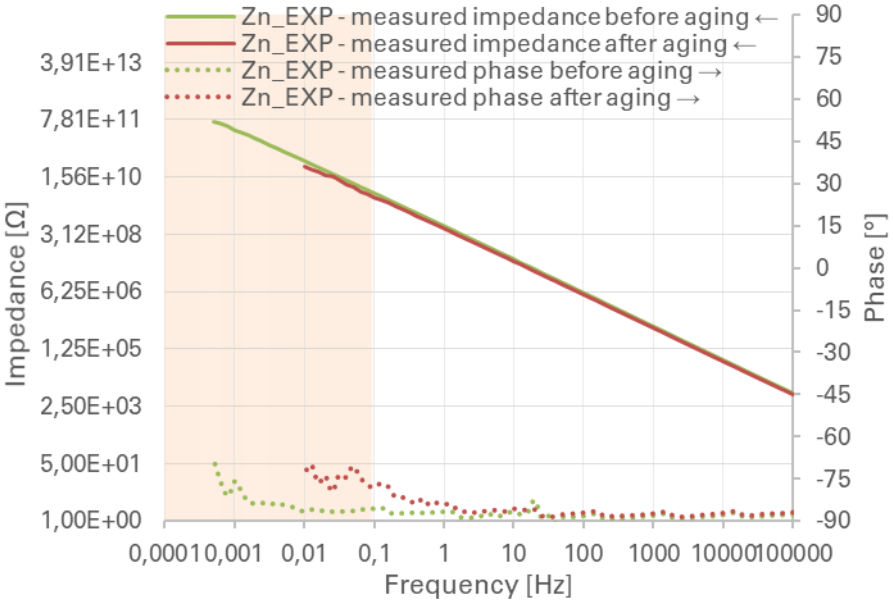

Appendix 24. Bode plot with matching phase plot for specimen Zn_EXP, measured in saturated sodium chloride solution, before (green lines) and after (red lines) 25 days of aging in 5% sodium chloride solution

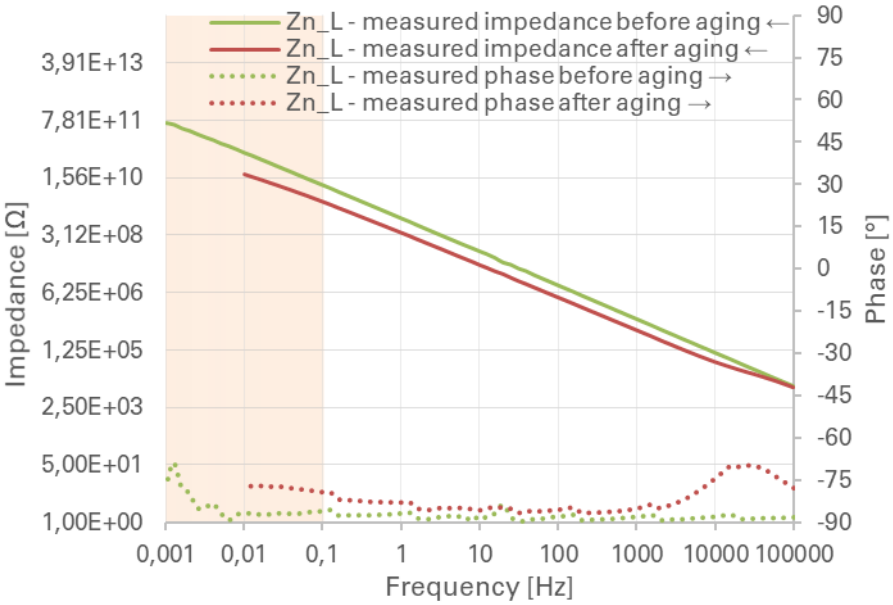

Appendix 25. Bode plot with matching phase plot for specimen Zn_L, measured in saturated sodium chloride solution, before (green lines) and after (red lines) 25 days of aging in 5% sodium chloride solution

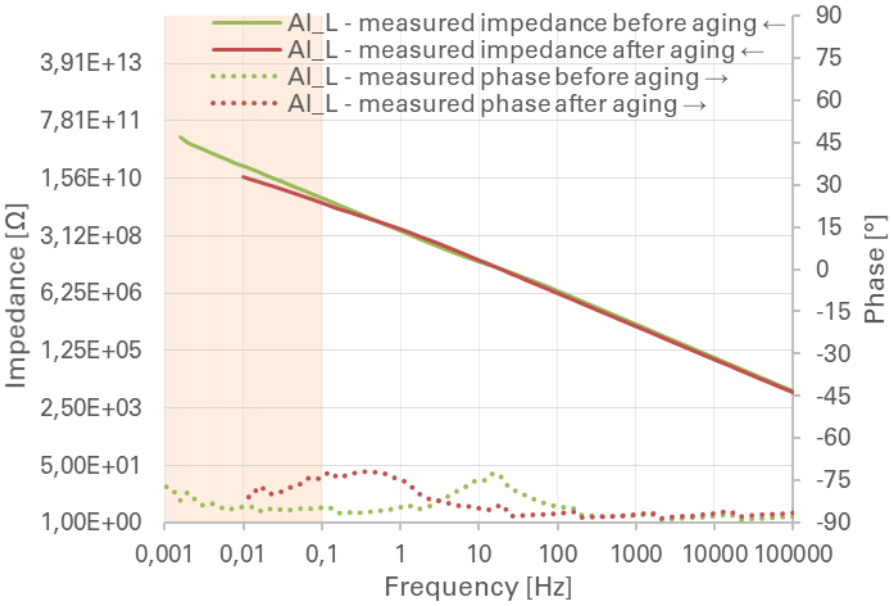

Appendix 26. Bode plot with matching phase plot for specimen Al_L, measured in saturated sodium chloride solution, before (green lines) and after (red lines) 25 days of aging in 5% sodium chloride solution